

LIPID KINASE REGULATION OF NOCICEPTIVE SIGNALING AND  
SENSITIZATION: IMPLICATIONS FOR ANALGESIC DRUG DEVELOPMENT

Brittany D. Wright

A dissertation submitted to the faculty of the University of North Carolina at Chapel Hill in partial fulfillment of the requirements for the degree of Doctor of Philosophy from the UNC Eshelman School of Pharmacy Department of Pharmaceutical Sciences (Division of Chemical Biology and Medicinal Chemistry).

Chapel Hill  
2013

Approved by:

Mohanish Deshmukh, Ph.D.

Stephen Frye, Ph.D.

Michael Jarstfer, Ph.D.

Ken McCarthy, Ph.D.

Mark Zylka, Ph.D.

© 2013  
Brittany D. Wright  
ALL RIGHTS RESERVED

## **ABSTRACT**

BRITTANY D. WRIGHT: Lipid kinase regulation of nociceptive signaling and sensitization: Implications for analgesic drug development  
(Under the direction of Mark Zylka)

Chronic pain affects approximately 35% of American adults resulting in annual treatment costs over \$600 billion. Unfortunately, current therapeutics have harmful side effects while only providing partial relief, highlighting the need for novel therapeutic targets for analgesic drug development. Neuropathic pain and inflammatory pain are the two most common forms of chronic pain in humans. In these conditions, nerve injury and inflammation lead to the release of pronociceptive molecules that signal through pronociceptive (pain-promoting) G protein-coupled receptors (GPCRs) and ion channels to sensitize nociceptive neurons in the dorsal root ganglia (DRG). Sensitization of these neurons leads to hyperalgesia and allodynia, two common symptoms of chronic pain.

The majority of these pronociceptive receptors and ion channels signal via phosphatidylinositol 4,5-bisphosphate (PIP<sub>2</sub>) hydrolysis. However, it is currently unknown which lipid kinases generate PIP<sub>2</sub> in DRG neurons and if these kinases regulate pronociceptive receptor signaling. The aim of this dissertation is to fully characterize the regulatory role of the predominant PIP<sub>2</sub>-synthesizing enzyme in

nociceptive signaling and sensitization using a combination of genetic and pharmacological approaches.

Our studies reveal that lipid kinase (LK) is expressed at the highest levels in DRG and, based on experiments with *LK*<sup>+/-</sup> mice, generates at least half of all PIP<sub>2</sub> in DRG neurons. Moreover, *LK* haploinsufficiency reduced pronociceptive receptor signaling and ion channel-mediated neuronal excitability in DRG neurons and reduced noxious thermal and mechanical sensitization in mouse models of chronic pain via PIP<sub>2</sub>-dependent mechanism(s). In parallel, we developed a high-throughput screening assay to identify the first reported small molecule inhibitor of LK, UNC1. UNC1 lowered PIP<sub>2</sub> levels in DRG neurons, reduced pronociceptive receptor signaling, and attenuated noxious thermal and mechanical sensitization when administered intrathecally. Collectively, this work demonstrates that LK regulates PIP<sub>2</sub>-dependent nociceptive signaling and sensitization and validates LK as a novel therapeutic target for chronic pain.

## **DEDICATION**

To my mom and dad. Thank you for endless love, inspiration, and support. I am  
forever grateful.

## **ACKNOWLEDGEMENTS**

I would like to extend my sincerest gratitude to my friends and family for their continued support, encouragement, and love throughout my graduate training. This would have never been possible without their continued support. Most importantly, I would like to thank my mom and dad, Cindy and Jackie Wright, for always being there and supporting me throughout life no matter what crazy dream I choose to follow and Dr. Robert Schuck for his unconditional love and support throughout every good and bad day of graduate school.

I would like to thank my dissertation committee for their guidance and continued commitment to my scientific development. I thank my advisor, Dr. Mark Zylka, who has always provided the motivation, resources, and creative scientific environment that have made this project successful. My committee chair, Dr. Michael Jarstfer, has always provided insightful advice on my scientific and professional development and for that, I am forever appreciative. I thank Dr. Stephen Frye for being amazing to work with and learn from during committee meetings, recruitment weekends, and our collaboration on this project. I thank Dr. Ken McCarthy for providing scientific advice and being an advocate for defined project endpoints, which is invaluable in the lengthy process that is graduate school. I thank Dr. Mohanish Deshmukh for always being a friendly face in the Neuroscience Center and providing insightful scientific guidance during committee meetings.

I am endlessly appreciative of current and past members of the Zylka laboratory that have made the challenges and obstacles encountered in graduate school easier to endure. I thank Bonnie Taylor-Blake, Walter Dutton, Brendan Fitzpatrick, Dr. Eric McCoy, Gabriela Salazar, Dr. Sarah Shoemaker and Dr. Sarah Street for their contributions to this project. I extend my sincerest gratitude to Dr. Julie Hurt, Dr. Angela Mabb, Dr. Jaeda Coutinho-Budd, Dr. Sarah Shoemaker, Dr. Brandon Pearson, and Gabriela Salazar for their friendship, encouragement, advice, support, and willingness to listen during my graduate training.

I would like to thank all members of the UNC Center for Integrative Chemical Biology and Drug Discovery that have welcomed me into their labs without hesitation. I thank William Janzen for his advice and guidance throughout the assay development process. I thank Dr. Jian Jin, Dr. Stephen Frye, and Dr. Anqi Ma for their scientific expertise in medicinal chemistry and providing an excellent collaborative environment. I thank Dmitiri Kireev for data analysis of our active compounds. I thank Cathy Simpson and Chatura Jayakody for all of their help with assay development and screening as well as their friendship.

The University of North Carolina at Chapel Hill has provided an excellent collaborative research environment for my graduate training. I am grateful that I had the chance to be a part of several different research programs at UNC including the Neuroscience Research Center, the department of Cell Biology and Physiology and my main appointment with the Division of Chemical Biology and Medicinal Chemistry (CBMC) in the UNC Eshelman School of Pharmacy. I would like to thank all of the CBMC staff, students, and faculty for being wonderful colleagues, always providing

support and encouragement, and having a continued commitment to scientific research. I would like to thank the UNC Eshelman School of Pharmacy and grants awarded to Mark Zylka for financial support that made this work possible.

Last but not least, I would like to thank my cats, Lewis and Clark, for forcing me to take time away from graduate school and enjoy the simple things in life.



## TABLE OF CONTENTS

LIST OF TABLES.....	xi
LIST OF FIGURES.....	xii
LIST OF ABBREVIATIONS.....	xiv
CHAPTER I: INTRODUCTION .....	1
Chronic pain and current therapeutics.....	1
Nociceptive Circuitry and Sensitization .....	2
G-protein-coupled receptor and ion channel mediated nociceptive signaling and sensitization.....	4
Phosphatidylinositol 4,5-bisphosphate (PIP <sub>2</sub> ).....	6
Type 1 Phosphatidylinositol 4-phosphate 5-kinases (PIP5K1s).....	8
Summary and Significance.....	10
Specific Aims .....	12
Figures.....	14
CHAPTER II: PIP5K1C REGULATES PRONOCICEPTIVE SIGNALING <i>IN VITRO</i> AND NOCICEPTIVE SENSITIZATION <i>IN VIVO</i> .....	18
Introduction.....	18
Methods.....	20
Results.....	28
Discussion .....	39
Figures.....	47

CHAPTER III: SENSORY NEURON-SPECIFIC GENETIC DELETION OF PIP5K1C IN MICE RESULTS IN PROPRIOCEPTIVE ABNORMALITIES .....	61
Introduction.....	61
Methods.....	62
Results.....	66
Discussion .....	69
Figures.....	75
CHAPTER IV: DEVELOPMENT OF A HIGH-THROUGHPUT SCREENING ASSAY IDENTIFIES A SMALL MOLECULE INHIBITOR OF PIP5K1C THAT ATTENUATES NOCICEPTIVE SIGNALING AND SENSITIZATION.....	80
Introduction.....	80
Methods.....	82
Results.....	88
Discussion .....	96
Tables.....	102
Figures.....	109
CHAPTER V: DISCUSSION AND PERSPECTIVE .....	121
Summary and Scope .....	121
Key Findings.....	124
Human implications .....	133
Conclusions.....	137
APPENDIX 1: PERSONAL CONTRIBUTIONS TO DISSERTATION CHAPTERS .....	138
REFERENCES.....	139

## LIST OF TABLES

Table 4.1. PIP5K1C HTS microfluidic mobility shift assay conditions.....	102
Table 4.2. Active compounds from the focused-kinases library. ....	103
Table 4.3. Active compound from the LOPAC library. ....	107
Table 4.4. Kinases screened for UNC3230 selectivity with numbers representing %activity/binding remaining in the presence of 10 $\mu$ M UNC3230. ....	108

## LIST OF FIGURES

Figure 1.1. Schematic of peripheral nociceptive circuitry.....	14
Figure 1.2. DRG-mediated nociceptive signaling in the three types of pain. ....	15
Figure 1.3. Phosphatidylinositol (PI) synthetic pathways.....	16
Figure 1.4. Type I PIP5Ks.....	17
Figure 2.1. PIP5K1C is the predominant PIP5K1 isoform in adult nociceptive DRG neurons. ....	47
Figure 2.2. PIP5K1C generates at least half of all PIP <sub>2</sub> in embryonic mouse DRG.....	48
Figure 2.3 PIP5K1C generates at least half of all PIP <sub>2</sub> in adult mouse DRG. ....	49
Figure 2.4. <i>Pip5k1c</i> haploinsufficiency attenuates TRPV1-mediated signaling and acute nociceptive sensitivity to heat. ....	50
Figure 2.5. <i>Pip5k1c</i> haploinsufficiency reduces ligand-evoked nociceptive signaling <i>in vitro</i> and nocifensive licking <i>in vivo</i> . ....	51
Figure 2.6. <i>Pip5k1c</i> haploinsufficiency attenuates PIP <sub>2</sub> -dependent ion channel-mediated neuronal excitability. ....	53
Figure 2.7. <i>Pip5k1c</i> haploinsufficiency alters the expression of cytoskeletal proteins. ....	54
Figure 2.8. Schematic representation of all PIP <sub>2</sub> -dependent mechanisms altered by <i>Pip5k1c</i> haploinsufficiency. ....	55
Figure 2.9. <i>Pip5k1c</i> haploinsufficiency reduces PIP <sub>2</sub> -dependent thermal and mechanical sensitization in models of chronic inflammatory and neuropathic pain.....	56
Figure 2.10. <i>Pip5k1c</i> haploinsufficiency does not alter motor function, gait or low-threshold (innocuous) mechanoreception.....	58
Figure 2.11. Nociceptive neuron markers and synaptic transmission between sensory neurons and spinal cord are not affected in <i>Pip5k1c</i> <sup>+/-</sup> mice. ....	59

Figure 3.1. Intrathecal PIP <sub>2</sub> injections selectively increase PIP <sub>2</sub> in the DRG.....	74
Figure 3.2. Generation of <i>Pip5k1c</i> <sup>fl/fl</sup> conditional knockout mice.....	75
Figure 3.3. Pip5k1c is selectively eliminated in sensory neurons of the DRG.....	76
Figure 3.4. Sensory-neuron specific deletion of <i>Pip5k1c</i> produces a proprioceptive phenotype.....	77
Figure 3.5 Sensory-neuron specific deletion of <i>Pip5k1c</i> reduces nerve innervation into the skin.....	78
Figure 4.1. Recombinant PIP5K1C can be used to generate fluorescein conjugated PIP <sub>2</sub> from fluorescein conjugated PI(4)P.....	109
Figure 4.2. PIP5K1C assay development to determine kinase concentration, ATP Km, and DMSO sensitivity.....	110
Figure 4.3. Assay validation using the LOPAC library.....	112
Figure 4.4. HTS of 4,727 compound kinase-focused library.....	113
Figure 4.5. The two most potent inhibitors of PIP5K1C have the same core structure and nanomolar potency.....	114
Figure 4.6. UNC3230 is a selective small molecule PIP5K1C inhibitor.....	116
Figure 4.7. UNC3230 reduces membrane PIP <sub>2</sub> levels in DRG neurons and GPCR signaling.....	117
Figure 4.8. UNC3230 reduces thermal and mechanical sensitization in models of chronic pain.....	118
Figure 4.9. Selectivity of UNC3230 relative to lipid kinases that generate phosphoinositides.....	120

## LIST OF ABBREVIATIONS

17-PT PGE <sub>2</sub>	17-phenyl trinor prostaglandin E <sub>2</sub>
<i>Acpp</i>	Prostatic acid phosphatase, murine gene
<i>ACTA1</i>	Alpha-actin, human gene
AP-2	Adaptor protein 2
ATP	Adenosine triphosphate
BBB	Blood-brain barrier
BDNF	Brain-derived neurotrophic factor
BK	Bradykinin
CFA	Complete Freund's adjuvant
CICBDD	Center for Integrative Chemical Biology and Drug Discovery
CGRP	Calcitonin gene-related peptide
CR-8	Coating reagent 8
Cre	Cre recombinase
DAG	Diacylglycerol
DRG	Dorsal root ganglion
EDTA	Ethylenediaminetetraacetic acid
ELISA	Enzyme-linked immunosorbent assay
EPAC	Exchange protein activated by cAMP
ER	Endoplasmic reticulum
F-actin	Filamentous actin
fl/fl	<i>Pip5k1c</i> gene floxed by LoxP sites
GDNF	Glial-derived neurotrophic factor

GPCR	G-protein coupled receptor
HTS	High-throughput screening
IB4	Isolectin B4
IP <sub>3</sub>	Inositol 1,4,5-triphosphate
kHz	Kilohertz
LCCS3	Lethal congenital contracture syndrome type 3
LOPAC	Library of pharmacologically active compounds
LK	Lipid kinase
LPA	Lysophosphatidic acid
NGF	Nerve growth factor
NSAID	Non-steroidal anti-inflammatory drugs
MAPK	Mitogen activated protein kinase
MSA	Mobility shift assay
PAP	Prostatic acid phosphatase
PGP9.5	Protein gene product 9.5
PI3K	Phosphatidylinositol 3-kinase
PI4K	Phosphatidylinositol 4-kinase
PI(3)P	Phosphatidylinositol 3-phosphate
PI(4)P	Phosphatidylinositol 4-phosphate
PI(5)P	Phosphatidylinositol 5-phosphate
PIP4K2A	Phosphatidylinositol 5-phosphate 4-kinase, type 2a, protein
PIP4K2C	Phosphatidylinositol 5-phosphate 4-kinase, type 2c, protein
<i>Pip5k1a</i>	Phosphatidylinositol 4-phosphate 5-kinase type 1a, murine gene

PIP5K1A	Phosphatidylinositol 4-phosphate 5-kinase type 1a, protein
<i>Pip5k1b</i>	Phosphatidylinositol 4-phosphate 5-kinase type 1b, murine gene
PIP5K1B	Phosphatidylinositol 4-phosphate 5-kinase type 1b, protein
<i>Pip5k1c</i>	Phosphatidylinositol 4-phosphate 5-kinase type 1c, murine gene
<i>PIP5K1C</i>	Phosphatidylinositol 4-phosphate 5-kinase type 1c, human gene
PIP5K1C	Phosphatidylinositol 4-phosphate 5-kinase type 1c, protein
PIP <sub>2</sub>	Phosphatidylinositol 4,5-bisphosphate
PKC	Protein kinase C
PLC	Phospholipase C
RNAseq	High-throughput RNA sequencing
SDS-PAGE	Sodium dodecyl sulfate polyacrylamide gel electrophoresis
shRNA	Small hairpin RNA
siRNA	Small interfering RNA
SNI	Spared nerve injury
<i>TNNT</i>	Skeletal troponin T
TRP	Transient receptor potential
TRPV1	Transient receptor potential vanilloid type 1
TRKA	Tyrosine receptor kinase receptor A
UNC	University of North Carolina at Chapel Hill
WT	Wild-type; C57Bl/6 mouse
wt/wt	Wild-type expressing <i>Advillin</i> driven Cre on one allele



# CHAPTER I

## INTRODUCTION

### **Chronic pain and current therapeutics**

Chronic pain affects approximately 100 million American adults, making it more prevalent than diabetes, cancer, and heart disease combined<sup>1</sup>. In addition to being in a perpetual state of discomfort, patients suffering from chronic pain are also plagued by depression, loss of sleep, and an inability to complete daily tasks, all of which lead to a significant decrease in overall quality of life<sup>1</sup>.

Unfortunately, non-steroidal anti-inflammatory drugs (NSAIDs), acetaminophen, and opioid-based analgesics such as morphine—the current first-line therapeutics for pain—have harmful side effects while only providing partial relief<sup>2</sup>. The complexity of nociception (detection of noxious stimuli) and subsequent pain processing, ultimately resulting in cognitive awareness, creates many challenges for analgesic drug discovery and contributes to the ineffectiveness and adverse effects associated with current therapeutics<sup>3</sup>.

Current therapeutic inadequacies highlight the need to identify novel molecular targets for analgesic drug development. In order to identify novel therapeutic targets, mechanisms of peripheral nociceptive signaling and sensitization need to be further elucidated<sup>4</sup>.

## **Nociceptive circuitry and peripheral sensitization**

Nociception is the detection and transduction of noxious stimuli by the peripheral and central nervous system, independent of cognitive awareness. In contrast, pain is associated with perception and requires cognitive awareness and intact cortical and subcortical processing<sup>5</sup>. Nociception is mediated by neurons (commonly referred to as nociceptors) whose cell bodies are located in dorsal root ganglia (DRG) (Figure 1.1). These nociceptors have a bifurcated axon that extends into the target tissue (organs, skin, muscle, etc.) via a peripheral terminal and onto second order neurons in the spinal cord (primarily lamina I and II) via a central terminal<sup>3, 4, 6</sup> (Figure 1.1). Nociceptive neurons are responsible for the detection of noxious thermal, mechanical, and chemical stimuli and can be divided into two groups. The first group consists of medium diameter neurons whose afferents are myelinated. These afferents, referred to as A $\delta$  fibers, are responsible for “fast” or “first” pain<sup>6</sup>. The second group is composed of small diameter neurons whose afferents are not myelinated. These unmyelinated afferents, referred to as C fibers, are responsible for the transduction of “slow” or “second” pain<sup>6</sup>.

The second group, the C fiber nociceptors, is further differentiated into two subgroups, peptidergic and nonpeptidergic neurons<sup>4, 6</sup> (Figure 1.1). Peptidergic and nonpeptidergic neurons differ in their molecular composition, anatomical projections, and contribution to different pain modalities. Peptidergic neurons express neuropeptides such as substance P and calcitonin gene-related peptide (CGRP) and their central termini project into the outer lamina (I and outer II) of the spinal dorsal horn<sup>7-9</sup>. In contrast, nonpeptidergic neurons express prostatic acid phosphatase,

bind the plant isolectin B4 (IB4), and project their central termini into lamina II of the spinal cord<sup>7-9</sup>. Importantly, peptidergic neurons primarily mediate detection of noxious thermal stimuli whereas nonpeptidergic neurons primarily mediate detection of noxious mechanical stimuli<sup>7-9</sup> (Figure 1.1). These molecular and anatomical distinctions are commonly used for differentiating various nociceptive signaling mechanisms *in vivo* and *in vitro*.

Under normal physiological conditions, nociceptors function as a defense mechanism to protect against dangerous stimuli and promote avoidance of situations that evoke pain<sup>10</sup>. This type of pain is called nociceptive or physiological pain<sup>3, 10, 11</sup>. In contrast, persistent or chronic pain results when nociceptors become sensitized (Figure 1.2B)<sup>12</sup>. Sensitization is characterized by a reduction in detection threshold and an increase in response to noxious stimuli which mediates two common symptoms of pain in humans, allodynia in which typically innocuous stimuli become painful and hyperalgesia in which a painful stimulus becomes more painful, respectively<sup>6, 10, 12</sup>. Sensitization of nociceptors occurs most commonly after inflammation and nerve injury<sup>6, 10</sup> giving rise to the two most common forms of chronic pain in humans, inflammatory and neuropathic pain, respectively<sup>2, 12</sup>. It is important to note that central sensitization takes place primarily at the level of the spinal cord in nociceptor transmission neurons in the dorsal horn while peripheral sensitization occurs in neurons of the DRG<sup>12</sup>. Central sensitization is dependent upon activity from the central terminal of the DRG (synaptic transfer from the nociceptor terminal to dorsal horn neurons) and is often preceded by peripheral

sensitization<sup>12</sup>. The focus of this dissertation is on mechanisms that mediate peripheral sensitization in DRG neurons.

### **G-protein-coupled receptor and ion channel mediated nociceptive signaling and sensitization**

Nociceptive, neuropathic, and inflammatory pain are mediated by several different molecular mechanisms; some of these mechanisms are unique to one type of pain while others are involved in multiple pain modalities<sup>13</sup>. Transient receptor potential (TRP) channels are responsible for the detection of noxious thermal, mechanical, and chemical stimuli and are the predominant mediators of nociceptive pain. Of particular interest to this dissertation is the non-selective cation channel, transient receptor potential vanilloid type I (TRPV1), as it is the predominant detector of noxious heat and is regulated by PIP<sub>2</sub><sup>14-17</sup> (Figure 1.2A). Furthermore, TRPV1 detection of noxious heat is commonly used in rodents as a model of nociceptive pain due to the ease of the corresponding assay and will be used as such for this dissertation. In addition, TRPV1 activation also contributes to the changes in nociceptor excitability that mediate persistent pain (Figure 1.2A).

Although TRPV1 is the main regulator of thermal acute nociceptive pain, GPCRs are the more predominant mediators of nociceptive sensitization and persistent pain (Figure 1.2B). It is well-established that nerve injury and inflammation result in the release multiple pronociceptive molecules, including bradykinin (BK), LPA, adenosine triphosphate (ATP) and prostaglandins<sup>3</sup>. These ligands signal through a diverse set of Gq and Gs-coupled GPCRs to sensitize

nociceptors<sup>18, 19</sup>. Activation of Gq-coupled GPCRs via canonical Gq-coupling results in phospholipase C (PLC)-catalyzed hydrolysis of phosphatidylinositol 4,5 bisphosphate (PIP<sub>2</sub>) to produce diacylglycerol (DAG) and inositol 1,4,5-triphosphate (IP<sub>3</sub>). DAG activates protein kinase Cs (PKCs) that subsequently activates the mitogen-activated protein kinase (MAPK) cascade. IP<sub>3</sub> binds to IP<sub>3</sub> receptors on the endoplasmic reticulum (ER), which results in an increase in cytoplasmic calcium from intracellular calcium stores. In addition, Gs-coupled GPCRs can contribute to this pathway by exchange protein activated by cAMP (EPAC) activation of PLC<sup>20</sup>. Activation these downstream effectors results in nociceptor sensitization (Figure 1.2B). Importantly, GPCR activation and subsequent downstream effector activation can potentiate the activity of a variety of ion channels and modulate the hyperexcitability of the nociceptors following nerve injury and inflammation (Figure 1.2B). As mentioned above, sensitization of nociceptors through activation of GPCRs is one of the predominant underlying mechanisms for neuropathic and inflammatory pain<sup>13</sup> (Figure 1.2B).

In addition to the previously mentioned TRP channels, a variety of ion channels are responsible for regulating neuronal excitability—and more importantly hyperexcitability following nerve injury and inflammation—via mechanisms that are both independent of and dependent upon modulation by GPCRs<sup>21, 22</sup>. Furthermore, an increase in excitability is crucial for prolonged nociceptive sensitization and persistent pain<sup>3, 6, 22</sup>. Many different classes of ion channels regulate neuronal excitability including sodium, potassium, calcium and hyperpolarization channels<sup>3, 6, 23-25</sup>. Although a review of the distinct function of each of these ion channels is

beyond the scope of this dissertation, it is important to note that many of these ion channels depend on PIP<sub>2</sub> for activity<sup>22, 24-26</sup> (Figure 1.2B).

Indeed, one important commonality between GPCR- and ion-channel mediated nociceptive signaling and sensitization is their dependence upon the lipid second messenger, PIP<sub>2</sub> (Figure 1.2A and B). PIP<sub>2</sub> regulates TRPV1, a predominant mediator of nociceptive pain, as well as other ion channels responsible for the regulation of neuronal excitability. Moreover, as discussed above, PIP<sub>2</sub> is a crucial component of the Gq-coupled GPCR signaling pathway, which mediates nociceptive sensitization following nerve injury and inflammation. Thus, PIP<sub>2</sub> represents a critical convergence point for many pain promoting pathways.

### **Phosphatidylinositol 4,5-bisphosphate (PIP<sub>2</sub>)**

Although PIP<sub>2</sub> is only a minor constituent (<1%) of the plasma membrane, it is very important to a multitude of cellular processes and serves as prerequisite to other regulatory lipids in the phosphatidylinositol (PI) synthetic cascade<sup>27, 28</sup> (Figure 1.3). As discussed above, PIP<sub>2</sub> hydrolysis regulates both GPCR- and ion channel-mediated signaling. As outlined previously, PLC hydrolysis of PIP<sub>2</sub> into DAG and IP<sub>3</sub> is crucial to GPCR signaling via a large number of downstream effectors including MAPKs and PKC. In addition, PIP<sub>2</sub> directly regulates channel activity of TRP channels and other ion channels via interactions with polybasic amino acids on the C terminus<sup>25</sup>. However, the regulation of nociceptive signaling and sensitization by PIP<sub>2</sub> most likely extends well beyond PIP<sub>2</sub> hydrolysis. Here, several additional PIP<sub>2</sub>

interactions that are pertinent to signaling in nociceptive DRG neurons will be discussed briefly.

PIP<sub>2</sub> is critical for cytoskeletal dynamics via its interactions with both actin and tubulin. PIP<sub>2</sub> has an important regulatory interaction with tubulin, the main constituent of cytoskeletal microtubules. Tubulin is responsible for the direct transfer of GTP to Gαq to initiate PLC activation and subsequent PIP<sub>2</sub> hydrolysis<sup>29-31</sup>. Importantly, high concentrations of tubulin inhibit PLC-mediated signaling via PIP<sub>2</sub> interactions<sup>29, 32</sup>. Moreover, intact microtubules contribute to TRPV1 stability and functionality<sup>33</sup>.

PIP<sub>2</sub> also interacts with actin and modulates actin dynamics through three distinct pathways: binding actin-capping proteins such as vinculin, serving as a scaffold for adaptor proteins such as adaptor protein 2 (AP-2), and regulating activity of Rho GTPases<sup>27</sup>. Furthermore, actin dynamics play a critical role in GPCR signaling and may contribute to GPCR-mediation of chronic nociceptive sensitization<sup>34, 35</sup>. For example, LPA receptor activation and subsequent calcium release plays an important role in the initiation of neuropathic pain<sup>16, 17, 39</sup>. Actin rearrangements that occur following LPA receptor activation are required for LPA-mediated calcium release (via LPA1 which also mediates LPA-induced neuropathic pain)<sup>36-39</sup>. Furthermore, prostaglandin-mediated nociceptive sensitization (via Gq activation of protein kinase C) requires an intact actin cytoskeleton to produce full inflammatory pain responses<sup>40</sup>. Thus, PIP<sub>2</sub>-actin and PIP<sub>2</sub>-tubulin interactions provide other potential mechanisms for attenuation of nociceptive signaling via decreases in PIP<sub>2</sub>.

Many of these processes are dependent upon adequate PIP<sub>2</sub> synthesis via phosphatidylinositol kinases. Type 1 phosphatidylinositol 4-phosphate 5-kinases (PIP5K1s) and type 2 phosphatidylinositol 5-phosphate 4-kinases (PIP4K2s) synthesize PI(4,5)P<sub>2</sub> by phosphorylating phosphatidylinositol 4-phosphate, [PI(4)P] and phosphatidylinositol 5-phosphate [PI(5)P], respectively (Figure 1.3). PI(4)P is the most abundant monophosphoinositide and is present at 10-fold greater concentrations than PI(5)P, suggesting that PIP5K1s are the predominant PIP<sub>2</sub> synthesizing enzymes. It must be noted that PIP5K1s can also phosphorylate phosphatidylinositol 3-phosphate, PI(3)P to form PI(3,5)P<sub>2</sub>; however, it has been shown that PIP5K1 generation of PI(4,5)P<sub>2</sub> is the major regulatory mechanism for GPCRs and ion channels<sup>25, 27, 41</sup> (Figure 1.3).

### **Type 1 Phosphatidylinositol 4-phosphate 5-kinases (PIP5K1s)**

There are three mammalian *Pip5k1* genes, *Pip5k1a*, *Pip5k1b*, and *Pip5k1c*, that express three PIP5K1 isozymes: PIP5K1A, PIP5K1B, and PIP5K1C (Figure 1.4). Due to patentability of portions of this work, PIP5K1C was previously referred to as lipid kinase (LK) in the abstract. The three isozymes are >80% identical at the amino acid level within the kinase catalytic domain. However, they have very little sequence homology within their N and C termini; these isozyyme-specific regions allow differentiated functions of each isoform within cells<sup>42, 43</sup> (Figure 1.4). Each isoform has differential expression within cells and across murine tissues. It must be noted that human PIP5K1A is homologous to murine PIP5K1B and human PIP5K1B is homologous to murine PIP5K1A (Figure 1.4). PIP5K1A is ubiquitously expressed



in murine tissue, is primarily expressed in the nucleus, and translocates to the membrane following receptor activation<sup>42-44</sup>. PIP5K1B is also ubiquitously expressed in murine tissue but is located in the perinuclear region<sup>44</sup>. Unlike PIP5K1A and PIP5K1B, PIP5K1C is not ubiquitously expressed and is instead expressed predominantly in neuronal tissue (with minimal expression in the lung and kidney). PIP5K1C localizes to the cytoplasm, plasma membrane, and intracellular membranes<sup>41, 45, 46</sup>.

Characterization of PIP5K1A and PIP5K1B has been carried out utilizing a variety of cell types and roles in membrane ruffling, endocytosis, and actin dynamics have all been elucidated<sup>47, 48</sup>. It is common for PIP5K1A and PIP5K1B to have overlapping functions; however, like the specialized expression profile of PIP5K1C, it is rare that PIP5K1C shares common functionality with PIP5K1A and PIP5K1B<sup>47, 48</sup>. Endocytosis is the one function in which all three isozymes play a role; however, it is suggested that PIP5K1C has a specialized role in interacting with AP-2 in this process<sup>48, 49</sup>. Furthermore, in bone marrow macrophages, PIP5K1A and PIP5K1C have very distinct functions that mediate different steps in phagocytosis<sup>47, 48</sup>. The role of PIP5K1C has primarily been studied in cortical synaptic transmission<sup>45</sup>, GPCR-mediated signaling<sup>41</sup>, regulation of focal adhesions<sup>50</sup>, and AP-2 mediated endocytosis<sup>49</sup>. Moreover, the functions of PIP5K1C can be further differentiated by the involvement of the two different splice isoforms, PIP5K1C635 and PIP5K1C661. Importantly, PIP5K1C635 is the primary splice variant responsible for the regulation of GPCR-mediated signaling whereas PIP5K1C661 is the primary splice variant

responsible for the interactions with talin and AP-2 which mediate endocytosis and focal adhesions<sup>41, 48-50</sup> (Figure 1.4).

Although the expression profile and functionality of PIP5K1s in DRG has yet to be determined, previous data suggest that PIP5K1C is the predominantly expressed isoform given its specialized expression in neuronal tissue. *Pip5k1c* homozygous mice (*Pip5k1c*<sup>-/-</sup>) exhibit a perinatal lethal phenotype (death within 24 hours of birth), presumably due to lack of mobility and an inability to feed<sup>45, 51</sup>. Heterozygous mice (*Pip5k1c*<sup>+/-</sup>) live to adulthood and reproduce normally. Previously characterized phenotypes in *Pip5k1c*<sup>-/-</sup> embryos include reduced synaptic transmission and impairment of clathrin-mediated endocytosis in cortical neurons and phagocytosis defects in bone marrow macrophages<sup>45, 47</sup>. In addition, calcium signaling in cochlear nonsensory cells hearing at high frequencies (> 20 kHz) is reduced in adult *Pip5k1c*<sup>+/-</sup> mice<sup>52</sup>.

### **Summary and Significance**

Therapeutic inadequacies and harmful side effects of current analgesics highlight the need to better understand the underlying signaling mechanisms of maladaptive pain pathology that would promote the identification of novel therapeutic targets and treatments. Structural features that are likely to interact with drug-like compounds determine the druggability of a potential therapeutic target<sup>53</sup>. The affinity of drug-like compounds to block the catalytic site of a kinase, which precisely abolishes the kinase's biological activity, makes kinases particularly attractive therapeutic targets<sup>53, 54</sup>. Discovery and characterization of novel regulatory kinases

that mediate peripheral sensitization offers the potential to develop new analgesics that are likely to improve efficacy. In addition, characterization of kinases that are primarily expressed in nociceptors will provide potential for mitigating unwanted side effects that plague current therapeutics.

Given that PIP5K1C, a potentially druggable kinase, is enriched in neuronal tissue and accumulating evidence indicates that many pronociceptive signaling mechanisms depend on PIP<sub>2</sub>, we hypothesize that PIP5K1C regulates PIP<sub>2</sub>-dependent pronociceptive signaling in DRG neurons. Furthermore, we hypothesize that reductions in PIP5K1C will reduce nociceptive sensitization via PIP<sub>2</sub>-dependent mechanisms. The aim of this work is to rigorously characterize the role of PIP5K1C in nociceptive signaling *in vitro* and sensitization *in vivo*. We seek to accomplish this aim using genetic deletion of *Pip5k1c* in mice (Aim 1 and 2) and pharmacological inhibition of PIP5K1C (Aim 3).

Completion of this work will improve our understanding of signaling mechanisms that mediate nociceptive sensitization, highlight lipid kinases as novel regulators of pronociceptive signaling, and provide insights into potential therapeutic treatments for chronic pain.

## Specific Aims

- 1) Utilize *Pip5k1c* genetic knockout mice to investigate the regulatory role of PIP5K1C in nociceptive signaling and sensitization

**Central Hypothesis:** Genetic deletion of *Pip5k1c* will attenuate PIP<sub>2</sub>-dependent nociceptive signaling and sensitization.

**Specific Hypotheses:**

- a) Genetic deletion of *Pip5k1c* will reduce PIP<sub>2</sub>-dependent GPCR- and ion channel-mediated pronociceptive receptor signaling in DRG neurons
  - b) Genetic deletion of *Pip5k1c* will reduce acute GPCR-mediated nocifensive behaviors and ion channel-mediated thermal sensitivity
  - c) Genetic deletion of *Pip5k1c* will attenuate PIP<sub>2</sub>-dependent nociceptive sensitization in mouse models of chronic pain
- 2) Characterize a sensory-neuron specific *Pip5k1c* knockout mouse to determine phenotypic site of action.

**Central Hypothesis:** Genetic deletion of *Pip5k1c* in sensory neurons only will reduce nociceptive signaling and sensitization similar to or greater than reductions observed in global heterozygotes.

**Specific Hypotheses:**

- a) Sensory neuron-specific deletion of *Pip5k1c* will reduce PIP<sub>2</sub>-dependent nociceptive signaling in DRG neurons
- b) Sensory neuron-specific deletion of *Pip5k1c* will attenuate PIP<sub>2</sub>-dependent nociceptive sensitization in mouse models of chronic pain

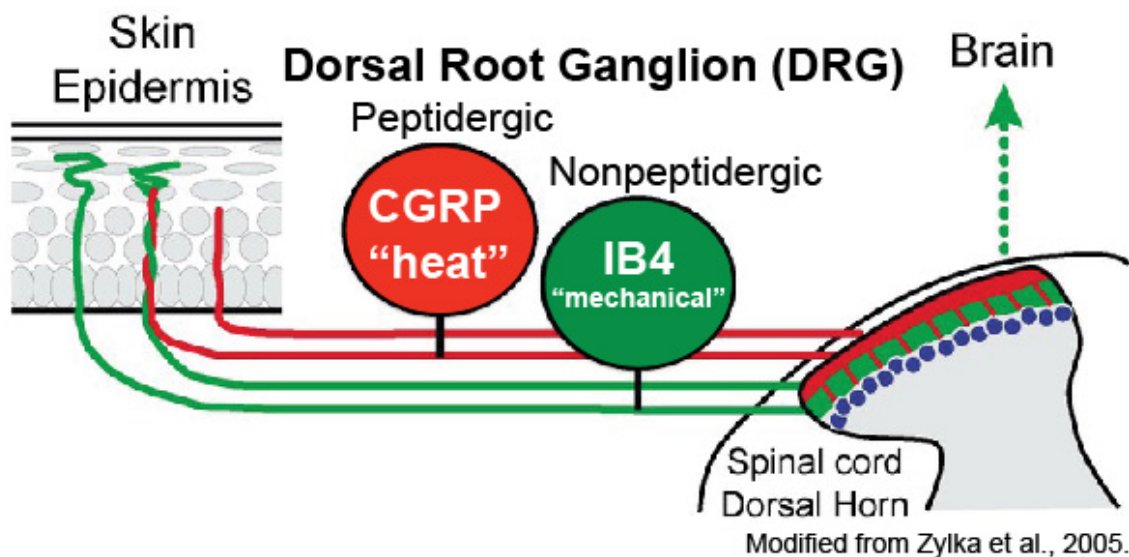
- 3) Develop a high-throughput screening assay to identify potent inhibitors of PIP5K1C that will be used to validate PIP5K1C as a novel therapeutic target.

**Central Hypothesis:** Development of a high-throughput screening assay will identify inhibitors (or promising scaffolds for medicinal chemistry optimization) of PIP5K1C that can be used to evaluate pharmacological inhibition of PIP5K1C in nociceptive signaling and sensitization.

**Specific Hypotheses:**

- a) Development of a high-throughput screening assay will identify inhibitors of PIP5K1C
- b) If identified, potent inhibitors will reduce nociceptive signaling in DRG neurons
- c) If identified, potent inhibitors will have antinociceptive effects when administered intrathecally.

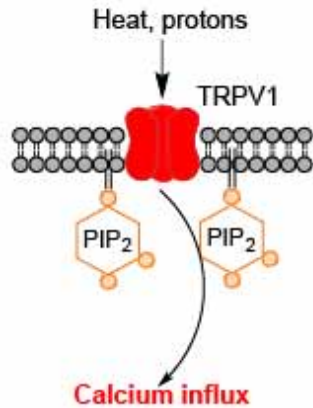
## Figures



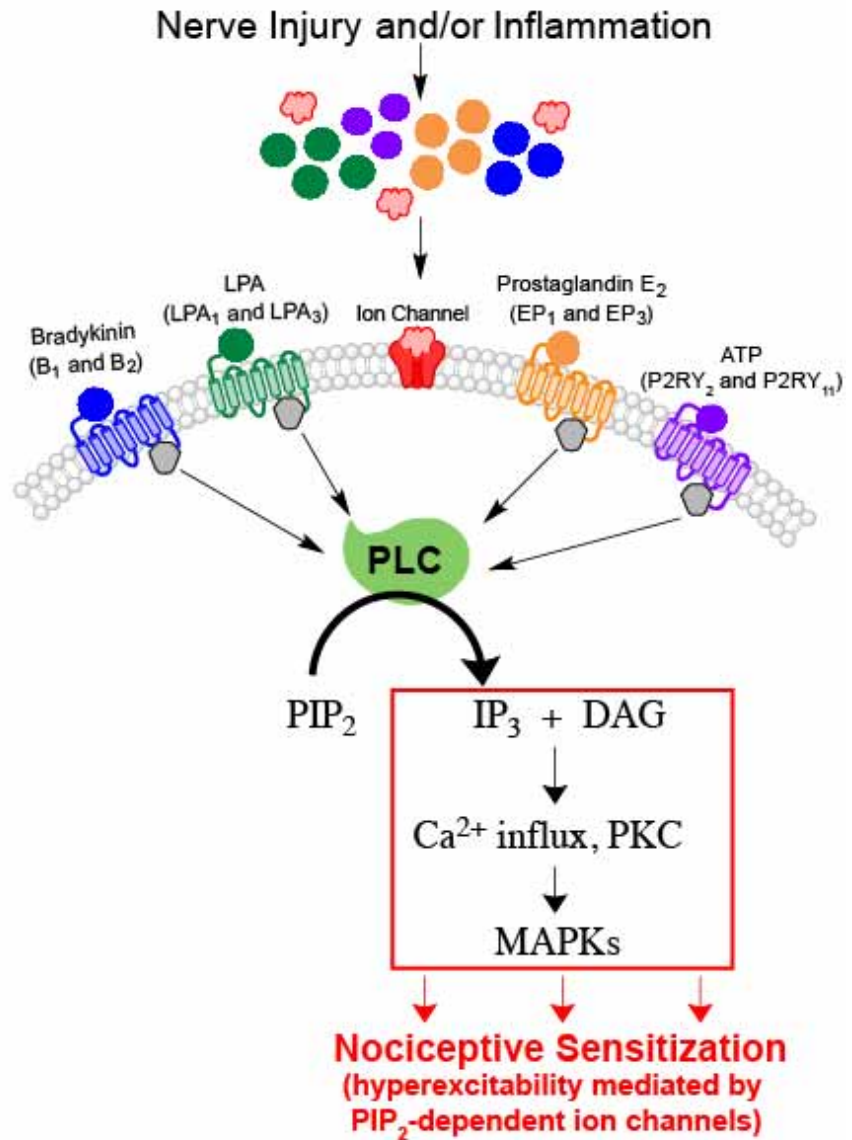
**Figure 1.1. Schematic of peripheral nociceptive circuitry.**

Dorsal root ganglion (DRG) neurons extend a bifurcated axon into the target tissue (such as the skin) and into the dorsal horn of the spinal cord to detect and process painful stimuli. Pain-sensing neuron in the DRG can be divided into two subgroups, peptidergic neurons that express calcitonin gene related peptide (CGRP) and mainly detect noxious thermal/heat stimuli and nonpeptidergic neurons that bind isolectin B4 (IB4) and primarily detect mechanical painful stimuli. This figure has been modified from Zylka et al., 2005<sup>8</sup>.

## A Nociceptive Pain



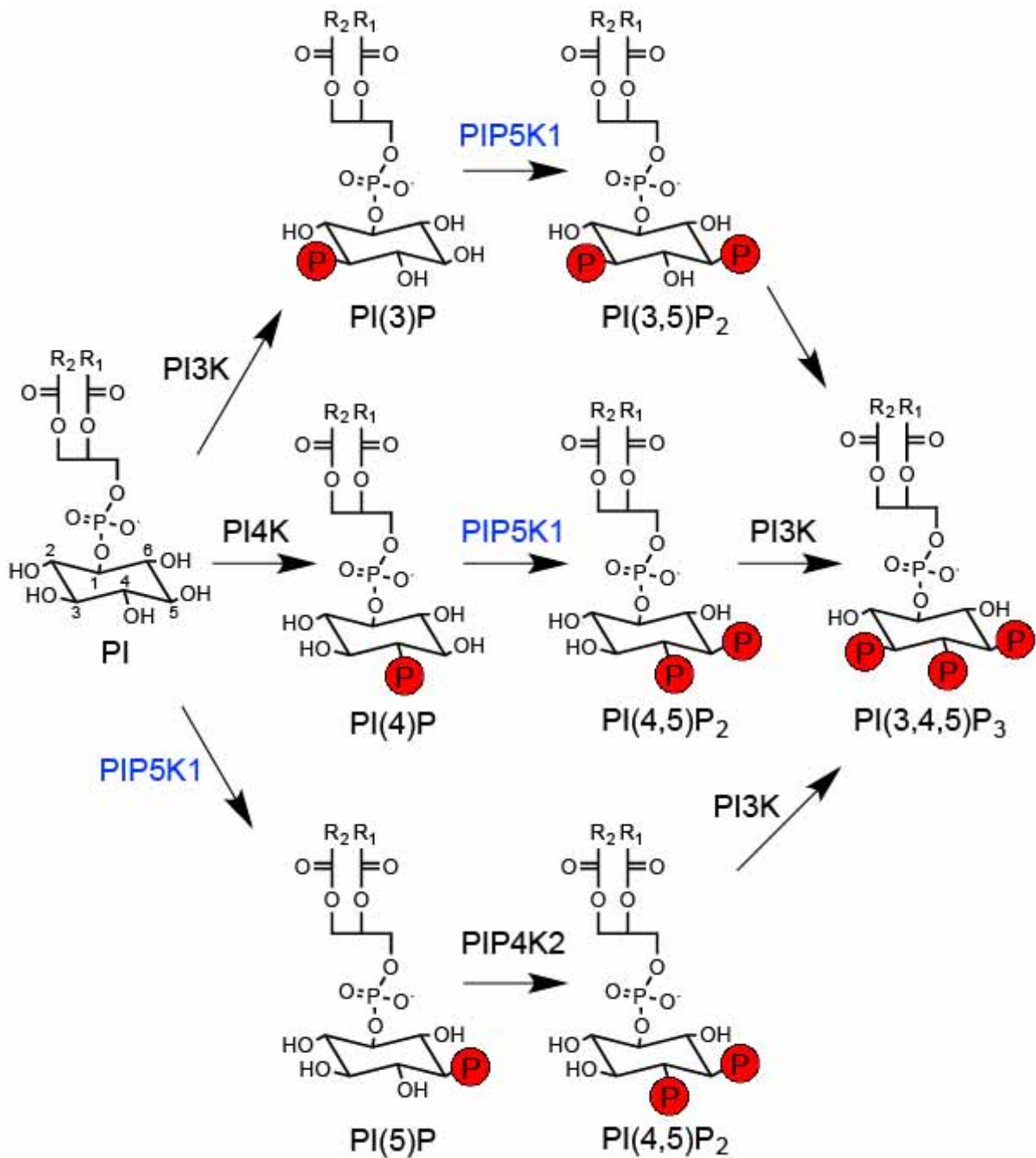
## B Neuropathic and Inflammatory Pain



**Figure 1.2. DRG-mediated nociceptive signaling in the three types of pain.**

**(A)** TRPV1-mediated signaling in nociceptive (acute, defense mechanism) pain.

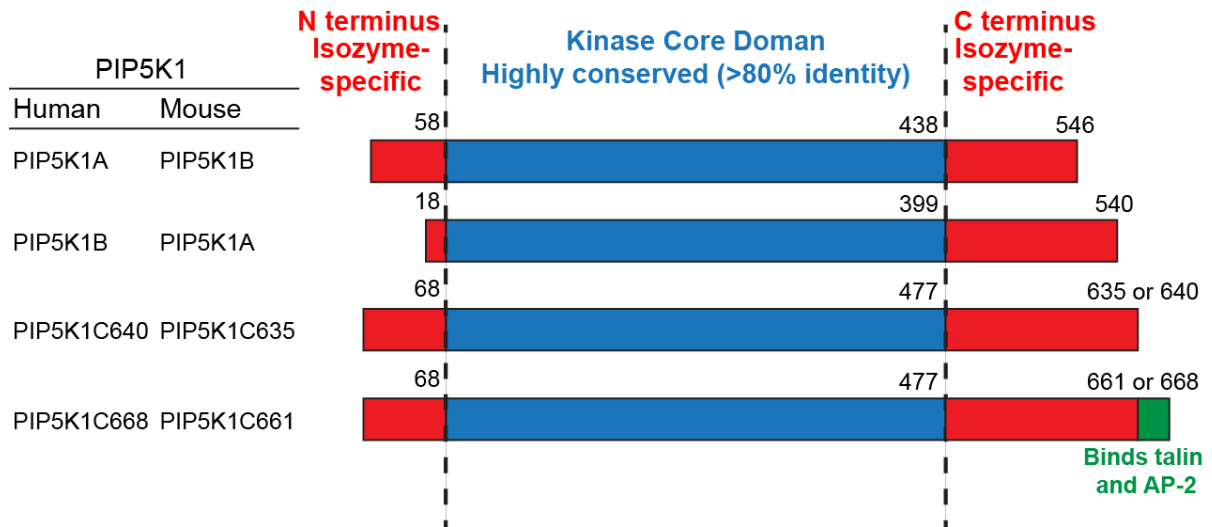
TRPV1 signaling is dependent on PIP<sub>2</sub>. **(B)** GPCR-mediated nociceptive signaling that leads to sensitization of nociceptors within the DRG. Nociceptive sensitization is dependent on PIP<sub>2</sub>-sensitive GPCRs and ion channels that mediate hyperexcitability following nerve injury and inflammation.



**Figure 1.3. Phosphatidylinositol (PI) synthetic pathways.**

PIP<sub>2</sub> is primarily synthesized from PI(4)P by type I PIP5K (blue). Kinases involved in the synthesis of all other phosphoinositides are shown. R<sub>2</sub> and R<sub>1</sub> are the fatty acid chains that make up diacylglycerol (DAG). Phosphate groups are red.





**Figure 1.4. Type I PIP5Ks.**

The three murine and human PIP5K1s have a highly conserved kinase core domain (blue). Isozyme-specific regions at the N and C termini of each protein allow for differentiated functionality within cells. PIP5K1C668/661 has a C terminal tail that is specialized in binding two cytoskeletal proteins, talin and adaptor protein-2 (AP-2).

## CHAPTER II

# PIP5K1C REGULATES PRONOCICEPTIVE SIGNALING *IN VITRO* AND NOCICEPTIVE SENSITIZATION *IN VIVO*

### Introduction

Tissue inflammation and nerve injury result in the release of a complex set of molecules that sensitize DRG neurons and contribute to chronic pain<sup>6</sup>. These molecules activate molecularly diverse pronociceptive receptors and ion channels found on the membrane of DRG neurons. While these receptors represent attractive targets for analgesic drug development, efforts to block individual pronociceptive receptors have so far failed to produce effective treatments for chronic pain<sup>3</sup>. This likely reflects the fact that multiple pronociceptive receptors and ion channels are activated during initiation and maintenance of chronic pain.

One approach to treat chronic pain that eliminates the issue of receptor diversity is to target points where different signaling pathways converge. Indeed, drugs that block signaling proteins that are several steps downstream from receptor activation, including protein kinase C $\epsilon$  (PKC $\epsilon$ ) and mitogen activated protein kinases (MAPKs), reduce nociceptive neuron sensitization, thermal hyperalgesia, and mechanical allodynia in animal models<sup>55-58</sup>. Unfortunately, drugs that inhibit MAPKs or PKC $\epsilon$  have shown modest to no efficacy in treating chronic pain in humans<sup>55, 59-61</sup>.

Ineffectiveness of these inhibitors has been attributed to several issues including trial design, subtherapeutic dosing, and inability to confirm inhibitor engagement with the target proteins.

Another convergence point, albeit one that has not been fully explored in the context of treating pain, is immediately downstream of multiple pronociceptive receptors and ion channels. Many pronociceptive receptors, including Gq-coupled receptors, Gs-coupled receptors (via EPAC), and receptor tyrosine kinases, initiate signaling upon phospholipase C (PLC)-catalyzed hydrolysis of the lipid second messenger PIP<sub>2</sub><sup>3, 6</sup>. PIP<sub>2</sub> hydrolysis produces diacylglycerol (DAG) and inositol-1,4,5-trisphosphate (IP<sub>3</sub>), which regulate nociceptive sensitization via multiple pathways, including PKC-dependent modulation of ion channels, MAPK activation, and IP<sub>3</sub>-mediated calcium influx<sup>3, 23, 62</sup>. In addition, many ion channels that detect noxious heat and regulate neuronal excitability are dependent upon PIP<sub>2</sub> for activity<sup>23, 25, 63</sup>. Thus, PIP<sub>2</sub> is a convergence point for diverse receptors, ion channels, and signaling pathways that promote and maintain nociceptive sensitization. In turn, this suggests it may be possible to reduce signaling through pronociceptive receptors and ion channels and reduce pain sensitization by inhibiting the lipid kinase(s) that generate(s) the majority of PIP<sub>2</sub> in DRG neurons.

Type 1 phosphatidylinositol 4-phosphate 5-kinases (*Pip5k1s*) generate PIP<sub>2</sub> by phosphorylating the 5 position on the inositol ring of phosphatidylinositol 4-phosphate [PI(4)P]. There are three mammalian *Pip5k1* genes (*Pip5k1a*, *Pip5k1b* and *Pip5k1c*)<sup>64</sup>. Of these, *Pip5k1c* is highly expressed in the brain<sup>46</sup>. PIP5K1C

regulates receptor-mediated calcium signaling, actin cytoskeletal dynamics, endocytosis, and exocytosis<sup>41, 46, 51, 65-67</sup>.

Previous studies examined the functions of *Pip5k1c* in the brain with knockout mice<sup>45, 51, 52, 68</sup>. Homozygous knockout mice (*Pip5k1c*<sup>-/-</sup>) have ~50% less PIP<sub>2</sub> in their brain and die within 24 hours of birth due to impaired mobility and an inability to feed<sup>45, 68</sup>. These data suggest a critical role for PIP5K1C in generating PIP<sub>2</sub> in neurons and in nervous system development. In contrast, heterozygous (*Pip5k1c*<sup>+/-</sup>) mice are viable, reproduce normally, have normal levels of PIP<sub>2</sub> in the brain and showed no phenotypes in an extensive battery of tests, including multiple tests of neurological function<sup>45, 68</sup>. The only phenotype observed thus far in *Pip5k1c*<sup>+/-</sup> mice is high-frequency (>20 kHz) hearing loss, a phenotype ascribed to *Pip5k1c* haploinsufficiency in non-sensory cells of the auditory system<sup>52</sup>.

Prior to completion of these studies, it was unknown which enzymes generated PIP<sub>2</sub> in nociceptive DRG neurons or if these enzymes regulated nociception *in vitro* or *in vivo*. Herein, we report that PIP5K1C is expressed in the majority of all DRG neurons, generates at least half of all PIP<sub>2</sub> in the DRG and regulates nociceptive sensitization in response to diverse stimuli that cause pain.

## Methods

### Animals

All procedures involving vertebrate animals were approved by the Institutional Animal Care and Use Committee at the University of North Carolina at Chapel Hill. *Pip5k1c*<sup>+/-</sup> mice were provided by Pietro de Camilli at Yale University (also available

from The Jackson Laboratory, #008515)<sup>45</sup>. Mice were genotyped using PCR on extracted tail DNA and the following primers: Neo4R, 5'-CAC CCC TTC CCA GCC TCT GA-3', PIPKRV1, 5'-CCT CAC ATC CTG CTC ACT CAG GAC C-3', and PKWT1, 5'-GCC TCA CAG AGA TTT GAC GTG TCA G-3'. *Pip5k1c*<sup>+/-</sup> mice were identified by the presence of a 650 bp knockout band (Neo4R and PIPKRV1) and a 250 bp WT band (PKWT1 and PIPKRV1). All mice were backcrossed to C57BL/6 mice for at least 10 generations.

### ***In situ* hybridization**

Mice were sacrificed using pentobarbital. Lumbar DRG were dissected from adult (6-8 weeks) male WT mice. Gene-specific probe preparation and *in situ* hybridization were completed as previously described<sup>69</sup>. Briefly, tissue was mounted in TissueTek immediately following dissection and cryosectioned at 20  $\mu$ m. Non-isotopic *in situ* hybridization was performed using digoxigenin-labeled cRNA probes for each of the three isoforms and standard nitro blue tetrazolium (NBT) and 5-bromo-4-chloro-3-indolyl phosphate (BCIP) stain. Double fluorescence *in situ* hybridization was performed by the UNC *in situ* hybridization core using previously described methods<sup>70</sup>.

### **Immunohistochemistry**

Mice were sacrificed using pentobarbital. Lumbar DRG and spinal cord were dissected from adult (6-8 week old) male mice and prepared as described previously<sup>71, 72</sup>. Briefly, tissues were immersion-fixed in 4% paraformaldehyde for 4 hours and

cryopreserved in 30% sucrose at 4°C for 3 days. Tissue was embedded in TissueTek and cryosectioned at 20 µm. Sections were immunostained thaw mounted onto SuperFrost Plus slides. The following primary antibodies were used for overnight incubations (at 4°C): sheep anti-CGRP (1:200; Enzo Life Sciences, CA1137), mouse anti-NeuN (1:250; Millipore, MAB377), and rabbit anti-PIP5K1C (1:200, generously provided by Hiroyuki Sakagami). Fluorescently conjugated secondary antibodies were purchased from Invitrogen and were used at 1:200 for 2 hours at room temperature. Alexa-conjugated Isolectin IB4 (1:1000; Invitrogen) was added to the secondary antibody incubation. All staining solutions were made in Tris-buffered saline containing Triton (0.05 M Tris, 2.7% NaCl, 0.3% Triton-X 100, pH 7.6). All images were obtained using a confocal microscope (Zeiss LSM 510).

### **Immunocytochemistry**

Biotinylated PIP<sub>2</sub> primary antibody was purchased from Echelon Biosciences (Z-B045) and used according to the manufacturer's instructions. All PIP<sub>2</sub> staining was completed at 37°C with Tris-buffered saline (50 mM Tris and 150 mM NaCl at pH 7.4). Chicken anti-NeuN (1:250; Aves) was added to the primary incubation. Alexa-conjugated streptavidin (1:2000; Invitrogen) and fluorescently labeled anti-chicken antibodies (1:1000; Invitrogen) were used for secondary detection. For evaluation of cytoskeletal dynamics, rabbit anti beta III tubulin (1:500, Abcam), and mouse anti-NeuN (1:250, Millipore) primary antibodies were used overnight at 4°C. Fluorescently conjugated secondary antibodies and fluorescently conjugated phalloidin were used at 1:1000 for 2 hours at room temperature. All solutions for

cytoskeletal staining were made in phosphate buffered saline (PBS) containing 0.3% Triton, 3% BSA, and 0.1% sodium azide. Additionally 10% normal goat serum was added to the primary antibody solution. All images were obtained using a Leica TCS-SL confocal microscope.

### **Western blot analysis**

Following decapitation, lumbar DRG (L3-L5, bilateral), lumbar spinal cord, and brain (frontal cortex) were dissected from adult male mice (6-8 weeks old) and embryos (E17.5-18.5). Tissue lysates were prepared in radioimmunoprecipitation buffer (RIPA) buffer (50 mM Tris, 1% Triton X-100, 0.25% sodium deoxycholate, 0.1% sodium dodecyl sulfate, 1 mM ethylenediaminetetraacetic acid and 150 mM sodium chloride) containing protease inhibitors (Roche Complete Mini Tablets, 11836153001 and 1 mM phenylmethylsulfonyl fluoride) and separated by sodium dodecyl sulfate polyacrylamide gel electrophoresis (SDS-PAGE). Gels were transferred onto polyvinylidene fluoride (PVDF) membranes and blocked with 5% dry milk (BioRad). Primary antibodies were prepared in Tris buffered saline with Triton (100 mM Tris, 165 mM sodium chloride, and 0.1% Tween 20) containing 5% BSA. PIP5K1C antibody (1:500) was a generous gift from P. De Camilli. Anti- $\beta$ -actin (1:3000; Abcam) served as a loading control. Secondary antibodies (1:10,000; Li-Cor IRDye 680 and 800) were prepared in TBS-T containing 5% dry milk.

### **ELISA PIP<sub>2</sub> quantification**

PI(4,5)P<sub>2</sub> mass enzyme-linked immunosorbent assay (ELISA) was purchased

from Echelon Biosciences (K-4500) and performed according to the manufacturer's instructions with the following alterations. Lumbar DRG (L3-L5, bilateral), lumbar spinal cord and cerebral cortex were dissected from adult male mice (6-8 weeks old) and frozen immediately on dry ice. All DRG were dissected from embryos (E17.5-18.5) and frozen immediately on dry ice. Tissue was homogenized and sonicated prior to lipid extraction. DRG samples were diluted 1:40 and spinal cord and brain samples were diluted 1:200 prior to use in the ELISA assay. Bicinchoninic acid (BCA) protein determination assay (ThermoScientific, 23225) was completed for each sample following the manufacturer's instructions. Protein content for each sample was used for normalization.

### **Neuron culture**

All DRG were dissected from 3-8 week old male mice following decapitation. Neurons were dissociated with manual trituration using a fire polished Pasteur pipette in a solution of 2 mg/mL collagenase (Worthington, CLS1) and 5 mg/mL dispase (Gibco, 17105-041). Neurons were cultured with Neurobasal A medium (Gibco, 10888) supplemented with 2% B27 (Gibco, 17504), 2 mM L-glutamine (Gibco, 25030), 1% penicillin/streptomycin (Gibco, 15140), 50 ng/mL glial derived neurotrophic factor (GDNF; Millipore, GF030) and 25 ng/mL nerve growth factor (NGF; Millipore, 01-125) in the absence of serum. Neurons were plated onto coverslips coated with 1 mg/mL poly-D-lysine (Sigma, P7886) and 10 µg/mL laminin (Sigma, L2020) and cultured for 18-24 hours prior to use.



## Calcium imaging

Calcium imaging of dissociated neurons was completed as described previously using Fura 2-acetoxymethyl ester (2  $\mu$ M; F1221, Invitrogen)<sup>73</sup>. Briefly, neurons were incubated with 2  $\mu$ M Fura 2-AM for 60' followed by 30' incubation with Hanks buffered saline solution (HBSS) prior to carrier/PIP<sub>2</sub> incubation. Neurons were then incubated with either carrier alone (2  $\mu$ M; Echelon Biosciences, P-9C2) or carrier + PIP<sub>2</sub> (2  $\mu$ M; Echelon Biosciences, P-4516) for 15 minutes prior to imaging. Carrier and PIP<sub>2</sub> complexes were formed by incubating together in HBSS at room temperature for 15 minutes prior to use. LPA (10  $\mu$ M; Avanti Polar Lipids, 857130), 17-PT-PGE<sub>2</sub> (10  $\mu$ M; Cayman Chemical 14810), Capsaicin (1  $\mu$ M; Sigma M2028) and KCl (100 mM; Fisher P330) were used for neuron stimulation.

## Electrophysiology

Recordings in DRG neurons were carried out as previously described<sup>74</sup>. Briefly, small (15-20  $\mu$ m), presumably nociceptive, DRG neurons were identified using an epifluorescence microscope (Nikon Eclipse FN1) equipped with IR-DIC optics, and visualized with a 40X water-immersion objective (NIR Apo 40X/0.80W, Nikon). DRG neurons were perfused at 2 mL/min with a bath solution that contained (in mM): 10 HEPES, 140 NaCl, 4 KCl, 2 MgCl<sub>2</sub>, 2 CaCl<sub>2</sub>, 5 glucose at pH 7.4, 300 mOsm. The electrode solution contained (in mM): 130 potassium gluconate, 5 NaCl, 1 MgCl<sub>2</sub>, 1 EGTA, 10 HEPES, 4 NaATP, with pH adjusted to 7.3 with KOH, and an osmolarity of 295 mOsm. For some experiments, PIP<sub>2</sub>-diC<sub>8</sub> (10  $\mu$ M) was added to the pipette solution. Patch pipettes made from borosilicate glass were pulled to a tip

resistance of 3-6 M $\Omega$  with a Sutter P-2000 electrode puller. Whole-cell, current clamp recordings were carried out using a Multiclamp 700B amplifier, and captured at 10kHz with an Axon Digidata 1440A and pClamp 10 software.

Field recordings in transverse mouse spinal cord slices were carried out as previously described<sup>75</sup>. Mouse spinal cords were dissected and sliced (800-900  $\mu$ m) at 4°C in buffer that contained (in mM): 87 NaCl, 2.5 KCl, 1.25 NaH<sub>2</sub>PO<sub>4</sub>, 25 NaHCO<sub>3</sub>, 0.5 CaCl<sub>2</sub>, 7 MgCl<sub>2</sub>, 75 sucrose, 10 glucose, 1.5 ascorbic acid. The tissue was continuously bubbled with 95%O<sub>2</sub>/5%CO<sub>2</sub>. Slices were incubated at 35°C for 45 minutes in artificial cerebrospinal fluid (ACSF) that contained (in mM) 125 NaCl, 2.5 KCl, 1.25 NaH<sub>2</sub>PO<sub>4</sub>, 26 NaHCO<sub>3</sub>, 2.5 CaCl<sub>2</sub>, 1.5 MgCl<sub>2</sub>, 25 glucose. The slices were then transferred to the recording chamber and the dorsal root was suctioned into a glass electrode in order to stimulate all sensory afferents. Field potential electrodes were pulled from borosilicate glass on a Sutter P-97 puller to a tip resistance of 1-2 M $\Omega$ . The field electrode was placed in lamina II then the dorsal root was stimulated for 0.5 ms at 5x the intensity needed to evoke a maximal response. The resulting signals were filtered at 1 kHz, amplified 1000 times, and captured at 10 kHz. Stimulus strength was then increased (0.1 Hz, repeated five times at each stimulus strength). To assess synaptic depletion and recovery, a maximal strength stimulus was presented to the slices at 10 Hz for 100 trials. Immediately after synaptic depletion stimulation, the slices were then stimulated at the same maximal stimulus strength, but at a frequency of 0.1 Hz for 15 minutes to measure fEPSP amplitude.

## **Rodent models of nociceptive and chronic pain**

This dissertation will use four rodent models of pain that have been designed to mimic human nociceptive, inflammatory, and neuropathic pain. To investigate nociceptive pain (detection of noxious stimuli as a defense mechanism), we will use noxious heat (>43°C) applied to rodent's hindpaw<sup>10, 72, 76</sup>. To investigate inflammatory pain, we will use the complete Freund's adjuvant (CFA) induced inflammatory pain model<sup>72</sup>. Two neuropathic pain models will be used: the spared nerve injury (two branches of the sciatic nerve are severed) and Lysophosphatidic acid (LPA) chemically induced neuropathic pain model<sup>38, 39, 77, 78</sup>. Radiant heating (Hargreaves method) will be used to assess thermal hyperalgesia and mechanical von Frey testing will be used to assess mechanical allodynia in the rodent models of chronic pain<sup>79, 80</sup>.

## **Behavioral assays**

Pronociceptive ligands (4.1 µg LPA; 1.2 µg 17-PT-PGE<sub>2</sub>, in 0.9% saline) were injected into the left hindpaw and the amount of time spent licking was measured for 5 minutes. Thermal sensitivity was measured using a Plantar Test apparatus (IITC) to heat each hindpaw and the latency for hindpaw removal was recorded. One measurement was taken for each hindpaw to determine the withdrawal latency in seconds. The radiant heat source intensity was calibrated so that the average withdrawal latency for WT mice was ~10 s. Cut off time was 20 s. Mechanical sensitivity was measured using an electronic von Frey apparatus (IITC) and a semi-flexible tip. Three measurements for each hindpaw were taken and averaged to

determine the withdrawal threshold in grams. Inflammatory (CFA) and neuropathic (LPA and spared nerve injury) models of chronic pain were performed as described previously<sup>71, 77, 78</sup>. Intrathecal injections (5  $\mu$ L) were performed in unanesthetized mice using the direct lumbar puncture method<sup>81</sup>. For the hot plate assay, the mice were restrained by scruffing and one hindpaw was placed on a metal surface of a given temperature (45°, 50°C, or 55°C). The latency for the animal to remove or shake the hindpaw was recorded once per animal per temperature. At least 30 minutes elapsed between measuring each temperature. Cut off was 20 seconds for all temperatures. The cotton swab assay was used to measure innocuous mechanical sensitivity<sup>82</sup>. For rotarod testing, the animals were placed on a rotating rod and the latency to fall off was recorded. Gait measurements were taken by painting the hindpaws with ink and allowing the mice to walk in a straight line down an enclosed runway. Stride was measured as the distance (in cm) between the left hindpaws (5 measurements per animal were averaged). Stance was measured as distance (in cm) between the left hindpaw and the subsequent step of the right hindpaw (5 measurements per animal were averaged). For all behavioral assays, mice were habituated to the testing apparatus/method and experimenter for 3-5 days prior to performing the assay.

## Results

### **PIP5K1C generates at least half of all PIP<sub>2</sub> in DRG neurons**

To determine which Type 1 *Pip5ks* were expressed in the DRG, we performed *in situ* hybridization with probes for the three known mammalian *Pip5k1*

genes. We found that *Pip5k1c* was expressed at higher levels in adult DRG than the other *Pip5k1* genes and was present in nearly all DRG neurons (Figure 2.1A-2.1C). PIP5K1C is also present in the brain at higher levels than PIP5K1A and PIP5K1B<sup>46</sup>. Consistent with widespread expression in all DRG neurons, we found that *Pip5k1c* was expressed in virtually all peptidergic (96.7%; n=220 counted) and nonpeptidergic (96.1%; n=210 counted) nociceptive neurons, marked by calcitonin gene-related peptide-alpha (*Cgrpa*) and Prostatic acid phosphatase (*Acpp*), respectively (Figure 2.1D and 2.1E)<sup>71, 72</sup>. Using a recently developed antibody to the c1 isoform<sup>83</sup>, we found that PIP5K1C was present on the plasma membrane and intracellular membranes of most DRG neurons (Figure 2.1F and 2.1G).

We next tested the extent to which PIP5K1C generated PIP<sub>2</sub> in DRG using *Pip5k1c* knockout mice and a competitive binding enzyme-linked immunosorbent assay (ELISA) for PIP<sub>2</sub><sup>45, 51, 84</sup>. We quantified PIP5K1C protein and PIP<sub>2</sub> levels in the DRG of wild-type (WT; *Pip5k1c*<sup>+/+</sup>), *Pip5k1c*<sup>+/-</sup>, and *Pip5k1c*<sup>-/-</sup> embryonic (E17.5-E18.5) mice. We found that PIP5K1C protein and PIP<sub>2</sub> levels were reduced (by ~50%) in the DRG of *Pip5k1c*<sup>+/-</sup> embryonic mice (Figure 2.2A-2.2C). No PIP5K1C protein was detectable in DRG from *Pip5k1c*<sup>-/-</sup> embryonic mice, confirming complete gene deletion and antibody specificity (Figure 2.2A and 2.2B). In addition, PIP<sub>2</sub> was reduced by ~70% in DRG from *Pip5k1c*<sup>-/-</sup> embryonic mice (2.2C), suggesting PIP5K1C generates the majority of all PIP<sub>2</sub> in DRG, at least in embryonic mice.

*Pip5k1c*<sup>+/-</sup> mice live into adulthood and reproduce normally<sup>45</sup>. Therefore, we quantified PIP5K1C protein and PIP<sub>2</sub> levels in the DRG from *Pip5k1c*<sup>+/-</sup> adult mice and WT littermate controls. PIP5K1C protein was reduced by ~40% and PIP<sub>2</sub> levels

were reduced by ~50% in the DRG of adult *Pip5k1c*<sup>+/-</sup> mice (Figure 2.3A-2.3C). In contrast, PIP<sub>2</sub> was not significantly reduced in spinal cord or brain from adult *Pip5k1c*<sup>+/-</sup> mice (Figure 2.3C). Likewise, others reported that PIP<sub>2</sub> was not reduced in the brain of embryonic *Pip5k1c*<sup>+/-</sup> mice using a different quantification method<sup>45, 51</sup>. In addition, we used immunofluorescence staining to examine PIP<sub>2</sub> levels at the membrane of cultured adult DRG neurons. Quantification of the average perimeter (membrane) staining intensity in confocal images revealed that membrane PIP<sub>2</sub> levels were reduced by ~50% in small-to-medium diameter ( $\leq 27 \mu\text{m}$ ) neurons of *Pip5k1c*<sup>+/-</sup> mice compared to WT controls (Figure 2.3C and 2.3D). Taken together, our data indicate that PIP5K1C generates at least half of all PIP<sub>2</sub> in the DRG, including small-to-medium diameter, presumably nociceptive, DRG neurons. Moreover, our data indicate that PIP<sub>2</sub> is selectively reduced in DRG of *Pip5k1c*<sup>+/-</sup> adult mice, but is not reduced in other regions of the nervous system that processes pain and somatosensory stimuli, including spinal cord and brain.

### ***Pip5k1c* haploinsufficiency attenuates TRPV1-mediated calcium signaling**

Since PIP<sub>2</sub> was reduced by 50% at the membrane of *Pip5k1c*<sup>+/-</sup> DRG neurons, we hypothesized that pronociceptive GPCRs and ion channels that require PIP<sub>2</sub> for activity would signal less efficiently in DRG neurons of *Pip5k1c*<sup>+/-</sup> mice. We began our signaling studies by focusing on TRPV1, the nonselective cation channel that mediates detection of noxious heat (“heat pain”) and is stimulated by capsaicin, the active ingredient in chili peppers<sup>76</sup>. As mentioned previously, we use TRPV1-mediated assays to investigate acute nociceptive pain *in vivo* using noxious thermal

assays; however, *in vitro* we use the potent agonist, capsaicin to study activity of the channel. It is well known that PIP<sub>2</sub> regulates TRPV1 signaling; although, the mechanism by which it regulates the channel is highly debated<sup>14-16, 63, 85</sup>. Regardless, we sought to determine the extent to which TRPV1 signaling was effected in *Pip5k1c*<sup>+/-</sup> neurons. We monitored capsaicin-evoked calcium responses in small diameter (≤27 μm) DRG neurons using the ratiometric calcium (Ca<sup>2+</sup>) indicator dye, Fura 2-AM. Potassium chloride (KCl) activates neuron-specific voltage-gated calcium channels and was used to distinguish neurons from other cell types in the culture and to assess cell health. We observed a ~40% reduction in TRPV1-evoked calcium responses (quantified as area under the curve of the capsaicin-evoked response in each responding neuron) in *Pip5k1c*<sup>+/-</sup> neurons compared to WT neurons (Figure 2.4A and 2.4B). Importantly, calcium responses were fully restored to WT levels when excess PIP<sub>2</sub> was delivered to *Pip5k1c*<sup>+/-</sup> neurons prior to imaging; indicating signaling deficits in *Pip5k1c*<sup>+/-</sup> neurons are PIP<sub>2</sub>-dependent (Figure 2.4A and 2.4B). There were no deficits observed in KCl-evoked responses further supporting the notion that deficits in *Pip5k1c*<sup>+/-</sup> neurons are due to PIP<sub>2</sub> reductions and not due to poor cell health (Figure 2.4A and 2.4B). Collectively, these data show that TRPV1-mediated signaling in *Pip5k1c*<sup>+/-</sup> DRG neurons is blunted via a PIP<sub>2</sub>-dependent mechanism and led us to hypothesize that TRPV1-mediated detection of noxious heat *in vivo* may also be reduced in *Pip5k1c*<sup>+/-</sup> mice.

### ***Pip5k1c* haploinsufficiency reduces acute thermal sensitivity presumably mediated by TRPV1**

To test this hypothesis, we evaluated withdrawal latencies of the hindpaw in *Pip5k1c*<sup>+/-</sup> and WT mice at noxious temperatures that require TRPV1 for detection (>43°C) in our model of acute nociceptive pain. *Pip5k1c*<sup>+/-</sup> mice had significantly increased withdrawal latencies compared to WT mice at all three noxious temperatures tested, 45°, 50°, and 55°C (Figure 2.4C). These data suggest that TRPV1 functions less efficiently *in vivo*, at least when detecting noxious heat. However, when capsaicin (2 µg) was injected into the hindpaw of *Pip5k1c*<sup>+/-</sup> and WT mice and nocifensive licking was monitored for 5 minute following injection, there was no difference in time spent licking between *Pip5k1c*<sup>+/-</sup> and WT mice (data not shown). Differing mechanisms of noxious heat activation of TRPV1 and agonist activation (capsaicin) of TRPV1 may explain the discrepancies observed in the *in vivo* thermal assay and nocifensive licking assay<sup>86</sup>. Additional testing at various concentrations of capsaicin (to obtain dose-response relationships) may be beneficial in evaluating differences in WT and *Pip5k1c*<sup>+/-</sup> mice. Collectively, these data suggest that TRPV1-mediated detection of noxious heat is blunted in *Pip5k1c*<sup>+/-</sup> mice; however, the extent to which capsaicin-induced acute nociceptive pain is altered is less clear and requires further investigation.

### ***Pip5k1c* haploinsufficiency attenuates pronociceptive GPCR signaling**

Nerve injury and inflammation release a complex set of molecules that activate GPCRs and lead to sensitization of DRG neurons. These GPCRs are



dependent on PIP<sub>2</sub> for activity. Since PIP<sub>2</sub> levels in the membrane were reduced by ~50% in DRG neurons, we hypothesized that pronociceptive GPCRs that couple to phospholipases and PIP<sub>2</sub> hydrolysis would signal less effectively in *Pip5k1c*<sup>+/-</sup> mice. To test this hypothesis we used the same calcium-imaging assay described above to quantify lysophosphatidic acid (LPA) and 17-phenyl trinor prostaglandin E<sub>2</sub> (17-PT PGE<sub>2</sub>) evoked calcium responses in small diameter DRG neurons. LPA evokes Ca<sup>2+</sup> influx in small-to-medium diameter DRG neurons and, when injected intrathecally (i.t.), produces a chemically-induced form of neuropathic pain that is dependent on LPA1 receptor activation<sup>38, 39</sup>. 17-PT PGE<sub>2</sub> is a selective agonist for G<sub>q</sub>-coupled prostanoid receptors, a class of receptors that are implicated in pain hypersensitivity following inflammation<sup>87-90</sup>. Following stimulation with LPA or 17-PT PGE<sub>2</sub>, calcium responses (quantified as area under the curve) were blunted in *Pip5k1c*<sup>+/-</sup> neurons compared to WT controls (Figure 2.5A-2.5D). Importantly, these signaling deficits could be fully restored to WT levels by delivering excess PIP<sub>2</sub> into *Pip5k1c*<sup>+/-</sup> neurons just prior to imaging (Figure 2.5A-2.5D). These data strongly suggest that the signaling deficits observed in *Pip5k1c*<sup>+/-</sup> neurons were the result of reduced PIP<sub>2</sub> levels and were not due to poor cell health or PIP<sub>2</sub>-independent signaling deficits. Moreover, KCl-evoked Ca<sup>2+</sup> responses were not altered, further indicating deficits were not due to cell health (Figure 2.5A, data not shown). Importantly, LPA or 17 PT-PGE<sub>2</sub>-evoked calcium responses in non-neuronal cells was not reduced, suggesting neuronal-specific deficits. The percentage of neurons responding to either ligand (LPA responders: mean 22.2 ± 2.9% for WT and 24.1 ± 3.7% for *Pip5k1c*<sup>+/-</sup>; 17-PT PGE<sub>2</sub> responders: 6.0 ± 1.2% for WT and 4.7 ± 1.1% for

*Pip5k1c*<sup>+/-</sup>) and the average diameter of responding neurons was not significantly different between WT and *Pip5k1c*<sup>+/-</sup> cultures (data not shown). We also found that delivering excess PIP<sub>2</sub> into WT neurons did not elevate LPA or 17-PT PGE<sub>2</sub> evoked calcium responses beyond control levels, suggesting that PIP<sub>2</sub> levels are already saturated in WT neurons under our culture conditions. Collectively, our data reveal that PIP5K1C regulates signaling downstream from two pronociceptive receptors, one associated with neuropathic pain and the other with inflammatory pain. Moreover, rescue experiments revealed that *Pip5k1c* regulates calcium signaling in DRG neurons via a PIP<sub>2</sub>-dependent mechanism, placing PIP5K1C upstream of multiple signaling pathways implicated in peripheral sensitization.

### ***Pip5k1c* haploinsufficiency reduces ligand-induced nocifensive behaviors**

LPA and 17-PT PGE<sub>2</sub> induce GPCR-mediated nociceptive responses when injected into the hindpaw and serve as a model of acute ligand-mediated nociceptive pain<sup>87, 91</sup>. To determine if these compounds signal less effectively in *Pip5k1c*<sup>+/-</sup> mice, we injected LPA (4.1 µg) or 17-PT PGE<sub>2</sub> (1.2 µg) into one hindpaw then monitored duration of licking for 5 minutes. We found that *Pip5k1c*<sup>+/-</sup> mice spent less time licking their ligand-injected hindpaws when compared to WT littermate controls (Figure 2.5E), indicating reduced nociceptive responses to noxious chemical stimuli.

## ***Pip5k1c* haploinsufficiency attenuates ion channel-mediated neuronal excitability**

In addition to regulating GPCR and TRPV1 activity that mediates nociceptive sensitization, PIP<sub>2</sub> is also required for a variety of ion channels that modulate neuronal excitability and more importantly, hyperexcitability following nerve injury and inflammation. Since membranous PIP<sub>2</sub> was reduced by ~50% and PIP<sub>2</sub>-dependent GPCR and TRPV1 signaling was reduced in *Pip5k1c*<sup>+/-</sup> neurons, we hypothesized that PIP<sub>2</sub>-dependent ion channel activity would also be attenuated. To test this hypothesis, we first examined intrinsic neuronal excitability, which is mediated by a variety of PIP<sub>2</sub>-dependent ion channels<sup>23, 26, 62</sup>. We assessed intrinsic excitability using whole cell recordings and quantified action potential firing rates (spikes per second) following current injections from 50 to 250 pA in small diameter (capacitance <20 pF; presumably nociceptive) neurons cultured from adult *Pip5k1c*<sup>+/-</sup> and WT mice. We observed that *Pip5k1c*<sup>+/-</sup> neurons were significantly less excitable (~30% reduction) at current injections ≥100 pA compared to neurons cultured from WT mice (Figure 2.6A and 2.6B). The addition of PIP<sub>2</sub> to the internal pipette solution completely restored excitability of *Pip5k1c*<sup>+/-</sup> neurons to WT levels suggesting that deficits in neuronal excitability are a direct result of decreased PIP<sub>2</sub> levels (Figure 2.6A and 2.6B). These data are consistent with reduced activity of ion channels that mediate excitability through PIP<sub>2</sub> dependent mechanism(s)<sup>26</sup>.

### ***Pip5k1c* haploinsufficiency alters actin and tubulin cytoskeletal dynamics**

PIP<sub>2</sub> is also important for actin assembly and polymerization at the membrane via interactions with actin binding proteins, such as ezrin 2 and vinculin<sup>92</sup>.

Furthermore, PIP5K1C facilitates actin organization at the membrane via interactions with the protein, talin<sup>93</sup>. Thus, we investigated filamentous actin (F-actin) staining at the membrane in *Pip5k1c*<sup>+/-</sup> and WT neurons using phalloidin, a specific antibody for F-actin (Figure 2.7A). Quantification of the membrane to cytoplasm ratio of F-actin in dissociated DRG neurons revealed that *Pip5k1c*<sup>+/-</sup> neurons have decreased membrane F-actin compared to WT neurons (Figure 2.7B). This finding is consistent with previous findings that sequestration of PIP<sub>2</sub> using a pleckstrin homology domain of phospholipase Cδ (PLCδ-PH) reduced filamentous actin at the membrane<sup>65</sup>. Actin organization at the cell membrane was partially restored in *Pip5k1c*<sup>+/-</sup> neurons incubated with PIP<sub>2</sub> suggesting that PIP5K1C regulates actin organization via mechanism(s) that are both independent of and dependent upon catalytic activity (data not shown).

Tubulin, the main constituent of cytoskeletal microtubules, also directly interacts with PIP<sub>2</sub> to regulate stability and functionality of ion channels at the membrane and PLC-catalyzed GPCR signaling<sup>29, 32, 33</sup>. Therefore, we sought to determine the extent to which tubulin was affected as a result of *Pip5k1c* haploinsufficiency and resulting reductions in PIP<sub>2</sub>. Immunocytochemical analysis with an antibody specific for neuronal beta III tubulin revealed that tubulin protein expression is increased by ~35% in *Pip5k1c*<sup>+/-</sup> neurons compared to WT controls (Figure 2.7C and 2.7D). A similar increase was observed at the RNA level using

high-throughput RNA sequencing (RNAseq; 30.6% increase; data not shown). Notably, genes that increased by at least 50% in *Pip5k1c*<sup>+/-</sup> DRG compared to WT DRG were clustered using the database for annotation, visualization, and integrated discover (DAVID). The top gene cluster (most enriched functional-related gene group) were genes involved in the cytoskeleton and contractile fibers (data not shown). Due to the availability of antibodies, we focused our immunocytochemical investigation of the cytoskeleton on actin and tubulin. Taken together, our immunocytochemical and RNA sequencing data suggest that *Pip5k1c* haploinsufficiency increases tubulin expression. Furthermore, taken together with our actin data, these data indicate that at least two important cytoskeletal proteins are altered as a result of *Pip5k1c* haploinsufficiency.

Collectively, our in vitro studies with ion channels and GPCR-mediated calcium signaling, cytoskeletal filament makers, and neuronal excitability reveal that *Pip5k1c* centrally regulates pronociceptive signaling via PIP<sub>2</sub>-dependent mechanism(s) (Figure 2.8). These data suggest that any one or combination of these deficits would result in reductions in nociceptive sensitization in models of chronic pain (Figure 2.8).

### ***Pip5k1c* haploinsufficiency attenuates thermal and mechanical sensitization in models of chronic pain**

Since pronociceptive receptors and ion channels signaled less effectively in DRG neurons, we hypothesized that thermal and mechanical sensitization would be blunted in *Pip5k1c*<sup>+/-</sup> mice following inflammation or injury. Indeed, it is well

established that pronociceptive receptor activation can sensitize animals to noxious thermal and mechanical stimuli<sup>3,6</sup>. Thermal hyperalgesia and mechanical allodynia were enduringly attenuated in *Pip5k1c*<sup>+/-</sup> mice in models of chemically induced neuropathic pain (i.t. injection of 1 nmol LPA), neuropathic pain caused by spared nerve ligation and inflammatory pain following an intraplantar injection of complete Freund's adjuvant (CFA) (Figure 2.9A-F). There were no significant differences in the contralateral (non-inflamed/non-injured) paw between WT and *Pip5k1c*<sup>+/-</sup> mice, and there were no significant differences in either paw at baseline (i.e. prior to LPA injection, nerve injury, or inflammation). Taken together, these data suggest that *Pip5k1c* regulates nociceptive sensitization in three different models (and two types) of chronic pain, with initiating events at three different anatomical locations (spinal, peripheral nerves and hindpaw).

**Phenotypes of *Pip5k1c*<sup>+/-</sup> are not due to motor impairment, loss of nociceptive neurons, or synaptic transmission deficits.**

The observed behavioral phenotypes were not due to motor impairment, as there were no significant differences between WT and *Pip5k1c*<sup>+/-</sup> mice in the rotarod assay (Figure 2.10A). Additionally gait (stride or stance) and responses to mechanical stimuli (innocuous touch and von Frey filaments) were not impaired in *Pip5k1c*<sup>+/-</sup> mice (Figure 2.10B-D).

These behavioral phenotypes were not due to a developmental loss of nociceptive neurons or terminals in spinal cord of *Pip5k1c*<sup>+/-</sup> mice (quantified by immunostaining for CGRP and IB4-binding, markers of nociceptive neurons; Figure

2.11A-J). Moreover, these phenotypes were not due to impaired excitatory synaptic transmission between sensory neurons and spinal dorsal horn neurons, assessed by measuring excitatory field potential (fEPSP) amplitude in spinal cord slices after stimulating the dorsal root with a suction electrode<sup>75</sup>. Specifically, we found no significant differences between genotypes in fEPSP amplitude at different stimulus strengths (Figure 2.11K), following synaptic depletion (Figure 2.11L and 2.11M) or during synaptic recovery (Figure 2.11N). These data also ruled out the possibility that synaptic transmission or synaptic vesicle trafficking was impaired in *Pip5k1c*<sup>+/-</sup> mice. Instead, our data suggest that the observed behavioral phenotypes reflect attenuated PIP<sub>2</sub>-dependent molecular mechanism(s).

## Discussion

Nerve injury and inflammation result in peripheral nociceptive sensitization via activation and modulation of pronociceptive receptors and ion channels that regulate neuronal excitability<sup>3, 6, 10, 11</sup>. Although these receptors and ion channels depend on PIP<sub>2</sub> for activity and previous data suggested that reductions in PIP<sub>2</sub> could reduce nociceptive sensitization<sup>84</sup>, it was unknown which kinase was responsible for the majority of PIP<sub>2</sub> production in nociceptive neurons. Our studies with *Pip5k1c*<sup>+/-</sup> mice reveal that PIP5K1C is the predominant PIP<sub>2</sub> synthesizing enzyme and generates at least half of the PIP<sub>2</sub> in the DRG. Our studies provide the first evidence that reductions in the catalytic activity of PIP5K1C attenuate pronociceptive signaling and nociceptive sensitization in rodent models of chronic pain. Importantly, our *in vitro*

studies with cultured DRG neurons reveal that PIP5K1C regulates at least three different mechanisms of pronociceptive signaling via PIP<sub>2</sub>-dependent processes.

Furthermore, our studies reveal that *Pip5k1c* haploinsufficiency selectively reduces PIP<sub>2</sub> in adult DRG without altering PIP<sub>2</sub> levels in adult brain or spinal cord making it unlikely that PIP<sub>2</sub>-dependent reduction in thermal and mechanical nociceptive sensitization in rodent models of chronic pain is due to PIP<sub>2</sub> decreases in other regions of the nervous system. In support of this, previous studies by Di Paolo et al. indicated there were no synaptic transmission deficits in *Pip5k1c*<sup>+/-</sup> cortical neurons. Furthermore, our *in vitro* studies reveal attenuated GPCR- and TRPV-mediated calcium signaling and ion channel-mediated neuronal excitability in DRG neurons and no deficits in synaptic transmission in the spinal cord. Taken together, these data support the hypothesis that reduced PIP5K1C and subsequent reductions in PIP<sub>2</sub> in the DRG are responsible for the antinociceptive phenotypes observed in *Pip5k1c*<sup>+/-</sup> mice.

Thermal and mechanical sensitization following LPA-induced neuropathic pain was prevented in *Pip5k1c*<sup>+/-</sup> mice. In contrast, our studies did not show that sensitization could be blocked entirely (maintain baseline withdrawal latency and threshold) in *Pip5k1c*<sup>+/-</sup> mice following SNI or CFA. This could reflect the fact that GPCR- and ion channel-mediated signaling was reduced, but not eliminated, in neurons from *Pip5k1c*<sup>+/-</sup> mice. Moreover, there are likely additional enzymes in DRG that generate PIP<sub>2</sub> and contribute to pronociceptive receptor signaling. Indeed, PIP<sub>2</sub> levels were not reduced to zero in DRG from *Pip5k1c*<sup>+/-</sup> or *Pip5k1c*<sup>-/-</sup> (embryonic)



mice. It is likely there are additional signaling pathways and cellular mechanisms that contribute to nociceptive sensitization independent of PIP5K1C and PIP<sub>2</sub><sup>3, 6</sup>.

***Pip5k1c* regulates pronociceptive GPCR and ion channel signaling via PIP<sub>2</sub>-dependent processes.**

Our *in vitro* studies with cultured DRG neurons reveal a critical regulatory role of PIP5K1C in three different pronociceptive signaling processes. First, PIP5K1C modulates TRPV1-mediated signaling which is important for the detection of noxious stimuli and physiological function of the peripheral nociceptive system. Second, PIP5K1C regulates GPCR signaling that mediates nociceptive sensitization following nerve injury and inflammation. Lastly, PIP5K1C regulates ion channels that mediate neuronal hyperexcitability and long-lasting adaptations of the peripheral circuitry following nerve injury and inflammation. Importantly, our data suggest all three processes are dependent on the catalytic activity of PIP5K1C because exogenous delivery of PIP<sub>2</sub> completely restored all signaling deficits.

Although the mechanism(s) by which PIP5K1C regulates pronociceptive signaling are PIP<sub>2</sub>-dependent, the exact PIP<sub>2</sub>-dependent mechanism(s) still need to be elucidated. We speculate that the signaling deficits observed in *Pip5k1c*<sup>+/-</sup> mice result primarily from the necessity of PIP<sub>2</sub> hydrolysis for efficient GPCR signaling and from direct regulatory interactions of PIP<sub>2</sub> with ion channels. PIP<sub>2</sub>-dependent reductions in GPCR signaling are likely due to attenuation of PLC-catalyzed hydrolysis of PIP<sub>2</sub> into DAG and IP<sub>3</sub>, downstream mediators required for GPCR-mediated calcium release. Similarly, reductions in PIP<sub>2</sub>-dependent TRPV1-mediated

calcium signaling and ion channel-mediated neuronal excitability are likely due to direct regulatory interactions of PIP<sub>2</sub> with ion channels<sup>16, 21, 23, 25, 62</sup>. However, we cannot rule out other potential PIP<sub>2</sub>-dependent processes that also influence signaling of GPCRs and ion channels.

For example, our studies reveal that actin and tubulin expression is altered in *Pip5k1c*<sup>+/-</sup> mice, both of which interact with PIP<sub>2</sub> to indirectly modulate signaling. It is reasonable to believe that increased tubulin expression and altered expression pattern of actin contribute to the observed signaling deficits. In fact, increases in tubulin have been shown to inhibit PLC-mediated GPCR signaling<sup>29, 32</sup>. In addition, intact microtubules are required for TRPV1 functionality following activation<sup>33</sup>. Thus, studies on the extent to which increases in beta-III tubulin effect microtubule polymerization and depolymerization dynamics are needed to determine how TRPV1 and other ion channel functionality may be altered. Lastly, it has been reported that an intact actin cytoskeleton is required for prostaglandin-mediated inflammatory pain<sup>40</sup> indicating that altered PIP<sub>2</sub>-actin interactions may contribute to the observed prostaglandin-mediated GPCR signaling deficits. Determining the exact mechanism(s) and to what extent each mechanism contributes to the observed signaling deficits is beyond the scope of this project and will require the development of new assays and techniques to separate each of the mechanisms. Collectively, our data indicate that PIP<sub>2</sub>-dependent mechanism(s) regulate pronociceptive signaling but the extent to which each mechanism is involved requires further investigation.

## ***Pip5k1c* haploinsufficiency attenuates PIP<sub>2</sub>-dependent nociceptive sensitization in models of chronic pain**

In addition to deficits in pronociceptive signaling *in vitro*, we observed reductions in nociceptive sensitization in *Pip5k1c*<sup>+/-</sup> mice *in vivo*. Acute nociceptive responses including detection of noxious heat and ligand-evoked nocifensive behaviors were reduced in *Pip5k1c*<sup>+/-</sup> mice. Ligand-evoked nocifensive licking in response to LPA and 17-PT PGE<sub>2</sub> was significantly reduced in *Pip5k1c*<sup>+/-</sup> mice; however nocifensive responses to capsaicin were not reduced. In contrast, responses to noxious thermal (>43°C) stimuli were reduced, indicating that PIP5K1C may contribute to differential signaling mechanisms following chemical or thermal activation of TRPV1. Taken together, our data suggest that the innate defensive mechanism of the nociceptive system is regulated by PIP5K1C and should be considered when evaluating PIP5K1C as a target for analgesic drug development.

The most profound reductions in nociceptive responses of *Pip5k1c*<sup>+/-</sup> mice were observed in models of chronic inflammatory and neuropathic pain. Thermal and mechanical nociceptive sensitization were attenuated in three models of chronic pain, LPA-induced neuropathic pain, SNI-induced neuropathic pain and CFA-mediated inflammatory pain, with initiating events at three different anatomical locations, spinal, peripheral nerve, and hindpaw, respectively. Importantly, reductions in thermal and mechanical nociceptive sensitization in *Pip5k1c*<sup>+/-</sup> mice in the three chronic pain models were completely restored to WT levels via exogenous intrathecal delivery of PIP<sub>2</sub> just prior to inflammation or injury. These data suggest that PIP5K1C regulation of nociceptive sensitization is dependent upon the catalytic

activity and subsequent PIP<sub>2</sub> concentrations at the time of injury or inflammation. Indeed, these findings are consistent with previous studies that indicated indirect (via adenosine receptor activation) reductions in PIP<sub>2</sub> concentration at the time of injury or inflammation reduced thermal and mechanical sensitization in modes of chronic pain<sup>84</sup>. Taken together, our studies validate PIP5K1C as a novel regulatory kinase in nociceptive sensitization and suggest there is enormous potential for developing PIP5K1C inhibitors as treatments for chronic pain.

### **Implications for humans carrying one or two non-functional mutation(s) in *PIP5K1C***

The cytoskeleton is made up of three types of filaments, microtubules (made from tubulin), microfilaments (made from actin) and intermediate filaments. *Pip5k1c* haploinsufficiency results in the alteration of actin and tubulin expression, two major components of microfilaments and microtubules, respectively. These changes are most likely due to reduced synthesis of PIP<sub>2</sub>, which interacts with both actin and tubulin to maintain stable cytoskeletal structure and mediate signaling<sup>27, 48</sup>. Neuronal-specific beta-III tubulin expression is increased by approximately 30% while the expression pattern of actin is altered in *Pip5k1c*<sup>+/-</sup> DRG neurons. Specifically, filamentous actin is reduced at the plasma membrane in *Pip5k1c*<sup>+/-</sup> DRG neurons. Importantly, actin serves as a scaffolding protein for tropomyosin and troponins during muscle contraction.

Human lethal congenital contracture syndrome type 3 (LCCS3) results from homozygous mutation in *PIP5K1C* in which aspartic acid 253 is mutated to

asparagine and renders the kinase inactive. LCCS3 is characterized by severe fetal akinesia, joint contractures, and muscle atrophy and results in death either embryonically or within 24 hours of birth. This mirrors the phenotype of *Pip5k1c*<sup>-/-</sup> mice, which also die within 24 hours of birth due to immobility and an inability to feed<sup>45, 94</sup>. Di Paolo et al. (mouse phenotype) and Narkis et al. (human phenotype) attribute the perilethality phenotype to reduced PIP5K1C-mediated synaptic vesicle release and endocytosis that is blunted following homozygous mutation. However, the link between homozygous mutations in PIP5K1C and the muscle-contraction based LCCS3 has never been investigated.

Although PIP5K1C expression is considered limited to neuronal tissue in mice and has been previously reported as having minimal expression in skeletal muscle<sup>45, 51</sup>, the expression profile in humans has not been determined. Furthermore, alterations in cytoskeletal proteins following mutations of *Pip5k1c/PIP5K1C* may be genome-wide and not tissue specific. Alternatively, the actin and tubulin phenotypes could be contributing to the phenotype via alterations in neuronal projections from the nervous system into the muscle. Nerve innervation into the muscle is required to transmit signals (in the form of action potentials) from the brain to the muscle to initiate contraction.

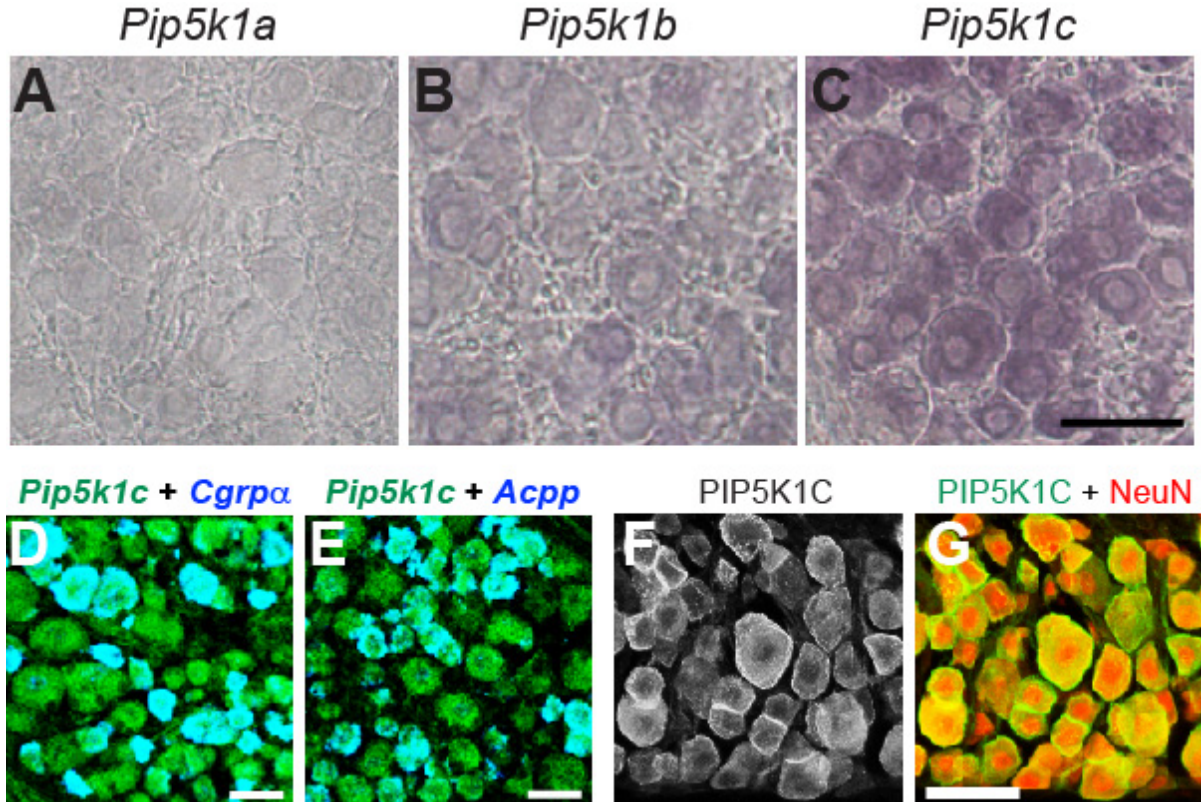
The exact mechanism by which muscle contraction is altered in the human phenotype are not known; however, these data suggest a link between alterations in cytoskeletal filaments that are required for muscle contraction and the LCCS3 phenotype that results from homozygous *PIP5K1C* mutation. A greater understanding of PIP5K1C in human physiology (particularly muscle and neuronal

tissue) is needed before further conclusions can be made. Interestingly, mutations in cytoskeletal filament genes such as alpha-actin (*ACTA1*) and skeletal troponin T (*TNNT*) have been implicated in arthrogryposis disorders similar to LCCS3<sup>95, 96</sup>. This further supports the hypothesis that alterations in cytoskeletal dynamics as a result of mutations in *PIP5K1C* likely contribute to the LCCS3 phenotype.

Importantly, although our preliminary studies with actin and tubulin may provide a potential link to the human LCCS3 phenotype as a result of homozygous mutation, muscle-contraction phenotypes are not observed in adult *Pip5k1c*<sup>+/-</sup> mice and were not reported in humans carrying a mutation in one allele of *PIP5K1C*. Additionally, the muscle/joint contractures and muscle atrophy are likely due to reduced PIP<sub>2</sub> synthesis during embryonic development. Thus, we conclude that alterations to muscle contraction are not contributing to the observed antinociceptive phenotypes of *Pip5k1c*<sup>+/-</sup> mice. Rather, the antinociceptive effects are due to reduced PIP<sub>2</sub>-dependent pronociceptive signaling and sensitization.

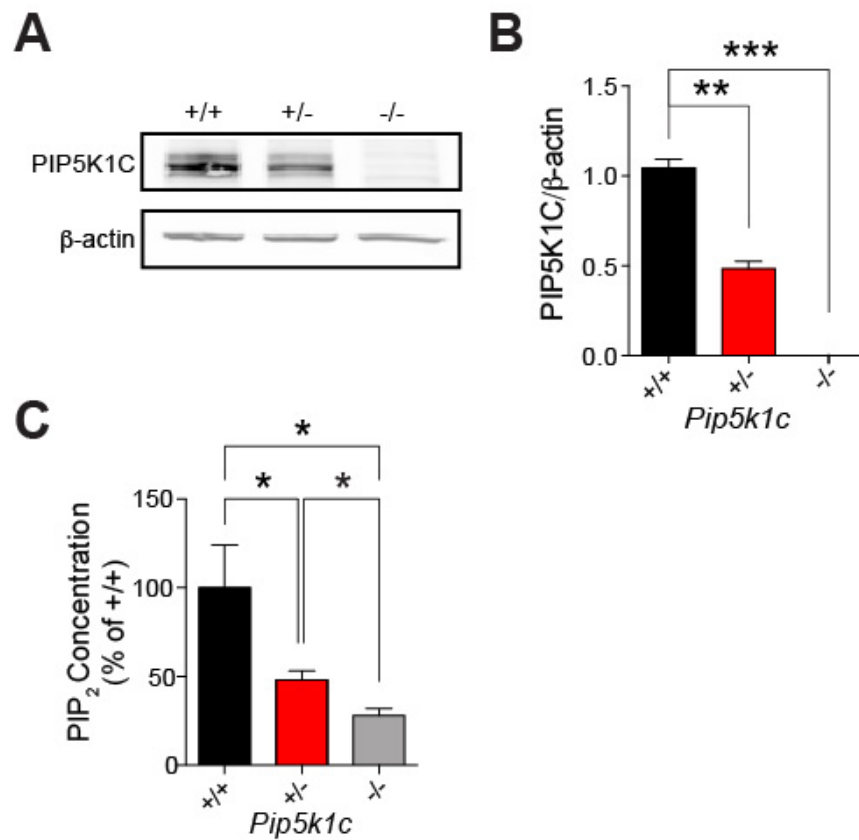
Interestingly, Israeli Bedouins that live in the Negev desert, an environment where somatosensory stimuli are extreme, frequently harbor a heterozygous mutation in *PIP5K1C* (LCCS3 that results from a homozygous mutation in *PIP5K1C* is prevalent in this community)<sup>94</sup>. Our studies with *Pip5k1c*<sup>+/-</sup> mice reveal reduced nociceptive responses to various somatosensory stimuli, suggesting that humans with one mutated allele may also have reduced nociceptive responses, which could provide a survival advantage in what is known to be an extreme environment. Although our data suggest a link, additional studies are needed to implicate *PIP5K1C* in human nociceptive processing pathways.

## Figures



**Figure 2.1. PIP5K1C is the predominant PIP5K1 isoform in adult nociceptive DRG neurons.**

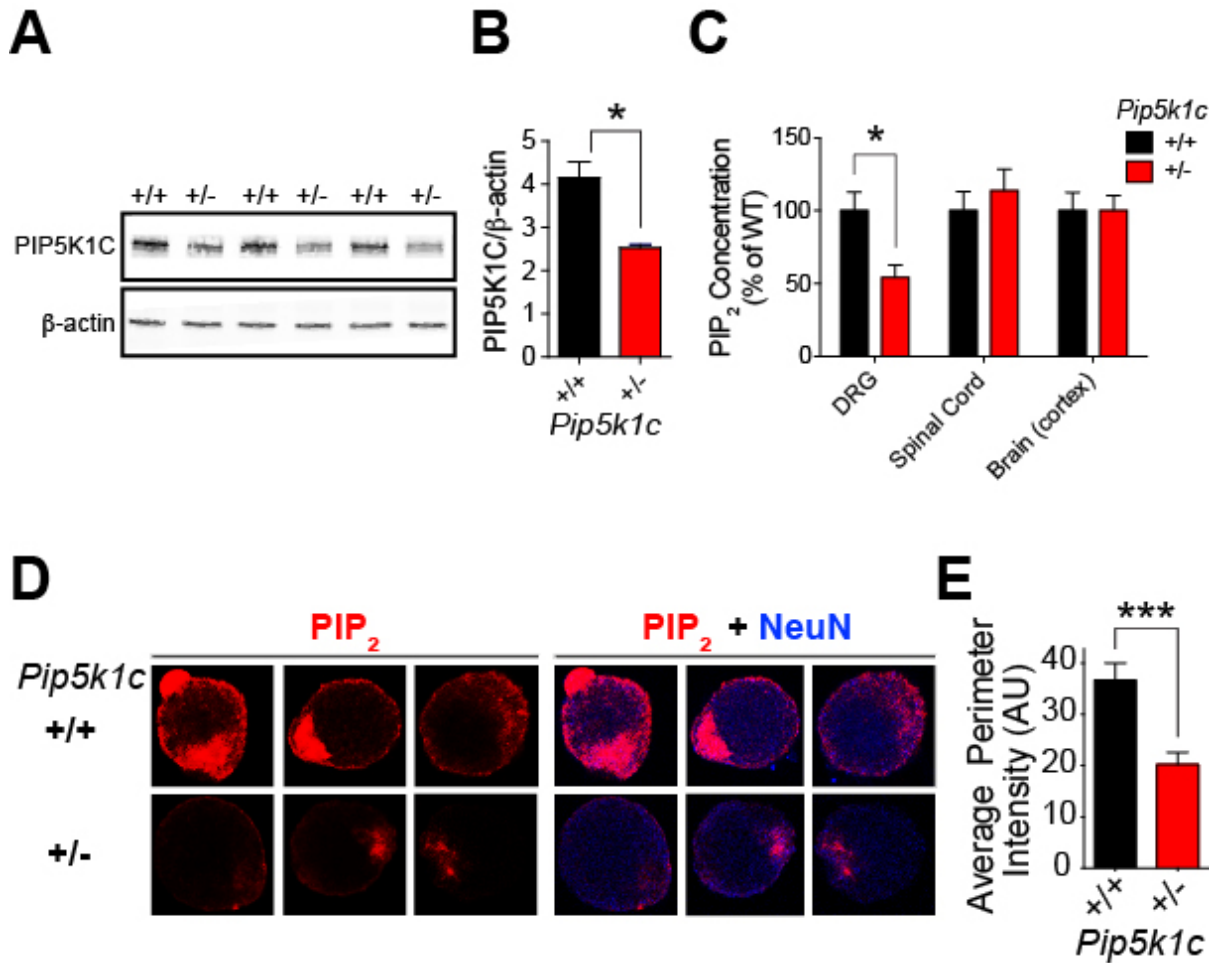
**(A-C)** *In situ* hybridization with gene-specific probes using sections from adult mouse lumbar DRG. Scale bar, 50  $\mu$ m. **(D,E)** Double fluorescence *in situ* hybridization using adult lumbar DRG. Confocal images. Scale bar, 50  $\mu$ m. **(F,G)** Sections from adult mouse DRG were immunostained for **(F)** PIP5K1C (c1 isoform) and **(G)** NeuN, merged. Confocal images. Scale bar, 50  $\mu$ m.



**Figure 2.2. PIP5K1C generates at least half of all PIP<sub>2</sub> in embryonic mouse DRG.**

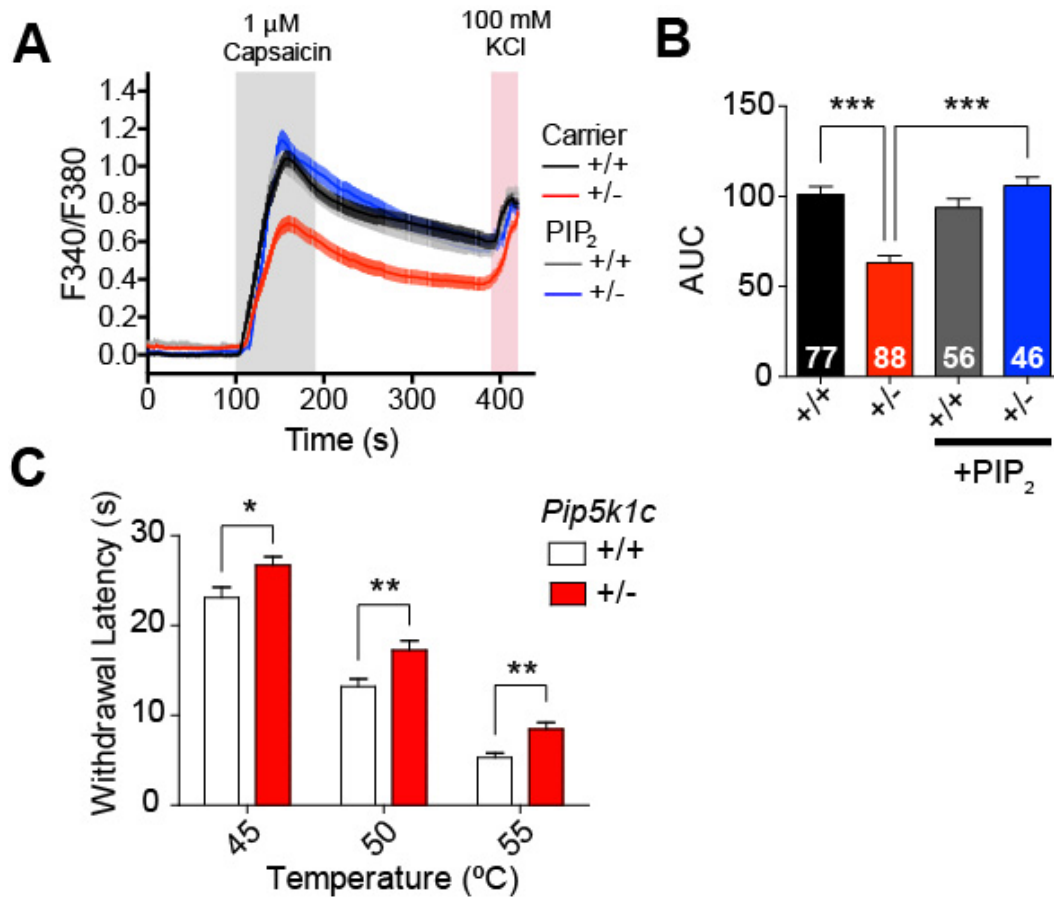
**(A, B)** PIP5K1C protein levels in the DRG of WT, *Pip5k1c*<sup>+/-</sup>, and *Pip5k1c*<sup>-/-</sup> embryonic (E17.5-18.5) mice relative to β-actin. **(A)** Representative western blots and **(B)** quantification; n=3 embryos per genotype. **(C)** PIP<sub>2</sub> levels in embryonic (E17.5-18.5) DRG quantified by mass ELISA from WT, *Pip5k1c*<sup>+/-</sup>, and *Pip5k1c*<sup>-/-</sup> mice. n=10 embryos per genotype.





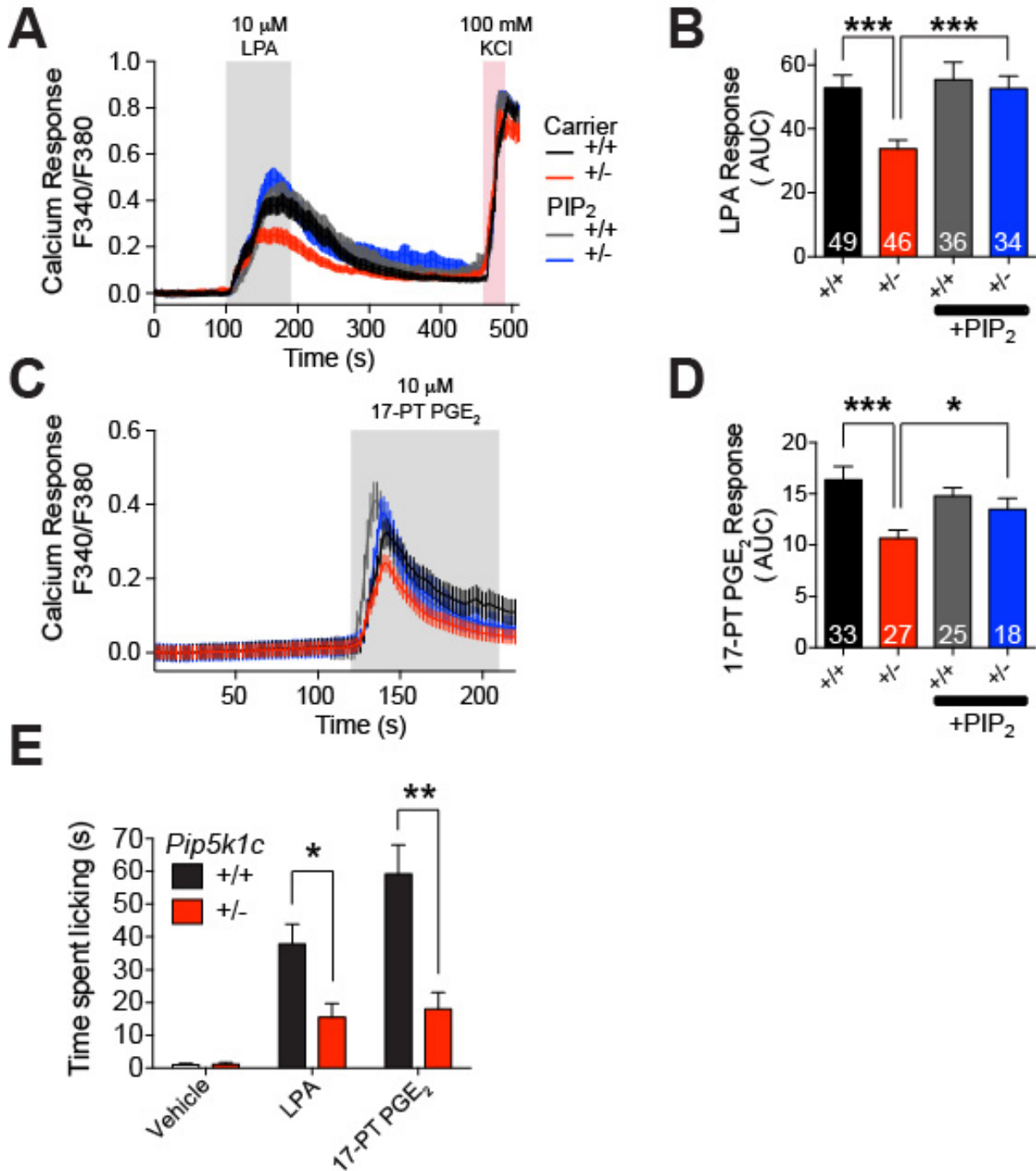
**Figure 2.3 PIP5K1C generates at least half of all PIP<sub>2</sub> in adult mouse DRG.**

(A, B) PIP5K1C protein levels in adult DRG of male *Pip5k1c*<sup>+/+</sup> and *Pip5k1c*<sup>+/-</sup> mice relative to β-actin. (A) Western blots and (B) quantification; n=3 per genotype. (C) PIP<sub>2</sub> levels in DRG, spinal cord, and brain (cerebral cortex) of adult male *Pip5k1c*<sup>+/+</sup> and *Pip5k1c*<sup>+/-</sup> mice, quantified by mass ELISA. n=10 mice per genotype. (D) Representative images of membrane PIP<sub>2</sub> staining in small diameter DRG neurons cultured from *Pip5k1c*<sup>+/+</sup> and *Pip5k1c*<sup>+/-</sup> adult mice relative to NeuN and (E) quantification of the average perimeter (membrane) intensity. n=28 small diameter neurons quantified per genotype. All data are mean ± SEM. \*p<0.05, \*\*\*p<0.0005.



**Figure 2.4. *Pip5k1c* haploinsufficiency attenuates TRPV1-mediated signaling and acute nociceptive sensitivity to heat.**

**(A)** Calcium responses and **(B)** quantification (area under the curve, AUC). Cultured adult DRG neurons were stimulated with 1  $\mu$ M capsaicin for 30 s, washed with HBSS for 4.5 minutes to remove the ligand, then stimulated for 30 s with 100 mM KCl to confirm neuron identity. Cultures were incubated with 2  $\mu$ M carrier or 2  $\mu$ M Carrier + 2  $\mu$ M PIP<sub>2</sub> for 15 minutes prior to calcium imaging. Number of neurons quantified is indicated in the bar graph. **(C)** WT and *Pip5k1c*<sup>+/-</sup> mice were restrained by scruffing and the right hindpaw was placed on a metal surface of the indicated temperature. The latency for the animal to withdrawal (lift, shake, or jump) its paw was recorded. **(B,C)** All data are mean  $\pm$  SEM. \* $p < 0.05$ , \*\* $p < 0.005$ , \*\*\* $p < 0.0005$ .

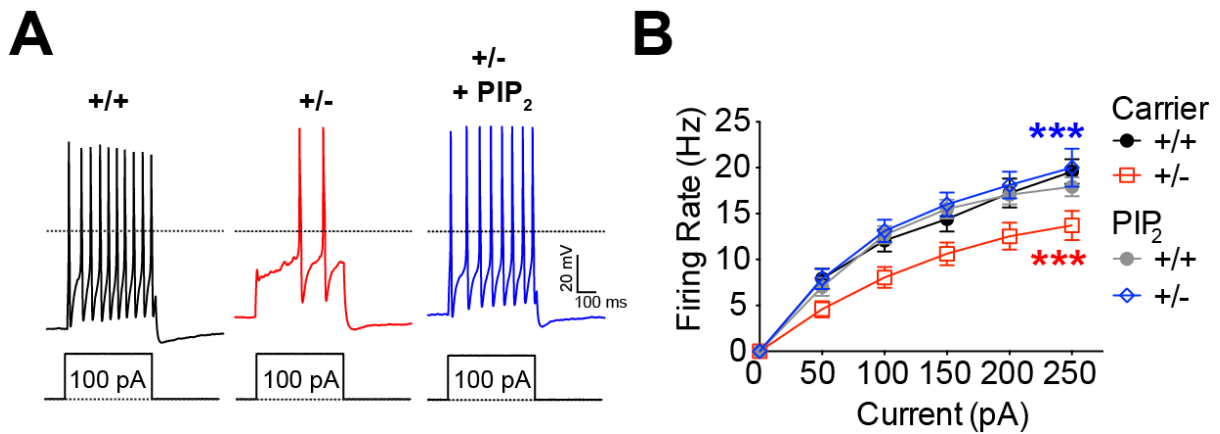


**Figure 2.5. *Pip5k1c* haploinsufficiency reduces ligand-evoked nociceptive signaling *in vitro* and nocifensive licking *in vivo*.**

**(A,C)** Calcium responses and **(B,D)** quantification (area under the curve, AUC).

Cultured adult DRG neurons were stimulated with **(A, B)** 10  $\mu$ M LPA or **(C, D)** 10  $\mu$ M

17-PT-PGE<sub>2</sub> for 90 s, washed with HBSS for 120 s to remove the ligand, then stimulated for 30 s with 100 mM KCl to confirm neuron identity (not shown for 17-PT PGE<sub>2</sub>). Cultures were incubated with 2 μM carrier or 2 μM Carrier + 2 μM PIP<sub>2</sub> for 15 minutes prior to calcium imaging. Number of neurons quantified is indicated in the bar graph. **(E)** Time spent licking for the first 5 minutes after injecting vehicle, 4.1 μg LPA, or 1.2 μg 17-PT PGE<sub>2</sub> into the left hindpaw of adult WT and *Pip5k1c*<sup>+/-</sup> male mice. n=10 mice per genotype per agonist. **(A-E)** Data are mean ± SEM. \*p<0.05, \*\*p<0.005, \*\*\*p<0.0005.

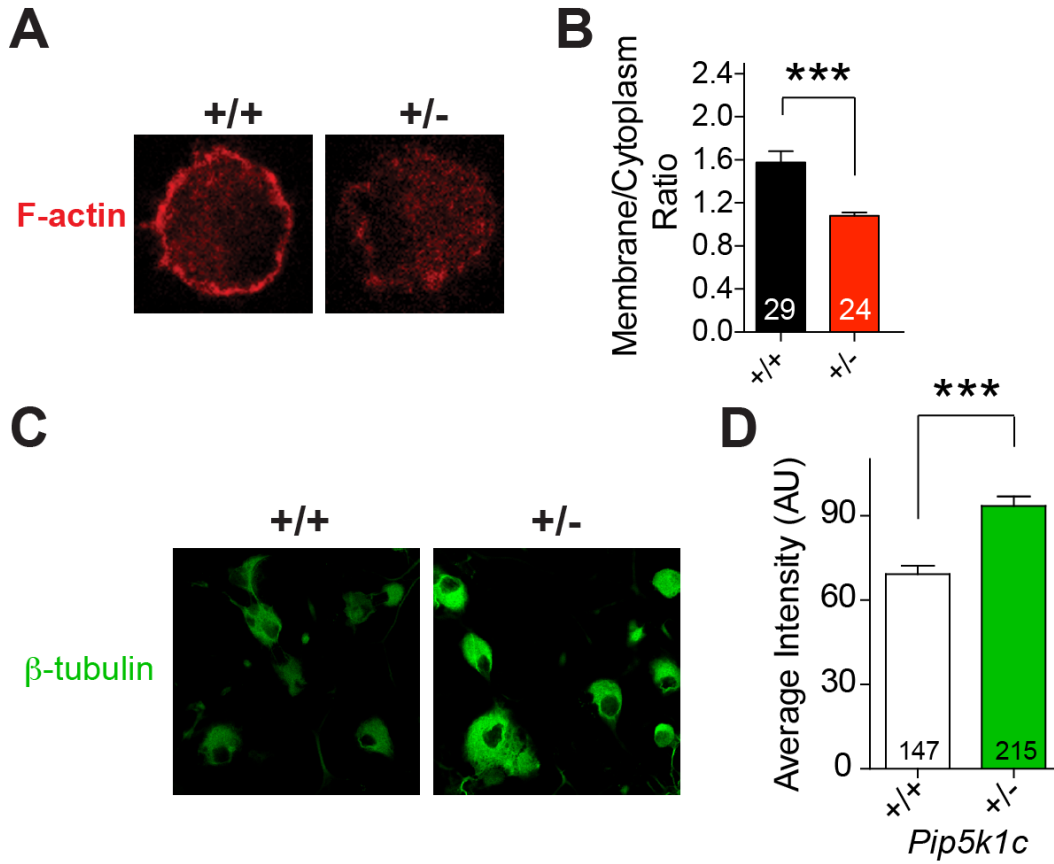


**Figure 2.6. *Pip5k1c* haploinsufficiency attenuates PIP<sub>2</sub>-dependent ion channel-mediated neuronal excitability.**

**(A)** Representative action potentials following 100 pA current injection. **(B)**

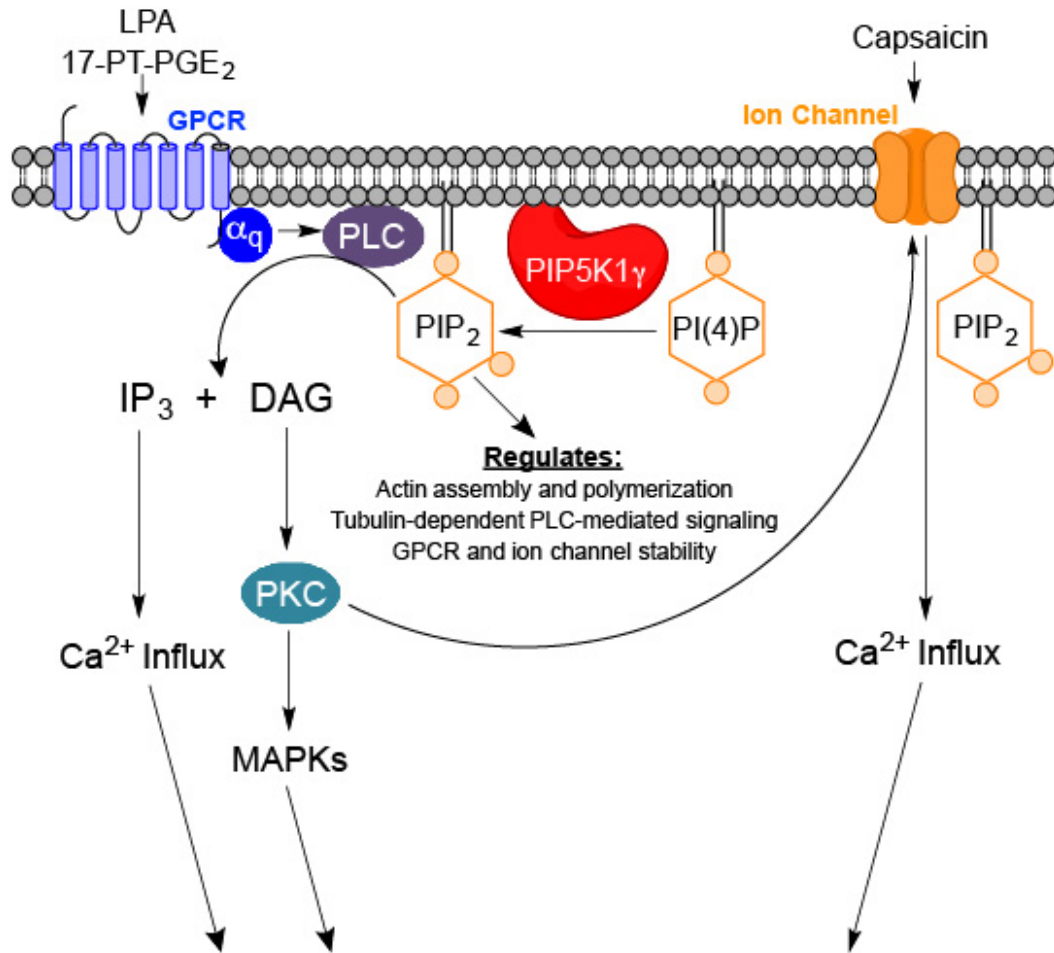
Quantification of firing rate (action potential spikes per second) for neurons cultured from *Pip5k1c*<sup>+/+</sup> and *Pip5k1c*<sup>+/-</sup> adult mice. Carrier (10 μM) or Carrier (μM) + PIP<sub>2</sub> (10 μM) were interleaved in the internal pipette solution. n=25-40 neurons per genotype.

Data are mean ± SEM. \*\*\*p<0.0005.



**Figure 2.7. Pip5k1c haploinsufficiency alters the expression of cytoskeletal proteins.**

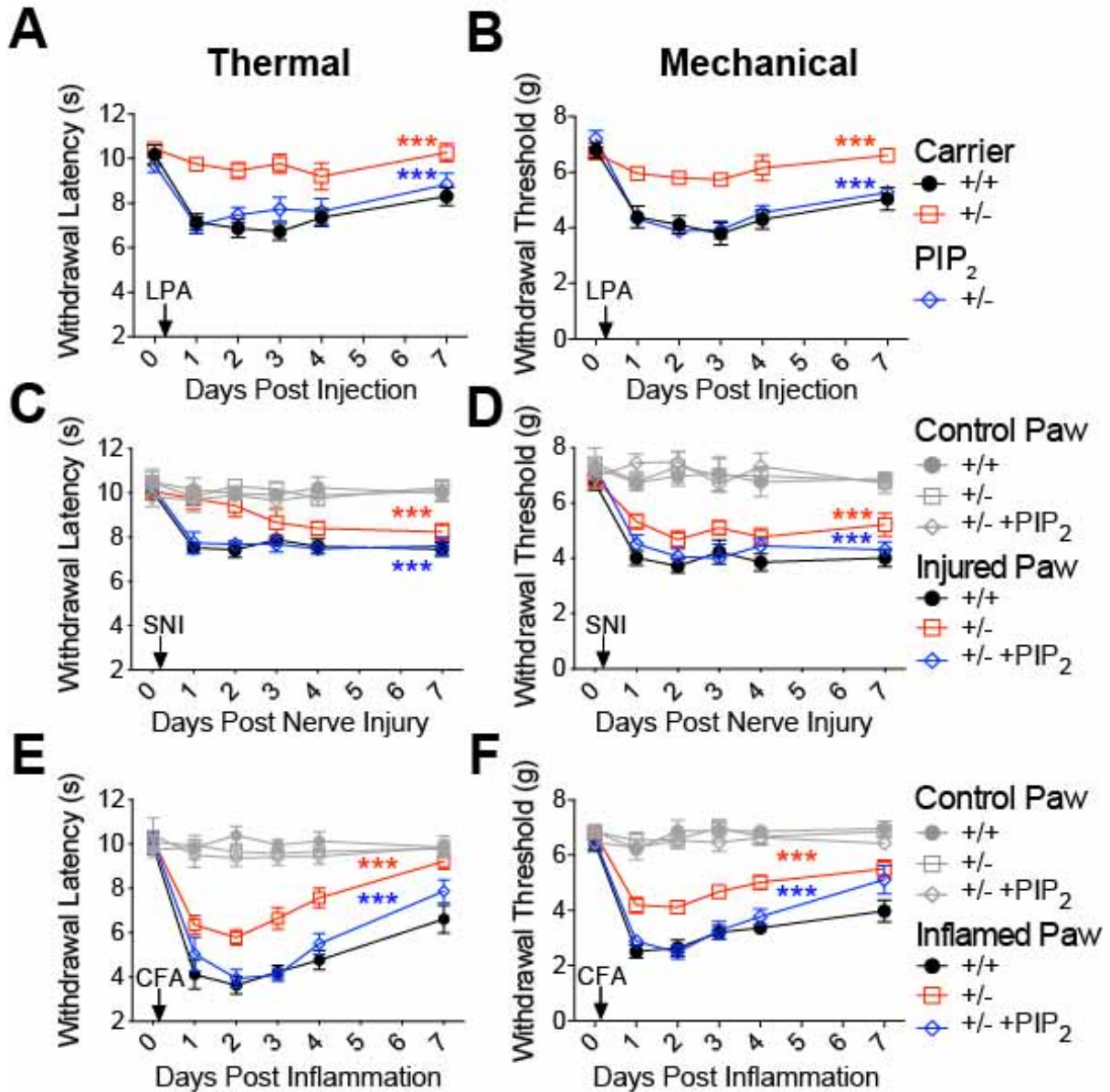
**(A)** Representative images of F-actin (phalloidin) staining **(B)** and quantification of the membrane to cytoplasmic ratio in small diameter DRG neurons cultured from *Pip5k1c*<sup>+/+</sup> and *Pip5k1c*<sup>+/-</sup> adult mice. Number of neurons quantified indicated in the bargraph. **(C)** Representative images of beta-III tubulin staining **(D)** and quantification of the membrane to cytoplasmic ratio in small diameter DRG neurons cultured from *Pip5k1c*<sup>+/+</sup> and *Pip5k1c*<sup>+/-</sup> adult mice. Number of neurons quantified indicated in the bargraph. **(B, D)** All data are mean  $\pm$  SEM. \*\*\*p<0.0005.



## Nociceptive Sensitization

**Figure 2.8. Schematic representation of all PIP<sub>2</sub>-dependent mechanisms altered by *Pip5k1c* haploinsufficiency.**

Model. PIP5K1C generates PIP<sub>2</sub> that is hydrolyzed downstream of pronociceptive GPCR and ion channel activation. Ca<sup>2+</sup> influx (from GPCRs and ion channels) and PKC activation of MAPKs contribute to nociceptive sensitization<sup>3,6</sup>. PIP<sub>2</sub> also regulates actin assembly, tubulin-dependent PLC-mediated signaling and GPCR and ion channel stability. *Pip5k1c* haploinsufficiency reduces the amount of PIP<sub>2</sub> that is available for signaling in DRG neurons.

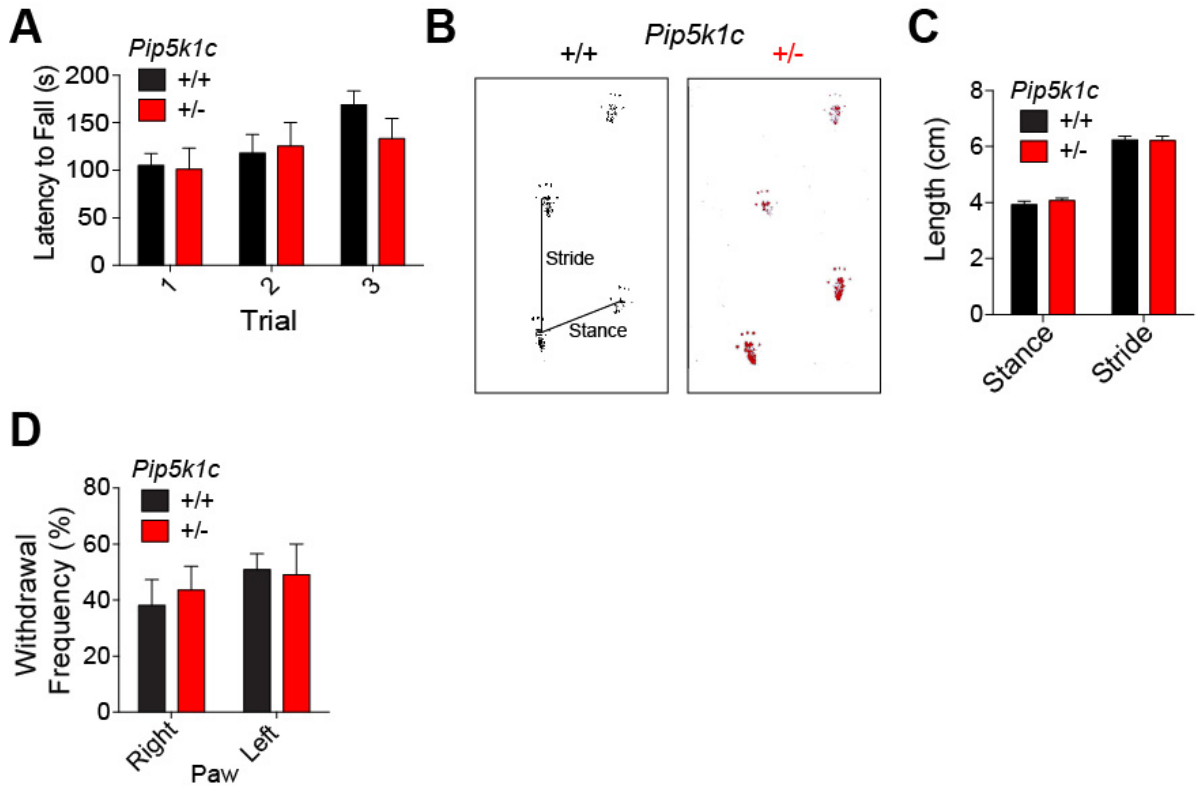


**Figure 2.9.** *Pip5k1c* haploinsufficiency reduces PIP<sub>2</sub>-dependent thermal and mechanical sensitization in models of chronic inflammatory and neuropathic pain.

(A) Thermal and (B) mechanical sensitivity in the chemically induced (LPA; 1nmol; intrathecal) neuropathic pain model in adult male *Pip5k1c*<sup>+/+</sup> and *Pip5k1c*<sup>+/-</sup> mice. Intrathecal injection of either carrier (0.3 nmol) or carrier (0.3 nmol) + PIP<sub>2</sub> (0.3 nmol) administered immediately prior to LPA injection. n=10 for WT+ Carrier and n=20 for

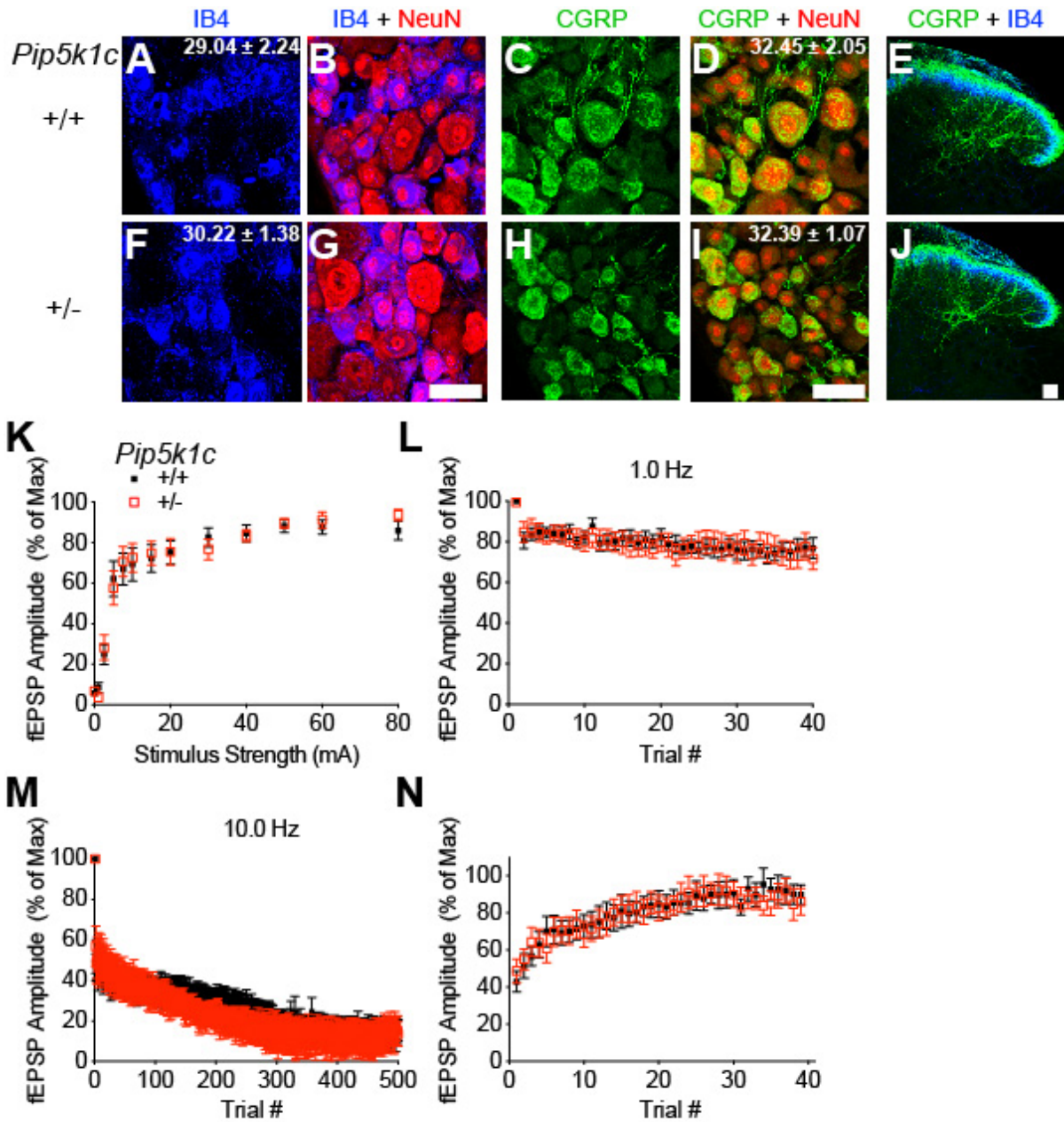


*Pip5k1c*<sup>+/-</sup> + Carrier and *Pip5k1c*<sup>+/-</sup> + PIP<sub>2</sub> **(C)** Thermal and **(D)** mechanical sensitivity in the spared nerve injury neuropathic pain model. Contralateral paw was not injured and served as a control. n=6 for WT + Carrier, n=10 for *Pip5k1c*<sup>+/-</sup> + Carrier and n=7 for *Pip5k1c*<sup>+/-</sup> + PIP<sub>2</sub>. **(E)** Thermal and **(F)** mechanical sensitivity in the CFA chronic inflammatory pain model. CFA (20 µL) was injected into one hindpaw. Contralateral paw was not injected and served as a control. n=10 for WT + Carrier, n=20 for *Pip5k1c*<sup>+/-</sup> + Carrier and n=10 for *Pip5k1c*<sup>+/-</sup> + PIP<sub>2</sub>. Intrathecal injection of either carrier (0.3 nmol) or carrier (0.3 nmol) + PIP<sub>2</sub> (0.3 nmol) administered immediately prior to and 2 hours following **(C,D)** injury or **(E,F)** inflammation. **(A-F)** All data are mean ± SEM. \*p<0.5, \*\*\*p<0.0005 (one-way ANOVA). Red asterisks indicate significance between *Pip5k1c*<sup>+/-</sup> mice and WT mice receiving carrier only. Blue asterisks indicate significance between *Pip5k1c*<sup>+/-</sup> mice receiving carrier and *Pip5k1c*<sup>+/-</sup> mice receiving carrier + PIP<sub>2</sub>.



**Figure 2.10. *Pip5k1c* haploinsufficiency does not alter motor function, gait or low-threshold (innocuous) mechanoreception.**

**(A)** Rotarod test of motor function. Three trials with adult WT and *Pip5k1c*<sup>+/-</sup> male littermates. n=10 mice per genotype. **(B,C)** Gait analysis with adult WT and *Pip5k1c*<sup>+/-</sup> male mice. **(B)** Representative gait measurements showing stride and stance and **(C)** quantification. Five stride and five stance measurements per animal. n=10 male mice per genotype. **(D)** Withdrawal frequency of each hindpaw to an innocuous mechanical stimulus (cotton swab). 5 trials per hindpaw. n=10 male mice per genotype **(A-D)** All data are mean ± SEM. No significant differences between genotypes in any of these assays.



**Figure 2.11. Nociceptive neuron markers and synaptic transmission between sensory neurons and spinal cord are not affected in *Pip5k1c*<sup>-/-</sup> mice.**

(A-J) IB4-binding (nonpeptidergic marker, blue) and immunofluorescence staining of CGRP (peptidergic marker; green) and NeuN (pan-neuronal marker, red). (A-D; F-I) lumbar DRG and (E,J) superficial dorsal horn of adult male WT and *Pip5k1c*<sup>-/-</sup> littermates. Insets show average percentage of IB4<sup>+</sup> or CGRP<sup>+</sup> neurons relative to

NeuN ( $\pm$  SEM). No significant differences between genotypes. Scale bar in (G, I, and J) is 50  $\mu$ m. **(K-N)** Field excitatory postsynaptic potential (fEPSP) recordings in spinal cord slices (lamina II) from adult male WT and *Pip5k1c*<sup>+/-</sup> mice. **(K)** fEPSP amplitude as a function of stimulus strength. **(L)** 1 Hz synaptic depletion. 1.0 mA stimulation at 1 Hz for 40 trials to deplete neurotransmitter. fEPSP peak amplitude was measured for each trial and plotted as trial number. **(M)** 10 Hz synaptic depletion. 1.0 mA stimulation at 10 Hz for 400 trials to deplete neurotransmitter. fEPSP peak amplitude was measured for each trial and plotted as trial number. **(N)** Synaptic recovery following 10 Hz depletion. Immediately after synaptic depletion, the slices were stimulated at 1.0 mA stimulation at 0.1 Hz for 10 minutes to assess recovery from synaptic depletion. n=12 WT, n=10 *Pip5k1c*<sup>+/-</sup> slices. No significant differences between genotypes (one-way ANOVA).

## CHAPTER III

### SENSORY NEURON-SPECIFIC GENETIC DELETION OF PIP5K1C IN MICE RESULTS IN PROPRIOCEPTIVE ABNORMALITIES

#### Introduction

Our studies in Chapter II focused on elucidating the role of PIP5K1C in nociceptive signaling and sensitization using a *Pip5k1c* haploinsufficiency model in which one allele of *Pip5k1c* was genetically deleted in all cells<sup>45</sup>. Given that pronociceptive receptors and ion channels located on the membrane of DRG neurons play a critical role in peripheral sensitization after nerve injury and inflammation, this chapter focuses on our characterization efforts in the DRG<sup>3, 6</sup>. Importantly, our previous studies revealed selective decreases in PIP<sub>2</sub> levels within the DRG while PIP<sub>2</sub> levels in the spinal cord and frontal cerebral cortex were unaffected in *Pip5k1c*<sup>+/-</sup> mice (Figure 2.3). In addition, we showed that synaptic transmission in the spinal cord was unaffected (Figure 2.9) and that intrathecal delivery of PIP<sub>2</sub> rescued thermal and mechanical nociceptive sensitization defects observed in *Pip5k1c*<sup>+/-</sup> mice. Significantly, these intrathecal injections specifically increased PIP<sub>2</sub> concentration in the DRG and not in the spinal cord (Figure 3.1). Collectively, these studies led us to hypothesize that PIP5K1C regulates nociceptive signaling and sensitization via PIP<sub>2</sub>-dependent mechanisms within the DRG.

Although our previous data suggest that PIP5K1C regulates peripheral nociceptive sensitization within the DRG and that PIP<sub>2</sub> reductions are DRG-specific in the haploinsufficiency model, we cannot completely rule out the possibility that deletion of the PIP5K1C protein alone is effecting activity, given that PIP5K1C regulates many cellular processes via mechanisms that may be independent of catalytic activity<sup>47-49, 97</sup>. In addition, we cannot rule out the possibility that PIP5K1C- and PIP<sub>2</sub>-dependent mechanisms are contributing to the observed phenotypes in tissues or cell types that were not tested. Thus, we sought to test our hypothesis using mice with conditionally deleted *Pip5k1c* using Cre recombinase (Cre) driven by the advillin promoter, which is exclusively expressed in sensory neurons of the DRG and trigeminal ganglia. Here, we report that although Advillin-Cre can be used to selectively reduce *Pip5k1c* in sensory neurons, mice lacking both alleles of *Pip5k1c* in the DRG exhibit a proprioceptive phenotype, rendering them unusable in standard nociceptive assays. In contrast, conditional *Pip5k1c* heterozygotes do not exhibit the proprioceptive phenotype and are currently being used to test our hypothesis that PIP5K1C reductions in the DRG mediate the observed reductions in peripheral sensitization.

## **Methods**

### **Animals**

All procedures involving vertebrate animals were approved by the Institutional Animal Care and Use Committee at the University of North Carolina at Chapel Hill. We obtained knockout-first, conditional-ready *Pip5k1c* mice from the UC Davis

knockout mice project (komp.org) via the Wellcome Trust Sanger Institute. Exon 5 which, encodes a portion of the catalytic domain, was flanked by LoxP sites. Upon arrival, the first litter of offspring was used for beta-galactosidase staining to confirm presence of transgene, via the presence of LacZ as confirmed by genotyping. Mice containing the transgene were then crossed with FlpE mice to remove the neomycin resistance cassette. Mice positive for the transgene with confirmed deletion of the neomycin cassette were crossed with Advillin-CRE mice (Adv) to conditionally delete *Pip5k1γ* only in sensory neurons<sup>98-100</sup>. The advillin promoter drives expression of Cre in sensory neurons only (DRG and trigeminal ganglia) in the Advillin-CRE mice, which have been extensively characterized<sup>98, 100</sup>. Mice were genotyped with the following primers (provided by Wellcome Trust Sanger Institute): CAS\_R1\_Term: TCGTGGTATCGTTATGCGCC, Pip5k1c\_Forward: TGGAGAGCATCTTCTTCCCC, Pip5k1c\_Reverse: TAACCATCATCCCTCCCTCG, LacZ\_Forward: ATCACGACGCGCTGTATC, and LacZ\_Reverse: ACATCGGGCAAATAATATCG. Cas\_R1\_Term and Pip5k1c\_Forward are used to observe a 210 base pair (bp) mutant band, Pip5k1c\_Forward and Pip5k1c\_Reverse are used to observe a 375 bp wild-type band. LacZ\_Forward and LacZ\_Reverse were used to confirm presence of LacZ prior to removal with FlpE mice. Female *Pip5k1c<sup>fl/fl</sup>*, *Advillin<sup>+/+</sup>* were crossed with male *Pip5k1c<sup>fl/fl</sup>*, *Advillin<sup>Cre/Cre</sup>* to produce the desired *Pip5k1c<sup>fl/fl</sup>*, *Advillin<sup>Cre/+</sup>* knockout animals. *Pip5k1c<sup>wt/wt</sup>*, *Advillin<sup>Cre/+</sup>* (wt/wt) mice served as controls. All mice were backcrossed to C57Bl/6 mice for at least 10 generations.

### ***In situ* hybridization**

Lumbar DRG were dissected from adult WT males 6-8 weeks old. Gene-specific probe preparation and *in situ* hybridization were performed as previously described<sup>69</sup>. Briefly, tissue was mounted in TissueTek immediately following dissection and cryosectioned at 20  $\mu$ m. Non-isotopic *in situ* hybridization was performed using digoxigenin-labeled cRNA probes for *Pip5k1c* and standard nitro NBT and 5-bromo-4-chloro-3-indolyl phosphate BCIP stain. *In situ* hybridization was completed by the UNC *in situ* hybridization core.

### **Western blot analysis**

Lumbar DRG, lumbar spinal cord, and brain (frontal cortex) were dissected from adult male mice (6-8 weeks old) and embryos (E17.5-18.5). Tissue lysates were prepared in RIPA buffer (50 mM Tris, 1% Triton X-100, 0.25% sodium deoxycholate, 0.1% sodium dodecyl sulfate, 1 mM ethylenediaminetetraacetic acid and 150 mM sodium chloride) containing protease inhibitors (Roche Complete Mini Tablets, 11836153001 and 1 mM phenylmethylsulfonyl fluoride) and separated by SDS-PAGE. Gels were transferred onto PVDF membranes and blocked with 5% dry milk (BioRad) in TBS-T (100 mM Tris, 165 mM sodium chloride, and 0.1% Tween 20). Primary antibodies were prepared in TBS-T containing 5% BSA. PIP5K1C antibody (1:500) was a generous gift from P. De Camilli. Anti- $\beta$ -actin (1:3000, Abcam, ab6276) served as a loading control. Secondary antibodies (1:10,000; Li-Cor IRDye 680 and 800) were prepared in TBS-T containing 5% dry milk.



## **Immunohistochemistry**

Mice were sacrificed using pentobarbital. Skin from the hindpaw (containing the volar pad, hairy skin, and glabrous skin) was dissected from adult (6-8 week old) male mice and prepared as described previously<sup>71, 72</sup>. Briefly, tissues were immersion-fixed in 4% paraformaldehyde for 4 hours and cryopreserved in 30% sucrose at 4°C for 3 days. Tissue was embedded in TissueTek and cryosectioned at 20 µm. Sections were then immunostained and thaw mounted onto SuperFrost Plus slides. The following primary antibodies were used for overnight incubations (at 4°C): rabbit anti-PGP9.5 (1:500; Ultraclone) and mouse anti-NeuN (1:250; Millipore, MAB377). Fluorescently conjugated secondary antibodies were purchased from Invitrogen and were used at 1:200 for for 2 hours at room temperature. All staining solutions were made in TBST (0.05 M Tris, 2.7% NaCl, 0.3% Triton-X 100, pH 7.6). All images were obtained using a confocal microscope (Zeiss LSM 510).

## **Behavioral Analysis**

Mice were observed for many days (starting from birth through adulthood) to monitor the proprioceptive phenotype. Animals were photographed and videotaped to document the phenotype. Gait measurements were taken by painting the hindpaws with ink and allowing the mice to walk in a straight line down an enclosed runway. Stride was measured as the distance (in cm) between the left hindpaws (5 measurements per animal were averaged). Stance was measured as distance (in cm) between the left hindpaw and the subsequent step of the right hindpaw (5 measurements per animal were averaged).

## Results

### ***Pip5k1c* is selectively eliminated in sensory neurons of *Pip5k1c<sup>fl/fl</sup>* mice crossed with Advillin-CRE.**

Mice provided from the Wellcome Trust Sanger Institute were confirmed to have the desired transgene upon arrival via beta-galactosidase staining (data not shown). These mice were crossed to FlpE mice (Jackson laboratory, 005703) to successfully remove the neomycin cassette, which was flanked by FRT sites (Figure 3.2). Mice bearing two copies of the floxed *Pip5k1c* allele in which the neomycin cassette was removed were crossed with Advillin-Cre mice to produce the desired *Pip5k1c<sup>fl/fl</sup>*, *Advillin<sup>Cre/+</sup>* knockout mice (Figure 3.2). Note that *Pip5k1c<sup>fl/fl</sup>*, *Advillin<sup>Cre/+</sup>* knockout mice will be referred to as *Pip5k1c<sup>fl/fl</sup>* (or simply fl/fl) whereas the *Pip5k1c<sup>wt/wt</sup>*, *Advillin<sup>Cre/+</sup>* controls will be referred to as wt/wt. *In situ* hybridization using a specific *Pip5k1c* RNA probe (used in Chapter II) revealed dramatic decreases in *Pip5k1c* mRNA expression in the DRG but not in the spinal cord of *Pip5k1c<sup>fl/fl</sup>* mice compared to wt/wt controls, suggesting that selective deletion of *Pip5k1c* was successful at the level of mRNA (Figure 3.3A-D). In addition, western blotting with a PIP5K1C-specific antibody revealed selective reductions of PIP5K1C protein in lumbar DRG but not lumbar spinal cord of *Pip5k1c<sup>fl/fl</sup>* mice compared to wt/wt mice, further suggesting that conditional deletion of *Pip5k1c* in sensory neurons only was successful (Figure 3.3E and 3.3F). It must be noted that neither *Pip5k1c* mRNA nor PIP5K1C protein was completely eliminated in the DRG of *Pip5k1c<sup>fl/fl</sup>* mice. PIP5K1C protein levels were reduced by approximately 75% in the *Pip5k1c<sup>fl/fl</sup>* DRG compared to wt/wt controls (Figure 3.3F).

### ***Pip5k1c*<sup>fl/fl</sup> mice exhibit a hindlimb proprioceptive phenotype**

Although the use of Advillin-Cre appears to specifically eliminate PIP5K1C in sensory neurons, *Pip5k1c*<sup>fl/fl</sup> mice develop what has been characterized in the literature as a hindlimb proprioceptive phenotype<sup>101, 102</sup>. The phenotype has been characterized as withdrawal of the hindlimbs close to the body when suspended by the tail (allowing the front paws to grip onto a wire surface), and awkward placement of the hindlimbs when sitting; both behaviors are exhibited by *Pip5k1c*<sup>fl/fl</sup> mice (Figure 3.4A and 3.4B). These behaviors can be observed by P7 (7 days after birth). Often, the *Pip5k1c*<sup>fl/fl</sup> mice will extend their hindlimbs vertically by their ears, a behavior not typical of WT (or wt/wt) mice (data not shown). Although certain proprioceptive behaviors were observed, there was no difference in gait (stride or stance—see methods for details) between *Pip5k1c*<sup>fl/fl</sup> mice and wt/wt controls (Figure 3.4C). Unfortunately, this proprioceptive phenotype makes it impossible to use these mice for standard nociceptive testing including the Hargreaves radiant heat test and electric von Frey mechanical test. Furthermore, when using the standard scruffing technique to restrain animals, it was noted that there appears to be excess “loose” skin on the *Pip5k1c*<sup>fl/fl</sup> mice compared to wt/wt controls (data not shown). This prevented completion of all other standard nociceptive assays including the restrained hot plate and tail immersion tests. Collectively, our behavioral analysis shows that phenotypes exhibited by *Pip5k1c*<sup>fl/fl</sup> mice are the same as those deemed as proprioceptive phenotypes in the literature and render these mice unusable for nociceptive studies<sup>101, 102</sup>.

### **Nerve innervation into the skin is reduced in *Pip5k1c*<sup>fl/fl</sup> mice**

Studies characterizing proprioceptive phenotypes in the literature have investigated these phenotypes by observing histochemical markers of nociceptive versus proprioceptive neurons, as well as nerve innervation from the DRG into various tissues including the skin<sup>101, 102</sup>. Protein gene product 9.5 (PGP9.5) is a neuronal marker that can be used to visualize nerve innervation from the peripheral nervous system (DRG) into skin. Given that all phenotypes in *Pip5k1c*<sup>fl/fl</sup> mice were observed in the hindlimbs, we evaluated PGP9.5 staining in the skin of the hindpaw. PGP9.5 staining in the hindpaw glabrous skin, the volar pad, and hairy skin of *Pip5k1c*<sup>fl/fl</sup> mice was dramatically reduced compared to wt/wt controls (Figure 3.5), although the differences cannot be easily quantified. Interestingly, histochemical analysis of parvalbumin—a metabolic marker of proprioceptive DRG neurons that has been characterized as absent in mice with the reported proprioceptive phenotype—revealed no differences between *Pip5k1c*<sup>fl/fl</sup> mice and wt/wt controls (data not shown). In addition, there were no histochemical differences when staining with a nociceptive marker, CGRP (data not shown). Taken together, our data suggests that neuronal development within the DRG is intact in both nociceptive and proprioceptive neurons but projection of DRG nerve terminals into the skin is disrupted.

## Discussion

The peripheral sensitization that mediates persistent/chronic pain results from prolonged hyperexcitability of neurons found in the DRG. Our previous data with global heterozygous *Pip5k1c* knockout mice suggested that reductions in PIP5K1C catalytic activity in the DRG significantly reduce peripheral sensitization (Chapter II); however, one allele of *Pip5k1c* was eliminated in all cells. To further investigate the site of action of PIP5K1C deletion on the observed phenotypes, we aimed to specifically delete *Pip5k1c* in sensory neurons only. Using a conditional deletion strategy, we reduced PIP5K1C expression in DRG and not in the spinal cord, suggesting successful targeting of sensory neurons using Advillin-CRE.

Unfortunately, homozygous deletion of *Pip5k1c* in sensory neurons resulted in a profound proprioceptive defect that made nociceptive studies impossible. We limited our *in situ* hybridization and Western blotting evaluations to the spinal cord and DRG due to the presence of this extreme phenotype and the fact that Advillin-CRE mice have been extensively characterized showing specific Cre expression in sensory neurons of the dorsal root and trigeminal ganglia with no expression of Cre in other areas of the mouse embryo including the spinal cord and brain<sup>98, 100</sup>.

Interestingly, behaviors observed in *Pip5k1c<sup>fl/fl</sup>* mice are characteristic of the reported hindlimb proprioceptive phenotype. However, preliminary immunohistochemical analysis of lumbar DRG neurons, which are responsible for projections into the hindlimbs, did not show a loss of parvalbumin-positive neurons, which are characteristically eliminated in proprioceptive phenotypes previously

reported<sup>101, 102</sup>. These data suggest that *Pip5k1c* elimination does not result in a loss of proprioceptive neurons, rather the proprioceptive phenotype is due to mechanisms independent neuron loss.

### **PIP5K1C regulates DRG peripheral afferent innervation**

Detection of noxious stimuli begins at the site of injury or inflammation via the peripheral (or afferent) terminal of DRG neurons that innervate target tissues such as the skin<sup>6, 10</sup>. Our immunohistochemical analysis of PGP9.5 staining in the hindpaw skin revealed dramatic, almost complete elimination, of peripheral terminal innervation from the DRG into the skin of *Pip5k1c*<sup>f/f</sup> mice. PGP9.5 is a non-specific marker of nerve innervation; therefore, we cannot make any conclusions regarding the type of innervations that are lost (free nerve endings versus encapsulated, for example). However, given the near-elimination of nerve endings in the glabrous skin and volar pad, it is reasonable to assume that both encapsulated (proprioceptive) and free nerve endings (nociceptive) are lost when *Pip5k1c* is reduced. These data suggest that *Pip5k1c* elimination in DRG produces a proprioceptive phenotype due to reduced afferent extension into target tissue rather than loss of proprioceptive neurons as reported by other gene/protein deletions.

PIP5K1C and PIP<sub>2</sub> play important roles in both actin and tubulin dynamics in many cell types<sup>27, 29, 32, 48, 66, 103</sup> including DRG (Chapter II). Given that DRG afferent innervation into target tissues requires concerted rearrangements of actin filaments and microtubules<sup>104</sup>, and PIP5K1C-interacting proteins such as talin and vinculin, it is reasonable to speculate that the reduced nerve innervation observed in *Pip5k1c*<sup>f/f</sup>

mice may be due to alterations in PIP5K1C regulation of actin and tubulin dynamics similar to those observed in *Pip5k1c*<sup>+/-</sup> mice (Chapter II). In support of this mechanism, cortical migration, another process that relies heavily on concerted cytoskeletal rearrangements, is disrupted when *Pip5k1c* is deleted using in utero electroporation of *Pip5k1c* small hairpin RNA (shRNA)<sup>83</sup>. Extensive studies of actin and microtubule dynamics in *Pip5k1c*<sup>fl/fl</sup> mice are needed and may provide a starting point for beginning to understand the mechanism(s) underlying the disrupted nerve innervation.

Neurotrophins (nerve growth factor, brain-derived growth factor, neurotrophin-3 and neurotrophin-4) activate receptor tyrosine kinases (Trks) to mediate DRG axonal guidance and nerve innervation into peripheral target tissues<sup>105, 106</sup>. Trk (A, B, and C) receptor stimulation leads to the activation of multiple downstream signaling pathways including PLC $\gamma$ -catalyzed hydrolysis of PIP<sub>2</sub><sup>105</sup>. It is therefore reasonable to speculate that deletion of *Pip5k1c* could reduce PIP<sub>2</sub>-mediated Trk signaling during developmental stages of axonal outgrowth and innervation, further contributing to the reductions in nerve innervation observed in *Pip5k1c*<sup>fl/fl</sup> mice. In fact, deletion of TrkA or NGF in mice dramatically reduces innervation into the epidermis, similar to the reductions in innervation observed in *Pip5k1c*<sup>fl/fl</sup> mice<sup>106</sup>. However, elimination of TrkA or NGF results in a loss of small diameter neurons, a phenotype not observed in *Pip5k1c*<sup>fl/fl</sup> mice. A less severe phenotype in *Pip5k1c*<sup>fl/fl</sup> mice (similar innervation phenotype but lack of cell death) compared to deletion of the entire receptor suggests a more subtle mechanism may be responsible for the phenotypes such as reduced receptor activity as a result of decreases in PIP<sub>2</sub> levels.

Further experiments such as calcium imaging using neurotrophin stimulation, as well as investigations of actin and tubulin dynamics, are needed to determine exactly which mechanism(s) underlie the PIP5K1C-mediated innervation phenotype. In addition, more in-depth immunohistochemical analysis of other tissues is needed to fully understand the extent to which innervation is reduced.

### **Moving forward: Alternatives for conditional *Pip5k1c* deletion**

Although conditional homozygous deletion of *Pip5k1c* produces a proprioceptive phenotype, conditional heterozygotes do not display this phenotype, rendering them useful for experiments to test our hypothesis that PIP5K1C-mediated reductions in nociceptive sensitization are due to specific reductions in the DRG. This research is still ongoing; conditional heterozygotes are being bred for behavioral and calcium imaging experiments in an effort to recapitulate our findings with global heterozygous knockout mice (Chapter II). Although *Advillin* is expressed in the majority of DRG neurons, a small subset of neurons that do not express *Advillin* may account for the 25% of PIP5K1C protein still detected in *Pip5k1c<sup>fl/fl</sup>* mice<sup>100</sup>. If *Advillin*-driven Cre reduces PIP5K1C protein expression by at least 40% (the level observed in the DRG of global *Pip5k1c<sup>+/-</sup>* mice) in the heterozygous conditional mice, we will be able to use the conditional heterozygotes to test our hypothesis.

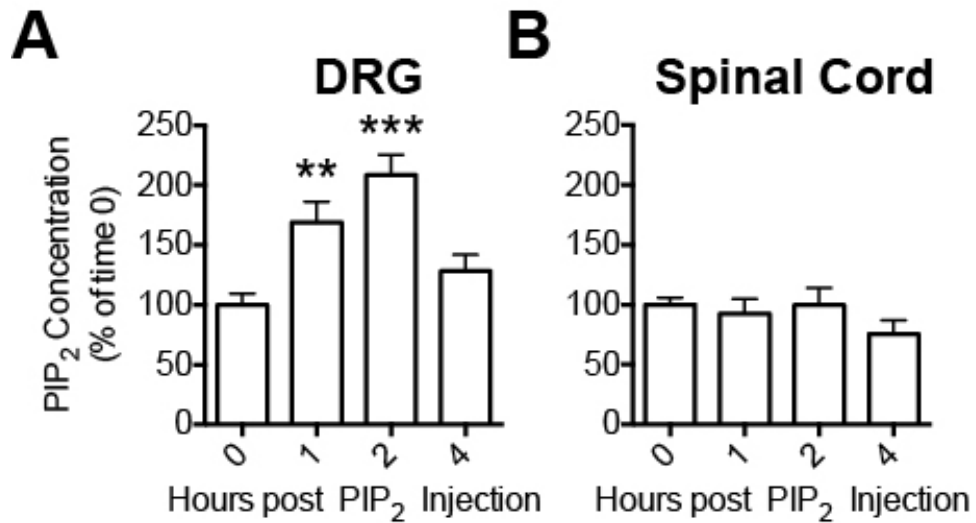
Additionally, there are other options for conditionally deleting *Pip5k1c* in sensory neurons only. For example, we can focus our efforts on specific subtypes of DRG neurons such as TRPV1- or sodium channel Na<sub>v</sub>1.8-expressing neurons, as



TRPV1- and Na<sub>v</sub>1.8-driven Cre recombinase lines have been well characterized<sup>107</sup>.<sup>108</sup>. Given the modest TRPV1-mediated phenotype in *Pip5k1c*<sup>+/-</sup> mice and the expression profile of Na<sub>v</sub>1.8, Na<sub>v</sub>1.8-driven Cre would be the best option. Na<sub>v</sub>1.8 is expressed in virtually all small-diameter nociceptive neurons but is absent in large-diameter DRG neurons and CNS tissue<sup>107</sup>. The lack of expression in large-diameter neurons may prevent the development of the proprioceptive phenotype.

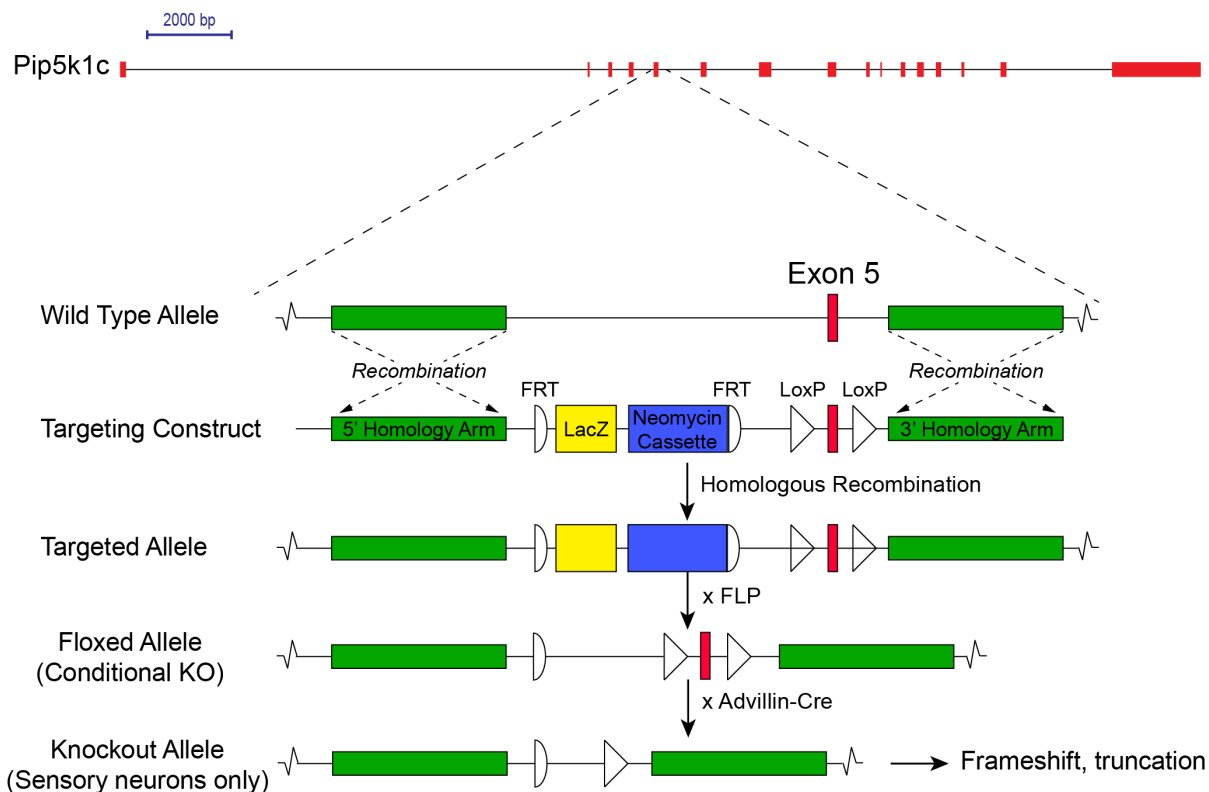
Another option for conditional deletion of PIP5K1C, and one that would be most likely to prevent the proprioceptive phenotype, would be an inducible Cre recombinase line. Several such lines exist including an inducible *Advillin*-driven Cre known as *Advillin-Cre-ERT2*. This line expresses Cre fused to a mutated ligand-binding domain from the human estrogen receptor (Cre-ERT2) which is driven by the *Advillin* promoter and only activated following administration of the synthetic estrogen receptor agonist, tamoxifen<sup>109</sup>. Use of the *Advillin*-driven inducible Cre recombinase system would allow for conditional deletion of *Pip5k1c* in adult sensory neurons only, and would likely prevent the proprioceptive phenotype that is likely due to defects in axonal outgrowth and innervation during development.

## Figures



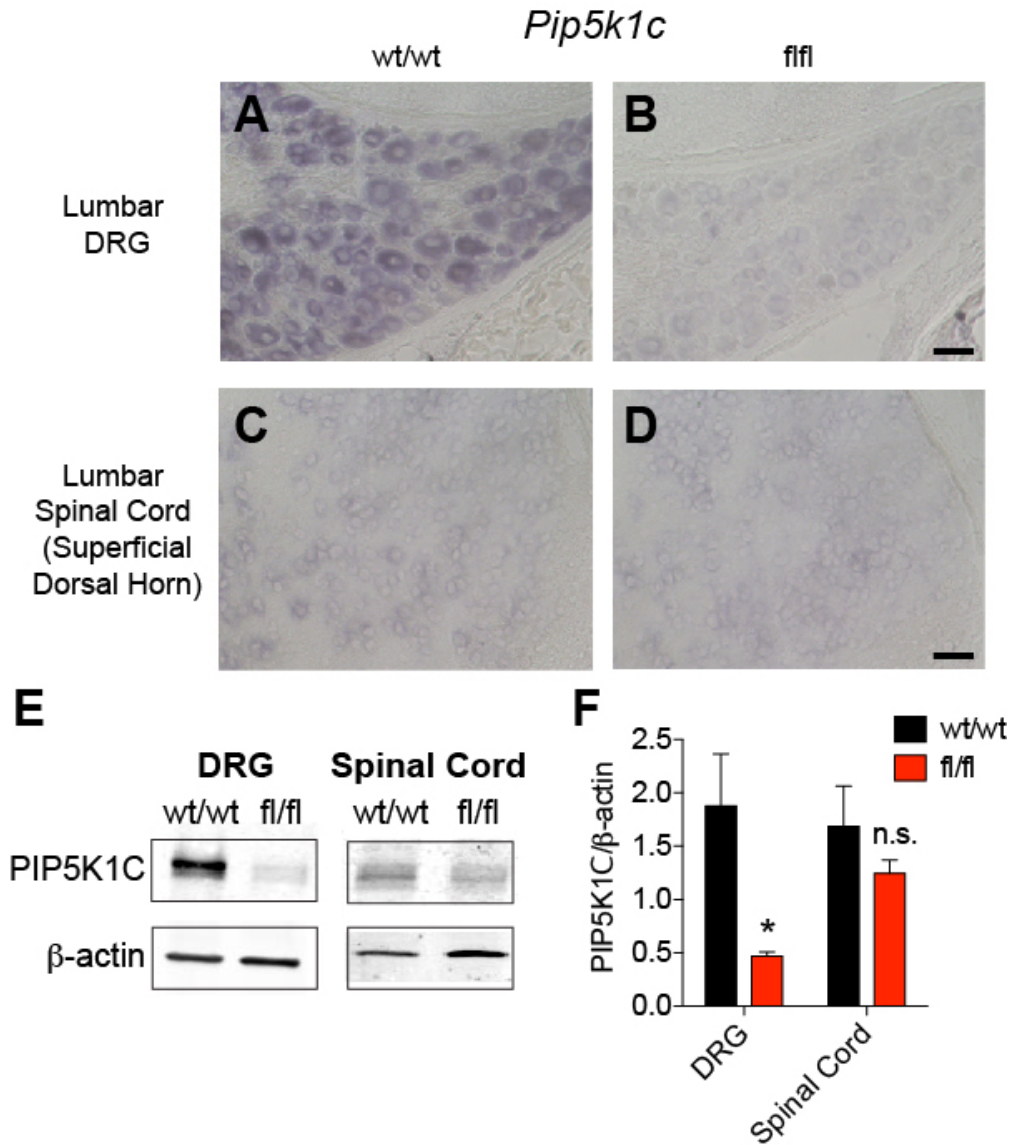
**Figure 3.1. Intrathecal PIP<sub>2</sub> injections selectively increase PIP<sub>2</sub> in the DRG.**

(A-B) Intrathecal injections of 0.3nmol carrier + 0.3 nmol PIP<sub>2</sub> elevate PIP<sub>2</sub> levels in (A) lumbar DRG but not in (B) lumbar spinal cord. Significant increases in PIP<sub>2</sub> levels are observed at 1 and 2 hours post injection. PIP<sub>2</sub> was quantified using a competitive binding mass ELISA specific for PI(4,5)P<sub>2</sub>. n=5 WT mice per time point. \*\*p<0.005, \*\*\*p<0.0005. Data are presented as mean ± SEM.



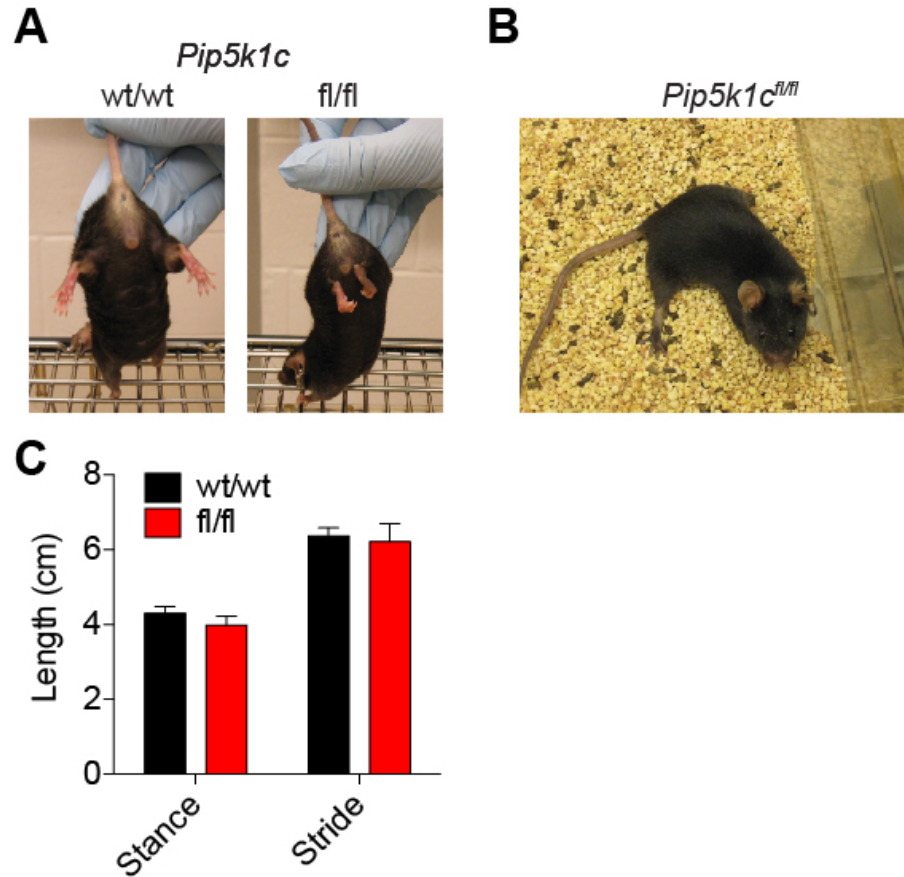
**Figure 3.2. Generation of *Pip5k1c<sup>fl/fl</sup>* conditional knockout mice.**

Diagram of the wild-type *Pip5k1c* allele and targeting construct. The neomycin cassette and LacZ reporter are removed using the FRT-FLP system. Mice expressing Cre driven by the *Advillin* promoter are used to delete *Pip5k1c* (Exon 5 flanked by LoxP sites) in sensory neurons only.



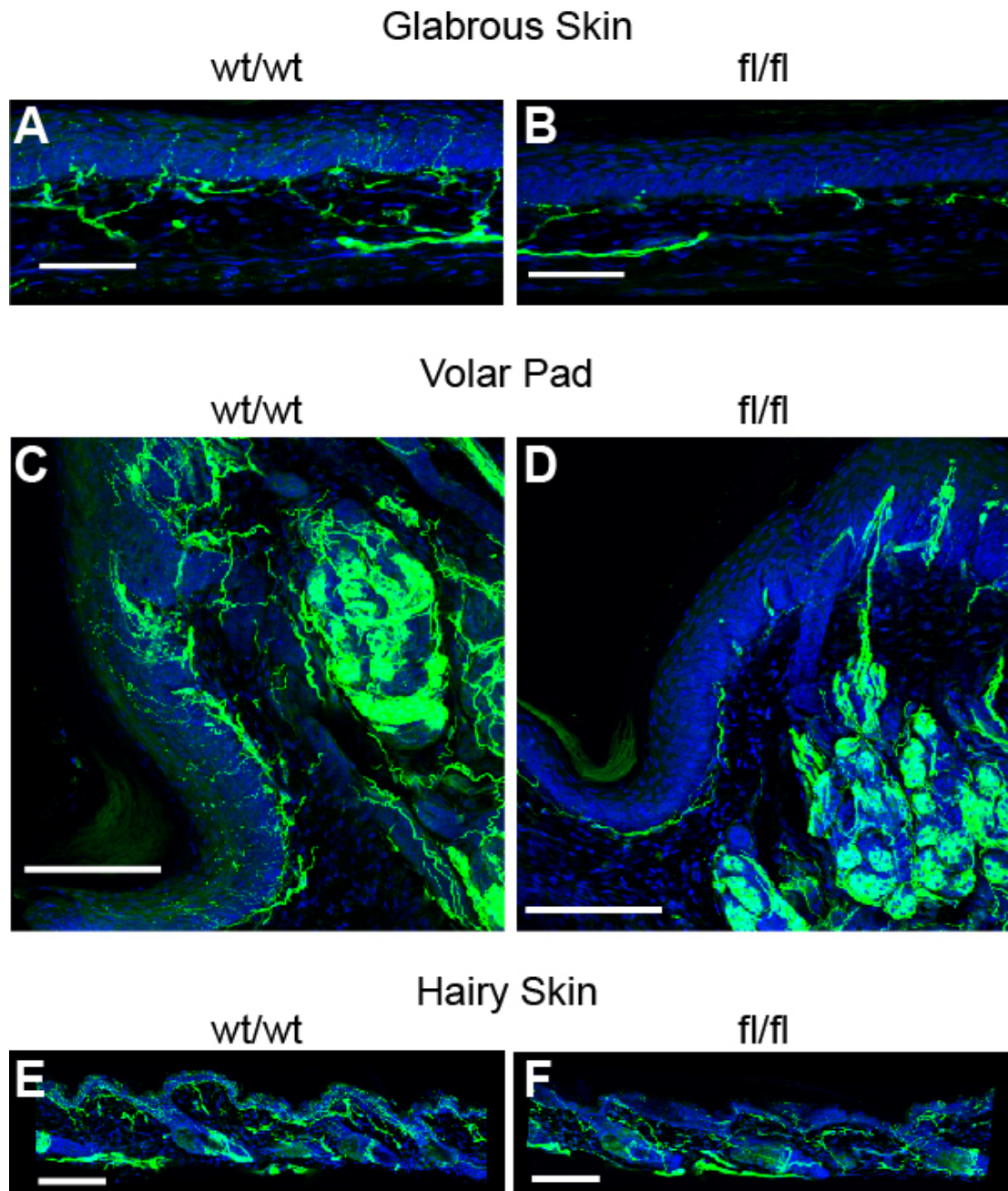
**Figure 3.3. Pip5k1c is selectively eliminated in sensory neurons of the DRG.**

(A-D) *Pip5k1c* *in situ* hybridization in (A, B) lumbar DRG and (C, D) lumbar spinal cord (superficial dorsal horn) from wt/wt controls and *Pip5k1c<sup>fl/fl</sup>* mice. Scale bar, 50 μm. (E, F) PIP5K1C protein levels in adult DRG of male *Pip5k1c<sup>+/+</sup>* and *Pip5k1c<sup>+/-</sup>* mice relative to β-actin. (E) Western blots and (F) quantification; n=3 per genotype. Data are presented as mean ± SEM. \*p<0.05 by unpaired t test.



**Figure 3.4. Sensory-neuron specific deletion of *Pip5k1c* produces a proprioceptive phenotype.**

**(A)** Images showing the difference in leg position between wt/wt controls and *Pip5k1c<sup>fl/fl</sup>* mice when held by the tail. **(B)** Image showing the extended hindlimb position exhibited by *Pip5k1c<sup>fl/fl</sup>* mice. **(C)** **(B,C)** Gait analysis with adult wt/wt and *Pip5k1c<sup>fl/fl</sup>* mice. Five stride and five stance measurements per animal. n=3 male mice per genotype. Data are presented as mean ± SEM.



**Figure 3.5 Sensory-neuron specific deletion of *Pip5k1c* reduces nerve innervation into the skin.**

(A,B) PGP9.5 (nerve innervations; green) and DRA15 (nuclei marker; blue) staining of glabrous hindpaw skin from (A) wt/wt and (B) *Pip5k1c*<sup>fl/fl</sup> mice. (C, D) PGP9.5 and

DRAQ5 staining of the hindpaw volar pad from **(C)** wt/wt and **(D)** *Pip5k1c<sup>fl/fl</sup>* mice.  
**(E, F)** PGP9.5 and DRAQ5 staining of hairy hindpaw skin from **(E)** wt/wt and **(F)** *Pip5k1c<sup>fl/fl</sup>* mice.

## CHAPTER IV

# DEVELOPMENT OF A HIGH-THROUGHPUT SCREENING ASSAY IDENTIFIES A SMALL MOLECULE INHIBITOR OF PIP5K1C THAT ATTENUATES NOCICEPTIVE SIGNALING AND SENSITIZATION

### Introduction

A large majority of phosphatidylinositol (PI) lipids contribute to tight regulation of cellular processes including migration, vesicle trafficking, endocytosis, exocytosis, proliferation, and survival<sup>110-113</sup>. However, because the role of phosphatidylinositol 3-kinases (PI3Ks) in cancer proliferation and survival has been extensively characterized, the vast majority of lipid kinase drug discovery efforts over the past 20 years (starting with the discovery of the first PI3K inhibitor, wortmannin) have been directed towards PI3Ks with relatively little investigation into other lipid kinase families. With more recent studies focused on the validation of additional lipid kinase families in disease pathophysiology such as of sphingosine 1-kinase in cancer proliferation<sup>114, 115</sup>, phosphatidylinositol 5-phosphate 4-kinase (PIP4K2) in insulin signaling<sup>116</sup>, and phosphatidylinositol 4-phosphate 5 kinase (PIP5K1C) in pain (Chapter II), there is renewed excitement around the development of high-throughput screening assays to identify inhibitors of these lipid kinases to promote a better understanding of the associated disease states.



Phosphatidylinositol 4,5-bisphosphate (PIP<sub>2</sub>), one of the most abundant phosphoinositides produced by the complex PI pathway, tightly regulates a multitude of cellular processes including G-protein-coupled receptor signaling, endocytosis, exocytosis, cytoskeletal dynamics, and vesicle trafficking<sup>45, 65, 67</sup>. Type I PIP kinases (PIP5K1s) and type II PIP kinases (PIP4K2s) synthesize PI(4,5)P<sub>2</sub> from phosphatidylinositol monophosphates (PIPs), PI(4)P and PI(5)P, respectively. Davis and colleagues developed a high-throughput assay to identify inhibitors of PIP4K2B that could advance the field of lipid kinase regulation of insulin signaling<sup>117</sup>. Similarly, we aimed to develop a high throughput screen (HTS) to identify small molecule inhibitors that could be used to further validate PIP5K1C as a therapeutic target in chronic pain.

Current assays to monitor PIP5K1-dependent PIP<sub>2</sub> synthesis include the use of lengthy lipid extraction protocols, radiolabeled ATP, and thin layer chromatography, which are not easily amenable to high throughput screening<sup>46, 51</sup>. Due to previous limitations in assay development, there are currently no reported inhibitors of PIP5K1s. Thus, we sought to develop our high-throughput screening (HTS) assay using fluorescently conjugated PI(4)P, the natural substrate for PIP5K1C, and full length recombinant PIP5K1C that would eliminate the use of radiolabeled ATP and lengthy lipid extraction and micelle preparation protocols. As such, we report the first high-throughput assay for PIP5K1 activity. In addition, we used the assay to identify a potent (IC<sub>50</sub>~40 nM) and selective PIP5K1C inhibitor, UNC3230 (previously referred to as UNC1 in abstract), which attenuates pain

signaling and sensitization in a manner similar to *Pip5k1c* haploinsufficiency (Chapter II).

## Methods

### Materials

Fluorescein conjugated phosphatidylinositol 4-phosphate [PI(4)P, 9000655] and fluorescein conjugated phosphatidylinositol 4,5-bisphosphate (PIP2, 10010388) were purchased from Cayman Chemical and reconstituted in 100% DMSO to 1.5 mM. N-terminal His<sub>6</sub>-tagged full length (90 kDa) recombinant human PIP5K1C was purchased from Millipore (14-845M). ProfilerPro separation buffer (760367) and coating-reagent 8 (CR-8; 760278) were purchased from PerkinElmer. PIP5K1C enzyme solution is used at a final concentration of 3 nM in assay buffer (Table 1) containing 0.01% BSA, 1mM DTT, 1x protease inhibitors (Roche mini complete tablets), and 1x phosphatase inhibitors. PI(4)P substrate solution is used at a final concentration of 1  $\mu$ M in assay buffer containing 0.05% DMSO and 15  $\mu$ M ATP (Km for PIP5K1C).

### Animals

All procedures involving vertebrate animals were approved by the Institutional Animal Care and Use Committee at the University of North Carolina at Chapel Hill. Wild-type (WT) C57Bl/6 mice were purchased from Jackson Laboratories (#000664) or bred in-house.

## **LOPAC Library**

The library of pharmacologically active compounds (LOPAC) library was purchased from Sigma and used as an assay validation library. The 1280 compounds were supplied as 1- $\mu$ L samples (10 mM) in 384-well polypropylene microplates (Grenier). On the day of screening, plates were thawed and diluted (1:100) to 0.1 mM (1000x the final assay concentration) with assay buffer (Table 1) in the 384-well plate. The Multidrop was used to add 100  $\mu$ L of 1% DMSO to columns 1,2, 23, and 24 which did not contain compound and serve as control columns. A Multimek NSX-1536 assay workstation system fitted with a 384-well head (Nanoscreen, Charleston, SC) was used to transfer 2  $\mu$ L of each sample into 384-well ShallowWell Nunc assay plates (ThermoScientific, 267459).

## **Kinase-focused Library**

The 4,727 compound kinase-focused library was prepared and generously provided by the UNC Center for Integrative Chemical Biology and Drug Discovery (CICBDD)<sup>118</sup>. On the day of screening, plates were prepared as described for the LOPAC library.

## **Screening**

A Multidrop Combi Reagent Dispenser was used for the addition of all reagents to assay plates. First 10  $\mu$ L of 90 mM EDTA (in assay buffer) was added to each well in columns 1 and 2 and serve as negative control reactions. Nine microliters of 2x enzyme solution was added to each well of the entire plate. Plates

were incubated at room temperature for 10 minutes then 9  $\mu$ L of 2x substrate solution was added to each well of the entire plate. Assay plates were incubated in the dark for 40 minutes at room temperature. Ten microliters of 90mM EDTA (in assay buffer) was then added to columns 3-24 to stop the reactions. Fluorescently conjugated substrate, PI(4)P, and product, PIP<sub>2</sub>, were detected using the LabChip EZ Reader II microfluidic mobility shift assay (MSA) platform from PerkinElmer. ProfilerPro separation buffer containing 1.5% CR-8 was used. Separation conditions: -2000 V downstream voltage, -500 V upstream voltage, -2.0 psi pressure, post-sample sip time of 120 seconds, final delay of 120 seconds.

For dose response curves, compounds were plated as 3-fold serial dilutions starting with a top concentration of 10 mM. The lowest concentration tested in the 10-point dose response was 0.0005 mM. Dose response compound plates were prepared using a Tecan Genesis200 (Research Triangle Park, NC). Dose response plates were heat-sealed and stored at -20°C until day of use. On the day of use, plates were prepared as described the LOPAC library (see above). The final top concentration was 10  $\mu$ M.

### **Data analysis**

Screening data was analyzed using Screenable software (Screenable Solutions, Chapel Hill, NC). Screenable was used to calculate the mean of the positive and negative controls, the percent inhibition (with respect to on-plate controls) for each reaction and the common assay performance measure,  $z'$ , for

each plate.  $Z' = \frac{3\sigma_{max} + 3\sigma_{min}}{|\mu_{max} - \mu_{min}|}$  where max is the negative control (no compound;

no inhibition) and min is the positive control (+90 mM EDTA; 100% inhibition). A  $Z' > 0.5$  was considered acceptable for the plate to be included in the overall data analysis. The LabChip software calculated percent conversion for each reaction.

Compounds from the kinase library were considered hits if they inhibited PIP5K1C at  $\geq 80\%$ . The 80% threshold was determined as greater than 3 standard deviations from the mean percent inhibition for the entire screen. Mean inhibition was 14% with a standard deviation of 21%. Dose response curves were calculated using Screenable Software by converting the % conversion to % inhibition with respect to on-plate controls and using a 3 or 4-parameter curve fit. Dose responses for kinases tested at DiscoverX for selectivity were calculated (after normalization to the positive control—no inhibition) using GraphPad Prism software and a 4 parameter curve fit with variable slope.

### **Selectivity screening**

Two different assays were used to assess selectivity. ProfilerPro (PerkinElmer) was used to assess selectivity of UNC3230 on 48 kinases. For the ProfilerPro assay, UNC3230 was added to reaction-ready (384-well) assay plates (PerkinElmer) containing each of the 48 kinases in duplicate and incubated for 15 minutes. Matching fluorescent substrates for each kinase (also provided in reaction-ready 384-well plates) and ATP at the  $K_m$  for each kinase were added then the plate was incubated for 90 minutes. Fluorescent substrates and products were separated

and quantified using the LabChip EZ Reader II microfluidic mobility-shift assay (PerkinElmer). Data for this assay are reported as percent of control (product produced in the absence of UNC3230).

The DiscoverX KINOMEScan competitive binding assay was used to quantitatively measure interactions between UNC3230 and 100 different kinases. Briefly, UNC3230 and each DNA-tagged kinase were added simultaneously to 384-well plates containing immobilized ligands for each of the 100 kinases tested. Plates were incubated for 1 hour and the amount of kinase bound to the immobilized ligand was quantified using quantitative PCR and the associated DNA tag. Binding interactions were determined by the amount of kinase that bound to the immobilized ligand. Competitive interactions between the kinase and UNC3230 would prevent binding of the kinase to the immobilized ligand. Data for this assay are reported as percent of control (binding of a control compound to the kinase).

### **Neuron culture**

All DRG were dissected from 3-8 week old male mice following decapitation. Neurons were dissociated with manual trituration using a fire polished Pasteur pipette in a solution of 2 mg/mL collagenase (Worthington, CLS1) and 5 mg/mL dispase (Gibco, 17105-041). Neurons were cultured with Neurobasal A medium (Gibco, 10888) supplemented with 2% B27 (Gibco, 17504), 2 mM L-glutamine (Gibco, 25030), 1% penicillin/streptomycin (Gibco, 15140), 50 ng/mL glial derived neurotrophic factor (GDNF; Millipore, GF030) and 25 ng/mL nerve growth factor (NGF; Millipore, 01-125) in the absence of serum. Neurons were plated onto

coverslips coated with 1 mg/mL poly-D-lysine (Sigma, P7886) and 10 µg/mL laminin (Sigma, L2020) and cultured for 18-24 hours prior to use.

### **Immunocytochemistry**

Biotinylated PIP<sub>2</sub> primary antibody was purchased from Echelon Biosciences (Z-B045) and used according to the manufacturer's instructions. All PIP<sub>2</sub> staining was completed at 37°C with Tris-buffered saline (50 mM Tris and 150 mM NaCl at pH 7.4). Chicken anti-NeuN (1:250; Aves) was added to the primary incubation. Alexa-conjugated streptavidin (1:2000; Invitrogen) and fluorescently labeled anti-chicken antibodies (1:1000; Invitrogen) were used for secondary detection.

### **Calcium imaging**

Calcium imaging of dissociated neurons was completed as described previously using Fura 2-acetoxymethyl ester (2 µM; F1221, Invitrogen)<sup>73</sup>. Briefly, neurons were incubated with 2 µM Fura 2-AM for 60' followed by 30' incubation with Hanks buffered saline solution (HBSS) prior to carrier/PIP<sub>2</sub> incubation. Neurons were then incubated with either carrier alone (2 µM; Echelon Biosciences, P-9C2) or carrier + PIP<sub>2</sub> (2 µM; Echelon Biosciences, P-4516) for 15 minutes prior to imaging. Carrier and PIP<sub>2</sub> complexes were formed by incubating together in HBSS at room temperature for 15 minutes prior to use. LPA (10 µM; Avanti Polar Lipids, 857130) and KCl (100 mM; Fisher P330) were used for neuron stimulation.

## Behavioral Assays

Thermal sensitivity was measured using a Plantar Test apparatus (IITC) to heat each hindpaw and the latency for hindpaw removal was recorded. One measurement was taken for each hindpaw to determine the withdrawal latency in seconds. The radiant heat source intensity was calibrated so that the average withdrawal latency for WT mice was ~10 s. Cut off time was 20 s. Mechanical sensitivity was measured using an electronic von Frey apparatus (IITC) and a semi-flexible tip. Three measurements for each hindpaw were taken and averaged to determine the withdrawal threshold in grams. Inflammatory (CFA) and neuropathic (LPA) models of chronic pain were performed as described previously<sup>71, 77, 78</sup>. Intrathecal injections (5  $\mu$ L) were performed in unanaesthetized mice using the direct lumbar puncture method<sup>81</sup>. UNC3230 was prepared at a 0.4 mM (2 nmol in 5  $\mu$ L) in 20% DMSO (in saline).

## Results

### Assay design and development

Prior to the development of this assay, standard methods to monitor PIP5K1 activity included the use of radiolabeled ATP, thin layer chromatography, and lengthy lipid extraction protocols<sup>46, 51</sup>. To avoid lengthy lipid extraction protocols required when using eukaryotic cell lysates, we decided to use recombinant PIP5K1C and a fluorescein conjugated PI(4)P substrate in a strictly *in vitro* reaction (Figure 4.1A). Although there are no reported assays that monitor PIP<sub>2</sub> from any of the three natural substrates, there was an assay recently developed that used the



PerkinElmer LabChip microfluidic mobility shift assay (MSA) to monitor the phosphorylation of PIP<sub>2</sub> to phosphatidylinositol 3,4,5-triphosphate (PIP<sub>3</sub>) by PI3K<sup>119</sup>. Using the reported PI3K assay buffer and the PerkinElmer LabChip MSA, we were able to observe baseline separation of 1 μM fluorescein-conjugated PIP<sub>2</sub> and 1 μM fluorescein conjugated PI(4)P (both purchased from Cayman chemical and prepared in assay buffer) using ProfilerPro separation buffer with 1.5% coating reagent 8 (CR-8) (Figure 4.1B; Table 4.1). Notably, the presence of sodium cholate in the assay buffer is imperative to achieve separation and prevent aggregation of lipids (data not shown). The proprietary CR-8 allows for run-to-run separation consistency and prevents aggregation and adsorption of the substrate and kinase to the microchannel surfaces<sup>120</sup>. Baseline separation of the substrate and product indicated that the LabChip MSA would be suitable for continued assay development.

Fluorescein conjugated PI(4)P (1 μM) was incubated with 100 μM full length (668 amino acid; 90 kDa) recombinant human PIP5K1C and varying concentrations of adenosine triphosphate (ATP; three fold serial dilution starting at 1000 μM) to determine the ATP K<sub>m</sub>. The LabChip MSA was used to monitor the reactions kinetically (every 5 minutes for ~80 minutes) and Michaelis-Menten analysis revealed an ATP K<sub>m</sub> of 15 μM (Figure 4.2A, 4.2B, and Table 4.1). Next, reactions containing 1 μM PI(4), 15 μM ATP, and varying concentrations (two-fold serial dilution starting at 10 nM; 7 concentrations total) of PIP5K1C were read kinetically (every 6 minute for 45 minutes) to determine the concentration of enzyme that would give ~30% conversion of substrate to product at an end-point within the linear range of the reaction. A final concentration of 3 nM PIP5K1C and a 40-minute incubation

time were chosen (Figure 4.2C and Table 4.1). Kinase titrations were performed for every vial of enzyme purchased over the course of assay development to account for slight differences in kinase activity from lot to lot.

Given that compound libraries are dissolved in 100% DMSO, reactions containing 1  $\mu$ M PI (4), 15  $\mu$ M ATP, 3 nM PIP5K1C, and varying concentrations of DMSO (two-fold serial dilutions starting at 10%; 9 concentrations total) were performed to determine DMSO tolerance after 40 minute reactions (Figure 4.2D). There was decreased activity in reactions containing >1% DMSO indicating the final concentration of DMSO within the reaction must be lower than 1% (Figure 4.2D). Compounds are prepared as 10 mM stocks in 100% DMSO then diluted to a final concentration of 10  $\mu$ M (1:1,000) and 0.1% DMSO which is well within the DMSO tolerability of the reaction. Finalized reactions containing 1  $\mu$ M PI(4), 15  $\mu$ M ATP, 3 nM PIP5K1C, and 0.1% DMSO produce the envisioned 30% conversion of substrate to product following a 40 minute incubation, indicating completion of the assay design stage (Figure 4.2E).

Next, we transitioned this assay into a high-throughput screening format which began with automation validation using a Multidrop Combi Reagent Dispenser for delivery of the enzyme and substrate solutions. We initially observed inconsistent delivery of lipid substrate and kinase to the plate, most likely due to lipid adsorption to the silicone tubing of the Multidrop delivery cassette<sup>121</sup>. To overcome adsorption problems, a final concentration of 0.01% BSA and 0.05% DMSO were included in the enzyme and substrate solutions, respectively, to serve as carriers and mitigate adsorption<sup>122</sup> (Table 4.1). In addition, the silicone lines of the multidrop

delivery cassette were primed with 5 mL of 0.02% BSA prior to kinase dispensing and 5 mL of 1% DMSO prior to substrate dispensing. Addition of BSA and DMSO to the enzyme and substrate solutions, respectively, allowed for consistent delivery of both solutions to multiple plates (data not shown). Incorporating these changes, automation validation was completed over three days and all plates had coefficients of variation less than 10%.

### **Assay validation**

Following automation validation, HTS validation was completed using the Nanoscreen MultiMek to transfer 1% DMSO (mimics compound delivery) to each assay plate followed by Multidrop delivery of the enzyme and substrate solutions. During this stage we confirmed the plate layout for the assay in which negative controls (+90 mM EDTA in assay buffer; 100% inhibition) would occupy columns 1 and 2 while positive controls (no compound; no inhibition) would occupy columns 23 and 24. All plates were run in this manner for HTS validation and screening. HTS validation was carried out over three days, 2 plates per day. HTS validation revealed excellent assay performance with  $Z'$  values above 0.9 on all three days (Figure 4.3A). We then used the library of pharmacologically active compounds (LOPAC) as a validation library to examine reproducibility of our assay. The 1280 LOPAC compounds were run in duplicate over two days (4 plates per day). The assay was deemed excellent with respect to  $Z'$  in which all plates ranged from 0.7 to 0.9 (Figure 4.3A). The data fit with a linear regression line revealed an  $r^2$  and slope of 0.966, indicating a highly reproducible assay (Figure 4.3B).

## Screening

A kinase-focused library of 4,727 compounds that was designed and made available by the UNC Center for Integrative Chemical Biology and Drug Discovery (CICBDD) was screened at 10  $\mu$ M in 0.1% DMSO<sup>118</sup>. Results from the kinase-focused library were found to follow a normal distribution (Figure 4.4A and 4.4B). All 16 plates of the kinase library had a Z' well over 0.5 with an average Z' of 0.862 (Figure 4.4C). Compounds that exhibited inhibition greater than three standard deviations from the mean value were considered active (>80% inhibition; mean of 14% and standard deviation of 21%). There were 22 compounds that exhibited >80% inhibition of PIP5K1C and were considered active (hit rate of 0.42%; Table 4.2). Primary hits were subjected to a set of structure- and property-based filters in order to remove the compounds whose physical properties would prevent them to penetrate through the cell membrane or induce substantial cellular toxicity. We made use of a softened version of the Lipinski rule<sup>123</sup> (2+ violations of Number of H-bond donors < 6, Number of H-bond acceptors < 12, Molecular Weight between 200 and 600, ALogP < 5.5) and REOS<sup>124</sup>. Likewise, we removed compounds featuring at least one reactive or toxicity-implicated substructure. After filtering, 20 compounds remained, all of which were classified as singletons (3 or more compounds with similar structures are considered clusters) (Table 4.2).

## Hit confirmation and follow up of select inhibitors

All available active compounds were re-tested in 10-point dose response curves (in triplicate) to confirm activity and provide potency information (Table 4.2).

Compound **20** was unavailable at the time of potency testing (Table 4.2). Potency values were obtained for 18 of the 19 compounds tested, revealing an overall 90% confirmation rate for our active compounds. In addition to active compounds from the kinase library, there were 6 active compounds (inhibition >80%; after drug-likeness filtering) in the LOPAC library; however, the LOPAC library was utilized as a validation library and potency information was not obtained for these literature compounds (Table 4.3).

Of the 20 active kinase-focused library compounds, compounds **1** (UNC3230) and **2** had identical thiazole carboxamide core structures and were the most potent inhibitors of PIP5K1C ( $IC_{50}$  of 0.130 and 0.120  $\mu$ M, respectively; Figure 4.5A, 4.5B, and Table 4.2). Further optimization of the assay (incubation of kinase with compound for 20 minutes prior to the addition of kinase), using a new lot of kinase and a tighter dose response curve (10 point; 1  $\mu$ M highest concentration) gave a reproducible potency value of ~40 nM for UNC3230 (Figure 4.6B). There were 3 additional compounds with  $IC_{50}$  values less than 1  $\mu$ M and a total of 7 compounds with  $IC_{50}$  values less than 5  $\mu$ M (Table 4.2). Based on preliminary secondary screening and the nanomolar potency, we continued our focused nociceptive studies with UNC3230.

### **UNC3230 reduces membrane PIP<sub>2</sub> levels and reduces pronociceptive receptor signaling**

To assess selectivity, we screened UNC3230 against 148 kinases (see methods), covering all major branches of the kinome (Figure 4.6C). Remarkably,

UNC3230 inhibited (ProfilerPro assays) or competitively interacted (DiscoverRX binding assays) with only five other kinases at our relatively high (10  $\mu$ M) screening concentration (using 10% activity/binding remaining relative to control as the cutoff for each kinase group, except lipid kinases, where a more stringent 35% of control cutoff was used) (Figure 4.6C, Table 4.4). Based on dose-responses with the five inhibited kinases, UNC3230 showed remarkable selectivity ( $K_d < 0.2$   $\mu$ M; using competitive binding assays) for PIP5K1C and PIP4K2C (Phosphatidylinositol-5-phosphate 4-kinase, type II, gamma) (Figure 4.6D-F). PIP5K1C and PIP4K2C directly generate PIP<sub>2</sub>, albeit using different substrates; PI(4)P versus PI(5)P, respectively. Importantly, UNC3230 represents the first reported inhibitor for these lipid kinases.

Inhibition of PIP5K1C and/or PIP4K2C would be predicted to reduce PIP<sub>2</sub> levels, so we assessed how UNC3230 affected PIP<sub>2</sub> levels in DRG neurons using the PIP<sub>2</sub>-specific antibody (described in Chapter II). We found that membrane PIP<sub>2</sub> levels were significantly reduced by ~45% in DRG neurons treated with 100 nM UNC3230 (~2-fold IC<sub>50</sub>) relative to vehicle controls (Figure 4.7A and 4.7B). In addition, we found that UNC3230 significantly reduced LPA-evoked calcium signaling in cultured DRG neurons relative to vehicle (Figure 4.7C and 4.7D). KCl-evoked calcium release was not reduced indicating cell health is not contributing to the observed signaling deficits. Collectively, our data indicate that UNC3230 represents a novel pharmacological probe that can be used to inhibit two lipid kinases that directly generate PIP<sub>2</sub>. Moreover, our data suggest that UNC3230

blunts pronociceptive receptor signaling in DRG neurons in a manner that is analogous to *Pip5k1c* haploinsufficiency (Chapter II).

### **UNC3230 has antinociceptive effects when injected intrathecally**

We monitored acute thermal and mechanical sensitivity in WT mice before and shortly after i.t. administration of 2 nmol UNC3230 (limited solubility in a number of vehicle formulations prevented us from testing higher doses, data not shown). We found that paw withdrawal latency in response to radiant heating of the hindpaw was significantly increased one and two hours after i.t. injection of UNC3230 compared to controls (Figure 4.8A). In contrast, no acute effects on mechanical sensitivity were observed following UNC3230 administration (Figure 4.8B). Given that UNC3230 blunted LPA-evoked signaling, and that LPA enduringly enhances thermal and mechanical sensitivity by activating LPA receptors over a brief three hour critical period<sup>78</sup>, we next evaluated the extent to which UNC3230 could reduce LPA-evoked thermal and mechanical hypersensitivity. We administered UNC3230 (2 nmol; i.t.; versus vehicle) then 1 hour later co-injected 1 nmol LPA with UNC3230 (2 nmol, i.t.; versus vehicle). UNC3230 significantly blunted thermal hyperalgesia and mechanical allodynia compared to vehicle (Figure 4.8C and 4.8D). Next, we administered UNC3230 (2 nmol; i.t.) 2 hours before and 2 hours after injecting CFA into one hindpaw. We found that UNC3230 significantly blunted thermal hyperalgesia and mechanical allodynia in the CFA-inflamed hindpaw (relative to vehicle control) but did not affect thermal or mechanical sensitivity in the control (non-inflamed) hindpaw over a multiday time course (Figure 4.8E and 4.8F). Taken

together, these data reveal that UNC3230 has acute thermal antinociceptive effects in uninjured mice and can attenuate thermal and mechanical hypersensitivity when administered prior to the onset of LPA-evoked neuropathic pain and CFA-evoked inflammatory pain.

## Discussion

Investigation of PIP5K1C regulation of cellular processes and disease physiology has been restricted to genetic approaches to reduce kinase activity due to the lack of reported inhibitors. Current studies have utilized genetic deletion of PIP5K1C using knockout mice, targeted small interfering RNA (siRNA) and shRNA, and kinase assays that require lengthy lipid extraction protocols and radiolabeled ATP<sup>45, 46, 51, 113</sup>. Unfortunately these kinase assays have not been amenable to high throughput screening, preventing the identification of PIP5K1C inhibitors. Moreover, the use of PIP5K1C genetic knockout mice is time- and resource-intensive and limits studies to chronic deletion of the enzyme, thwarting information on acute inhibition of just the catalytic activity<sup>125</sup>. Here, we report the successful development of a high-throughput assay for PIP5K1C activity, screening of a kinase-focused library to identify inhibitors of PIP5K1C, and characterization of the most potent compound, UNC3230 in nociceptive signaling and sensitization.



**UNC3230 is a potent and selective inhibitor of UNC3230 that has activity similar to *Pip5k1c* haploinsufficiency**

UNC3230 has an *in vitro* IC<sub>50</sub> of approximately 40 nM and shows remarkable selectivity when assayed against 148 kinases that cover each branch of the kinome. For the 100 kinases screened using the DiscoverX platform, the DiscoverX Selectivity Profile score for UNC3230 was 0.12 (on a scale from 0 to 1.0)<sup>126</sup>. To put this value in context, of 38 kinase inhibitors (several of them FDA-approved) benchmarked in this assay at 3 μM<sup>126</sup>, a majority (n=22) were less selective than UNC3230. The only other kinase UNC3230 inhibited with equal or greater potency was PIP4K2C, another enzyme that synthesizes PI(4,5)P<sub>2</sub>. In contrast to PIP5K1C, PIP4K2C phosphorylates PI(5)P which is at least 10x less abundant than PI(4)P<sup>67, 111</sup>. Given that PI(4)P is at much higher concentrations, the ~50% reduction in PIP<sub>2</sub> in DRG neurons following incubation with UNC3230 is most likely due to inhibition of PIP5K1C rather than PIP4K2C. Notably, UNC3230 did not interact with PIP5K1A at 10 μM, a PIP5K family member that is highly similar (69% amino acid identity across the entire protein and 82% identity within the kinase core domain) to PIP5K1C (Figure 4.9) Moreover, UNC3230 did not inhibit any of the other lipid kinases that regulate phosphoinositide levels, including phosphatidylinositol-4,5-bisphosphate 3-kinases (PIK3s, also known as PI3Ks) (Table 4.4). Note, PIP4K2C should not be confused with phosphatidylinositol 4-kinases (PI4Ks) that generate PI(4)P from phosphatidylinositol and that can be inhibited by wortmannin and phenylarsine oxide (PAO; Figure 4.9)<sup>127</sup>.

The most important finding of this Chapter is that PIP5K1C pharmacological inhibition with a small molecule reduces pronociceptive signaling analogous to reductions observed in the *Pip5k1c* haploinsufficiency model (Chapter II). This indicates that reduction of catalytic activity in adult neurons is sufficient for reducing the activity of pronociceptive receptors. Importantly, intrathecal injection of UNC3230 has antinociceptive effects in response to thermal stimuli. Furthermore, administration of UNC3230 just prior to induction of LPA-induced neuropathic pain or CFA-induced inflammatory pain (and a second co-injection with LPA and second injection 2 hour following CFA administration) attenuates nociceptive sensitization. It is worth noting that reductions in nociceptive sensitization following nerve injury and inflammation were less pronounced following UNC3230 administration compared to reductions observed in the *Pip5k1c* haploinsufficiency model, particularly reductions in mechanical sensitivity. This could be due to other phenotypes that were observed in the *Pip5k1c* haploinsufficiency model such as alterations to actin and tubulin dynamics that have yet to be evaluated following UNC3230 treatment. Likewise differing phenotypes may arise from chronic inhibition of catalytic activity and/or deletion of the PIP5K1C protein in the haploinsufficiency model that are not present following acute inhibition with a small molecule (Chapter II). To evaluate differences between acute and chronic inhibition (Chapter II), additional experiments are needed including evaluation of actin and tubulin dynamics, TRPV1-mediated calcium imaging, and ion channel-mediated neuronal excitability in DRG neurons incubated with UNC3230. These experiments will allow for more in-depth comparison between pharmacological inhibition and genetic deletion. Furthermore, in order to make

reliable assessments of differences/similarities of UNC3230 and *Pip5k1c* haploinsufficiency in models of chronic pain, the models should be performed with WT mice receiving vehicle, WT mice receiving UNC3230, and *Pip5k1c*<sup>+/-</sup> receiving vehicle simultaneously. Importantly, further characterization of UNC3230 is still ongoing, including evaluation of UNC3230's potential to reduce DRG neuronal excitability, the predominant mediator of prolonged pain hypersensitivity.

### **UNC3230 provides a scaffold for future compound development**

Unfortunately, UNC3230 has aqueous solubility issues that prevented in-depth analysis of the compound at a wide range of concentrations *in vitro* and *in vivo*, highlighting the need for medicinal chemistry optimization to increase solubility while maintaining or enhancing potency and selectivity. Unlike the PIP4K2s, there are no crystal structures of any of the PIP5K1s making structure-guided drug design difficult<sup>117</sup>; however, standard structure-activity relationship (SAR) studies are feasible and ongoing. Although there are no crystal structures available for PIP5K1Cs, it may be possible to generate a homology model using the crystal structure of PIP4K2C to aid in drug discovery efforts<sup>128, 129</sup>. Unfortunately, the sequence homology between PIP4K2C and PIP5K1C is only ~33% which is not considered ideal and will most likely prevent obtaining reliable and detailed information on UNC3230 interactions with PIP5K1C based on PIP4K2C<sup>128, 129</sup>. Nonetheless, we know that UNC3230 potently inhibits PIP4K2C and not PIP4K2A and we may be able to use computational modeling and the known crystal structures of PIP4K2A and PIP4K2C to determine possible interaction sites of UNC3230 with

PIP4K2C that are different from PIP5K2A and may be similar to PIP5K1C. The developed assay will allow for high-throughput evaluation of analogues derived from the identified thiazole carboxamide core structure as well as any other core structures identified via additional screening.

### **Implications for phosphoinositide signaling studies**

Although we describe the characterization of UNC3230 in pain signaling and sensitization, studies of UNC3230 in other PIP5K1C-regulated cellular processes are needed. Current techniques in the field of PIP5K1C-regulated cellular processes depend on overexpression of phosphatases and kinases that transiently eliminate or synthesize PIP<sub>2</sub>, respectively<sup>113, 130, 131</sup>. The identified inhibitors provide a new tool for these studies that eliminates the need for overexpression and allows transient inhibition while maintaining physiologically relevant protein levels of the phosphatase and kinases in the PI pathway.

As mentioned previously, many previous studies investigated the roles of PIP5K1C have relied on genetic deletion in mice that chronically eliminates the kinase which prevents understanding alterations of cellular processes following acute inhibition. Previous attempts to study differences in acute and chronic inhibition have relied on overexpression of PIP5K1 constructs containing a kinase dead mutation via transient transfection<sup>83</sup>. This is not ideal for many cell types including our cell type of interest, DRG neurons, due to an inability to transiently transfect cells with high efficiency (data not shown). DRG neurons can be transduced using lentiviral vectors; however making kinase dead mutant expression

constructs is time-intensive and prevents efforts to evaluate endogenous levels of PIP5K1s (data not shown). UNC3230 can now be used in DRG neurons to elucidate which cellular processes are affected by chronic inhibition or non-catalytic functions of PIP5K1C. Moreover, small molecule inhibitors provide a complementary pharmacological approach to reinforce findings from previously used genetic techniques, as we have demonstrated <sup>125</sup>.

### **High throughput screening assay can be expanded to include other lipid kinases**

The developed assay can be extended to the study of other lipid kinases that play important roles in cellular signaling and disease pathology. The only limitation to expansion of this assay is availability of fluorescently conjugated substrates and recombinant proteins. However, many fluorescently labeled lipid substrates are available for purchase from a variety of vendors and recombinant proteins are routinely expressed and purified from baculovirus and bacterial systems. Furthermore, this new assay can be expanded to screen larger-scale libraries such as the 100K Diversity compound library (available at the UNC CICBDD) to provide additional scaffolds for continued development of PIP5K1C inhibitors for analgesic drug development.

## Tables

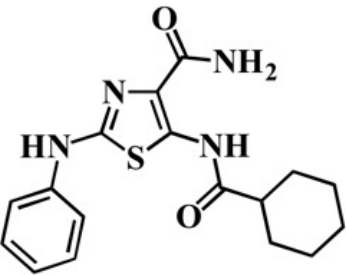
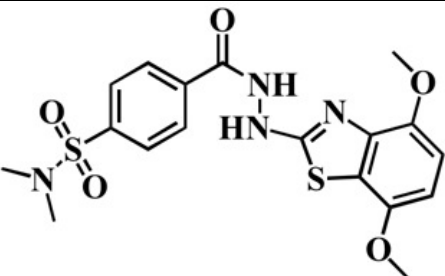
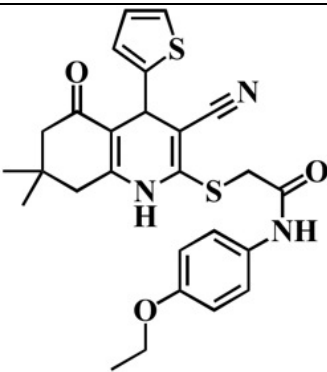
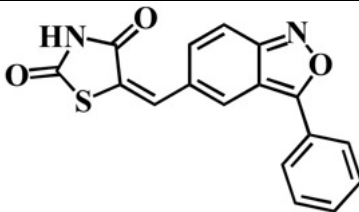
**Table 4.1. PIP5K1C HTS microfluidic mobility shift assay conditions.**

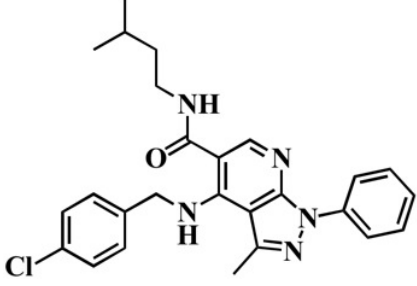
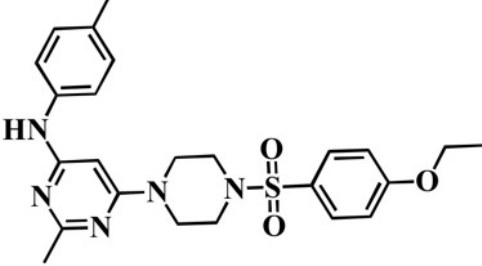
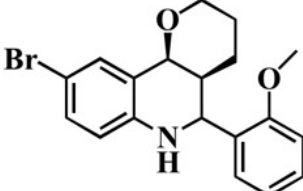
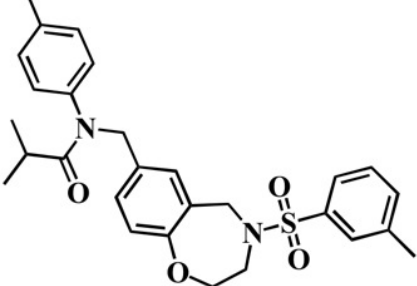
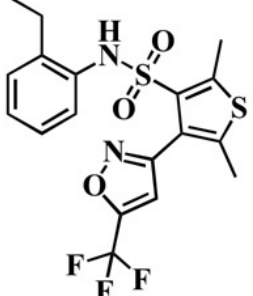
Assay buffer	50 mM MOPS, pH 6.5, 500 $\mu$ M sodium cholate, 10 mM $MgCl_2$ , 25 mM NaCl
Separation buffer	ProfilerPro separation buffer with 1.5% coating reagent 8 (CR-8)
Separation conditions	-2000 V downstream voltage, -500 V upstream voltage, -2.0 psi pressure, post-sample sip time of 120 seconds, final delay of 120 seconds.
Enzyme *	3 nM, prepared in assay buffer with 0.01% BSA (fatty acid free), 1 mM DTT, 1x protease inhibitors, 1x phosphatase inhibitors
Substrate	1 $\mu$ M prepared in assay buffer with 0.05% DMSO and 15 $\mu$ M ATP ( $K_m$ )
Endpoint assay setup	9 $\mu$ L 2x enzyme solution added to compound plate (2 $\mu$ L in 100% DMSO), incubate 10 minutes, 9 $\mu$ L 2x substrate solution added, incubate 40 minutes, 10 $\mu$ L stop solution added
Incubation	40 minutes at room temperature
Reaction plate	Nunc shallow 384 well
Stop solution	90 mM EDTA, pH 8.0 in assay buffer

\*Enzyme concentration is lot specific and must be titrated for each lot

**Table 4.2. Active compounds from the kinase-focused library.**

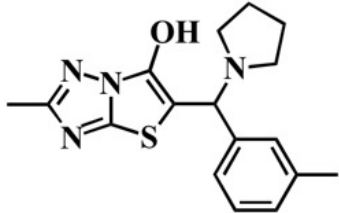
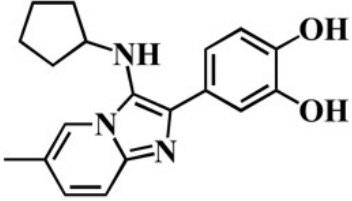
Active compound that passed drug-likeness filtering (22):

Compound #	Molecule	Inhibition (%) at 10 $\mu$ M (initial screen)	IC <sub>50</sub> ( $\mu$ M; mean $\pm$ SD)
1		94	0.12 $\pm$ 0.03
2	Not disclosed	93	0.13 $\pm$ 0.03
3		81	0.22 $\pm$ 0.01
4		81	0.23 $\pm$ 0.01
5		91	0.90 $\pm$ 0.08
6	Not disclosed	83	1.2 $\pm$ 0.06
7	Not disclosed	89	2.2 $\pm$ 1.0

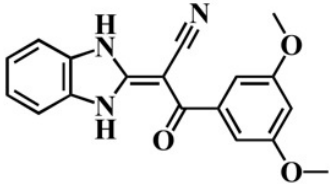
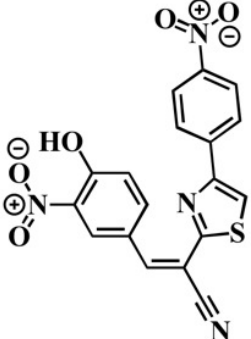
8		83	$5.1 \pm 0.77$
9		80	$6.1 \pm 0.44$
10		83	$6.2 \pm 0.35$
11		88	$6.5 \pm 0.64$
12		83	$7.3 \pm 0.21$



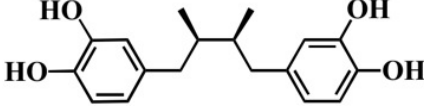
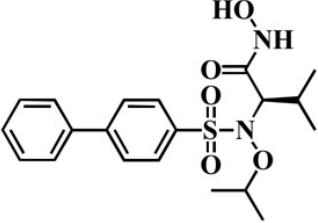
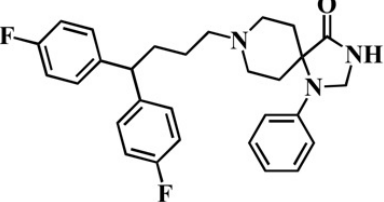
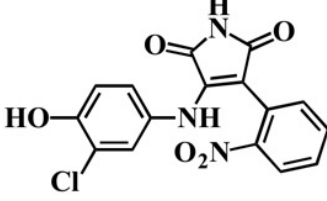

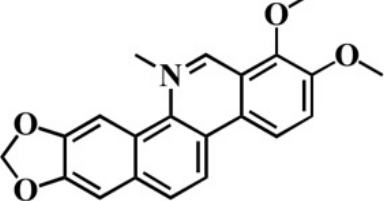
13		80	$7.9 \pm 1.2$
14		81	$9.1 \pm 0.56$
15		101	$9.6 \pm 0.77$
16		80	$9.7 \pm 0.31$
17		81	$10 \pm 0$
18		87	$10 \pm 0$

19		89	Not active
20		95	Not available for testing

Active compound that did **not** pass drug-likeness filtering (2)

21		81	Not tested
22		88	Not tested

**Table 4.3. Active compound from the LOPAC library.**

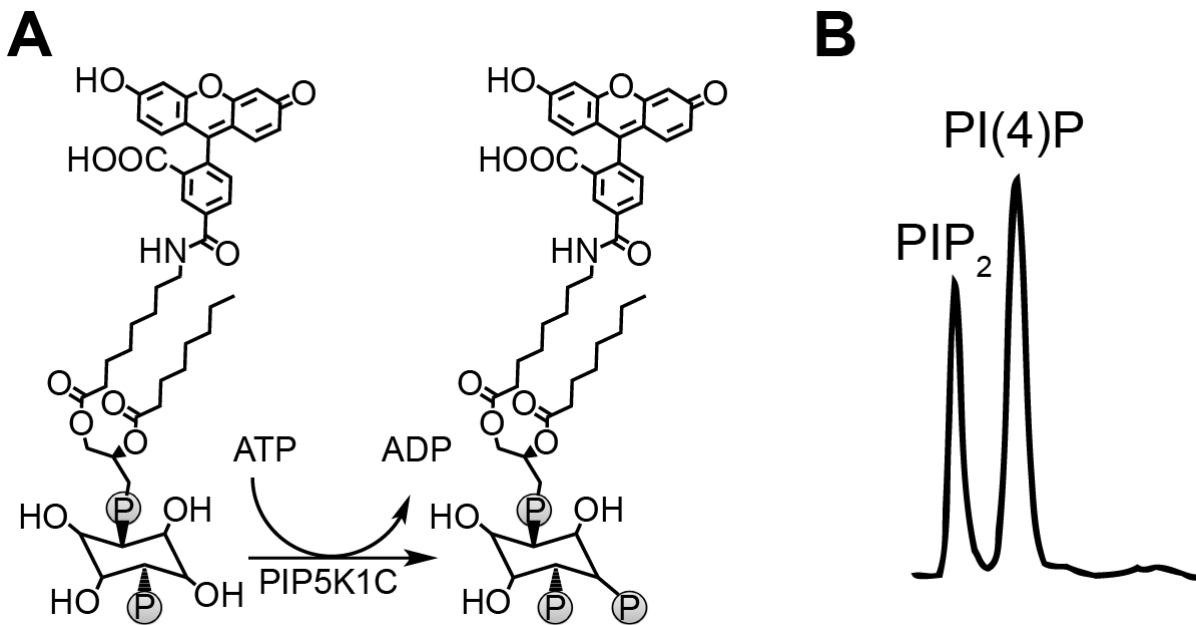
Molecule	Name	Description from LOPAC library	Inhibition (%) in PIP5K1C screen
	Nordihydroguaiaretic acid from <i>Larrea divaricata</i>	Lipoxygenase inhibitor	96
	ARP 101	A matrix metalloproteinase 2 (MMP-2) selective inhibitor.	92
	Fluspirilene	Dopamine receptor antagonist; antipsychotic	90
	SB 415286	Competitive glycogen synthase kinase-3 (GSK-3) inhibitor.	90
	BIO	Potent, selective, and ATP-competitive GSK3alpha/beta inhibitor.	89
	Chelerythrine chloride	PKC inhibitor	89

**Table 4.4. Kinases screened for UNC3230 selectivity. Numbers represent % activity/binding remaining in the presence of 10  $\mu$ M UNC3230.**

<b>AGC</b>		<b>CMGK</b>		<b>TK</b>	
AKT1	92*	CDK16	94	ABL	92*
AKT2	98*	CDK19	100	ALK	54
CDC42BPA	98	CDK2	93*	AXL	75
DMPK	91	CDK3	100	BTK	102*
GRK1	96	CDK7	85	CSF1R	100
P70S6K	74*	CDK9	99	EGFR	98
PDPK1	100	DYRK1A	12	EPHA2	100
PRKACA	99*	DYRK1B	16	ERBB2	97
PRKCB	109*	GSK3B	88, 57*	FGFR1	96*
PRKCD	87	MAPK1	109*	FGFR2	100
PRKCE	100	MAPK10	5.4	FLT3	90*
PRKCG	105*	MAPK11	95	FYN	88*
PRKCZ	94*	MAPK14	88, 130*	INSR	100*
ROCK2	99*	MAPK3	91*	ITK	94
RPS6KA5	96*	MAPK8	32	JAK2	70
RPS6KA3	85	MAPK9	15	JAK3	94
RPS6KA1	85*	SRPK3	100	KDR	100*
RPS6KB1	74*			KIT	100
SGK1	8, 23*	<b>LIPID</b>		LCK	93*
STK32C	80	PI4KB	67	LYN	97*
		PIK3C2B	78	MET	75*
		PIK3C2G	93	MUSK	100
<b>ATYPICAL</b>		PIK3CA	77	NTRK1	99
ADCK3	35	PIK3CB	95	NTRK2	83
PDK2	93*	PIK3CD	90	NTRK3	89
RIOK1	92	PIK3CG	82	PDGFRA	81
TRPM6	67	PIP4K2B	100	PDGFRB	100
		PIP4K2C	14	PTK2	97
<b>CAMK</b>		PIP5K1A	100	PTK2B	99
CAMK2A	98	PIP5K1C	7	RET	100
CAMK2G	85*			SRC	95*
CAMK4	93*	<b>OTHER</b>		SRMS	81
CHEK2	2.7	AAK1	47	SYK	93*
CHK1	101*	AURKA	76*	TEC	89
DCLK1	87	AURKB	91	TIE1	91
MAPKAPK2	85*	CHUK	82	TYK2	86
MAPKAPK5	89*	IKBKB	100	TYRO3	94
MARK1	89*	PLK1	73	ZAP70	89
MARK3	100, 93*	ULK2	79		
MKNK1	95				
MKNK2	46	<b>STE</b>		<b>TLK</b>	
MYLK3	46	MAP2K1	89	ACVR1B	89
NUAK2	100	MAP2K2	82	BMPR2	80
PHKG1	60	MAP3K4	93	BRAF	94
PHKG2	88	MAP4K4	28, 27*	IRAK4	93*
PIM2	82*	MINK1	35	LIMK1	100
PRKD1	84	MYO3A	64	MAP3K9	74
STK11	100	MYO3B	49	RAF1	91*
TSSK1B	76	PAK1	92	TGFBR1	96
		PAK2	99*		
<b>CK1</b>		PAK4	60		
CSNK1D	6.8, 54*	STK3	100*		
CSNK1G2	28				

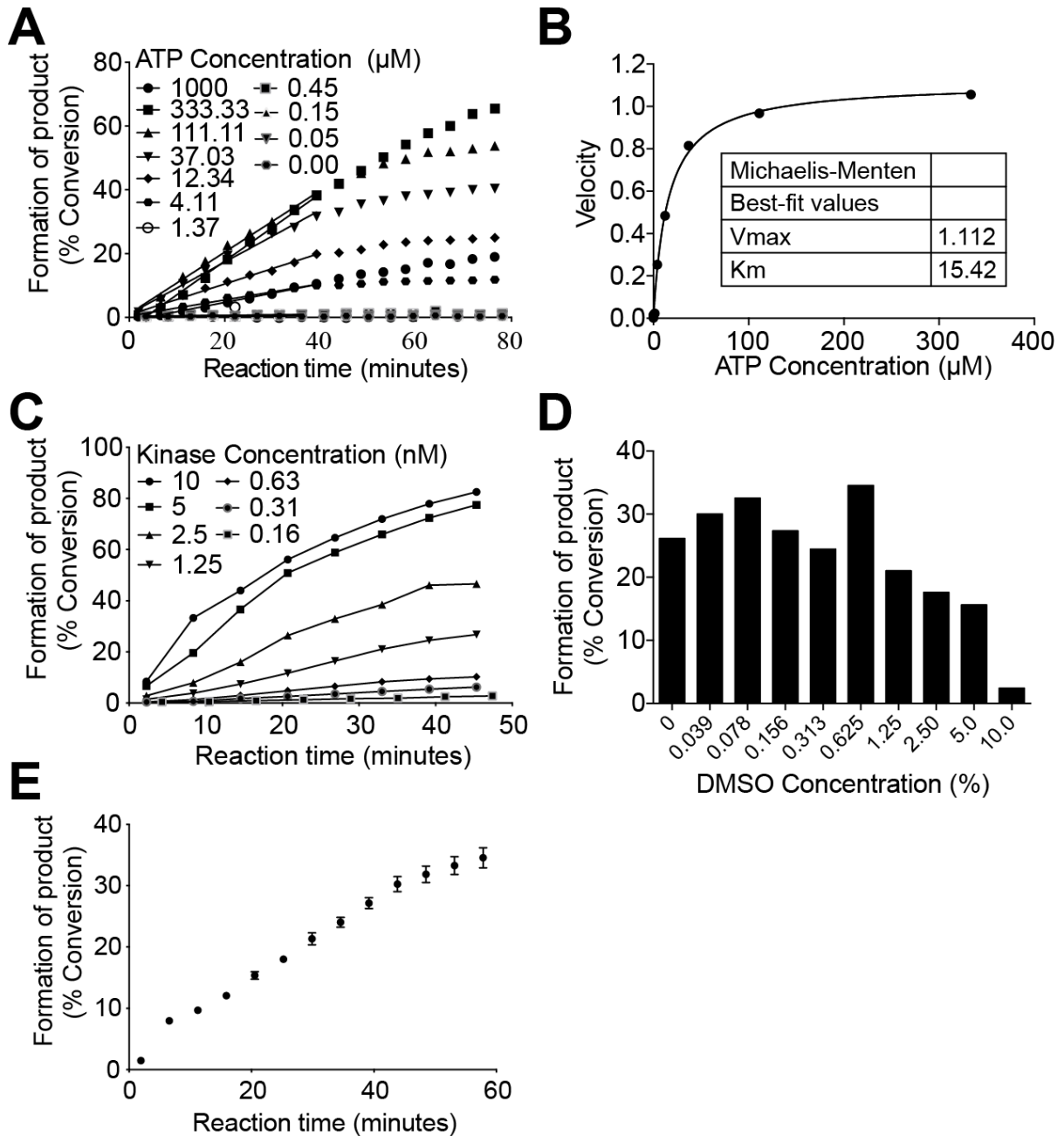
\* Screened using the PerkinElmer ProfilerPro assay, all others screened using the DiscoverX KINOMEScan assay.

## Figures



**Figure 4.1. Recombinant PIP5K1C can be used to generate fluorescein conjugated PIP<sub>2</sub> from fluorescein conjugated PI(4)P.**

(A) Schematic representation of the PIP5K1C reaction using fluorescein conjugated PI(4)P as the substrate. (B) PerkinElmer LabChip EZ Reader II and microfluidic platform can be used to achieve baseline separation of the fluorescein conjugated substrate, PI(4)P, and fluorescein conjugated product, PIP<sub>2</sub>.



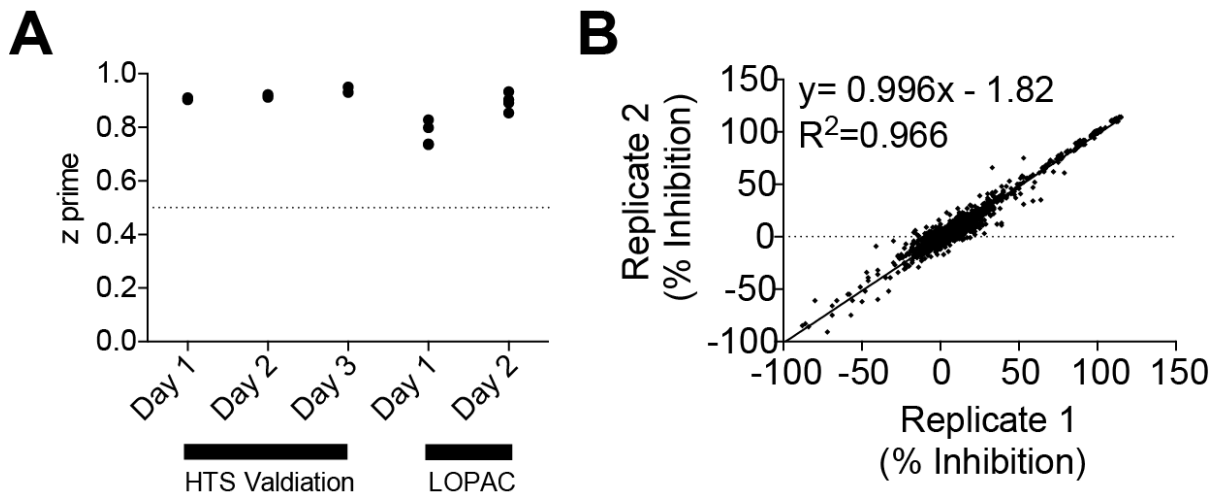
**Figure 4.2. PIP5K1C assay development to determine kinase concentration, ATP Km, and DMSO sensitivity.**

**(A)** Progression curves for PIP5K1C reactions with varying concentrations of ATP.

**(B)** Michaelis-Menten analysis of initial rates in **(A)** to determine ATP Km for PIP5K1C.

**(C)** Progression curves for PIP5K1C with varying concentrations of

PIP5K1C to determine the optimal kinase concentration to obtain ~30% conversion after 40-minute incubation. **(D)** Percent conversion of PIP5K1C reactions at various DMSO concentrations after 40-minute incubation to determine DMSO sensitivity of the reaction. **(E)** Final progression curve for reactions containing all optimized parameters. Mean  $\pm$  SEM. n=12 reactions. **(A-E)** Percent conversion of substrate to product is calculated using PerkinElmer EZ Reader II software.

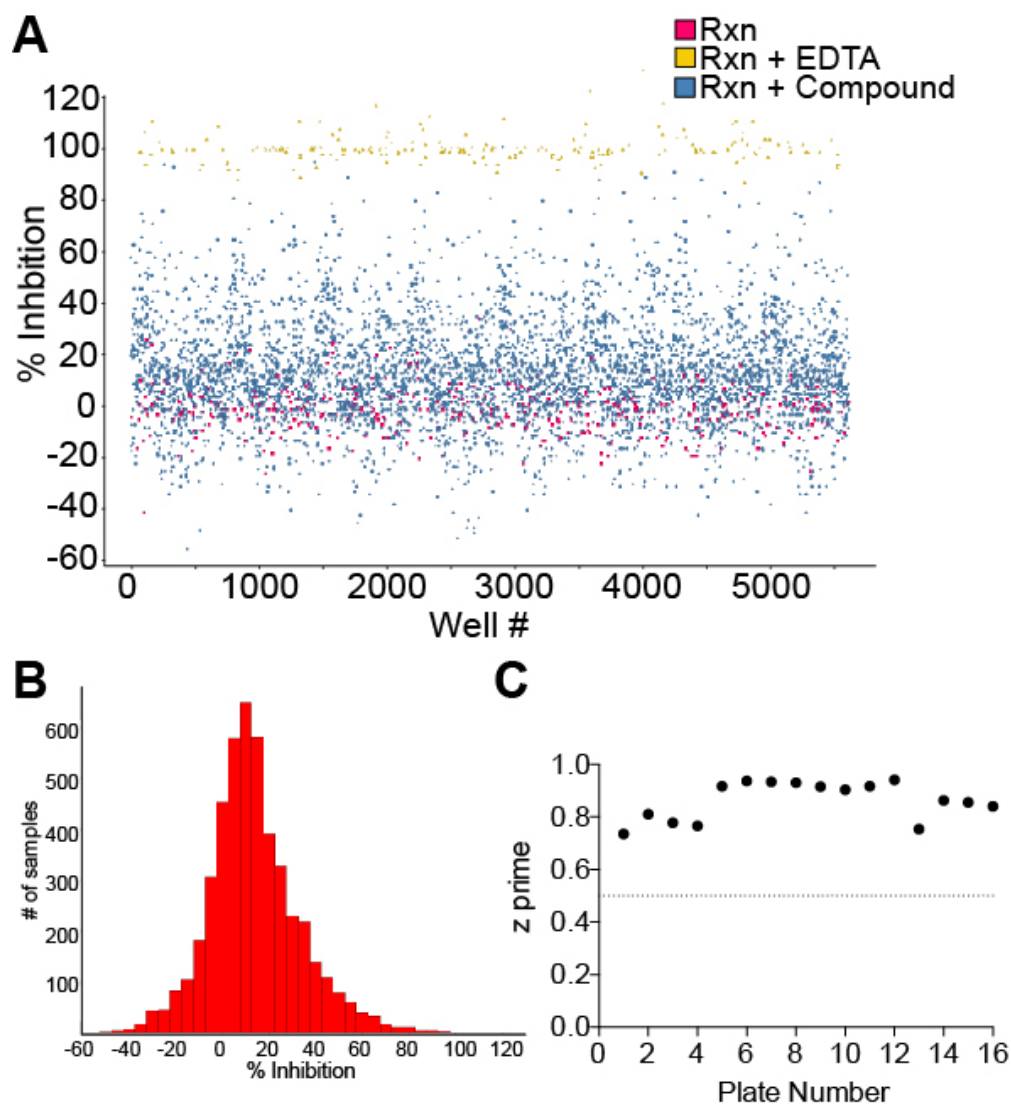


**Figure 4.3. Assay validation using the LOPAC library.**

**(A)** The common assay performance measurement,  $z'$ , for 6 plates (over 3 days) of HTS validation and 4 plates of the LOPAC library in duplicate (2 days). **(B)**

Duplicate runs (each on a different axis) of the LOPAC library (1280 compounds) to assess reproducibility of the developed assay. Data are presented as % inhibition calculated by on-plate controls.



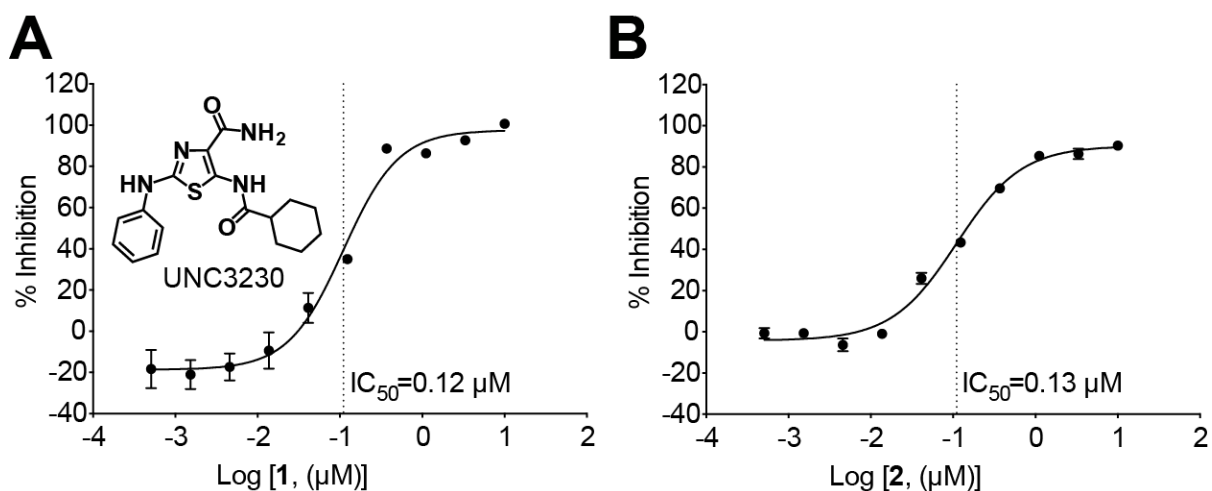


**Figure 4.4. HTS of 4,727 compound kinase-focused library.**

**(A)** PIP5K1C reactions (expressed as % inhibition determined by on-plate controls) for each well of the assay including all negative (yellow) and positive controls (red).

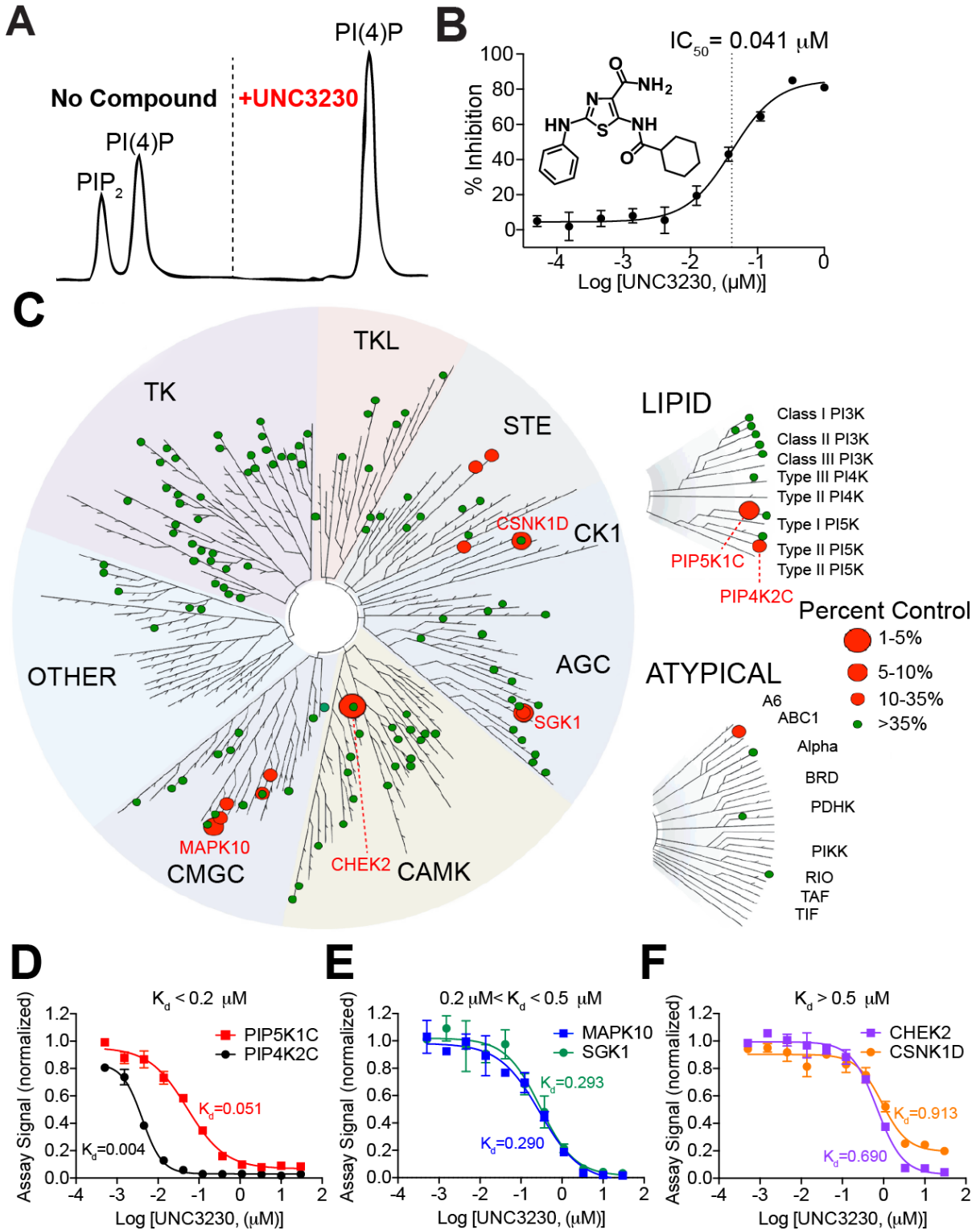
**(B)** Distribution of compound activity for the kinase-focused library. The number of compounds with a given activity level (% inhibition) are plotted in a frequency histogram.

**(C)**  $z'$  values for each of the 16 plates of the kinase-focused library.



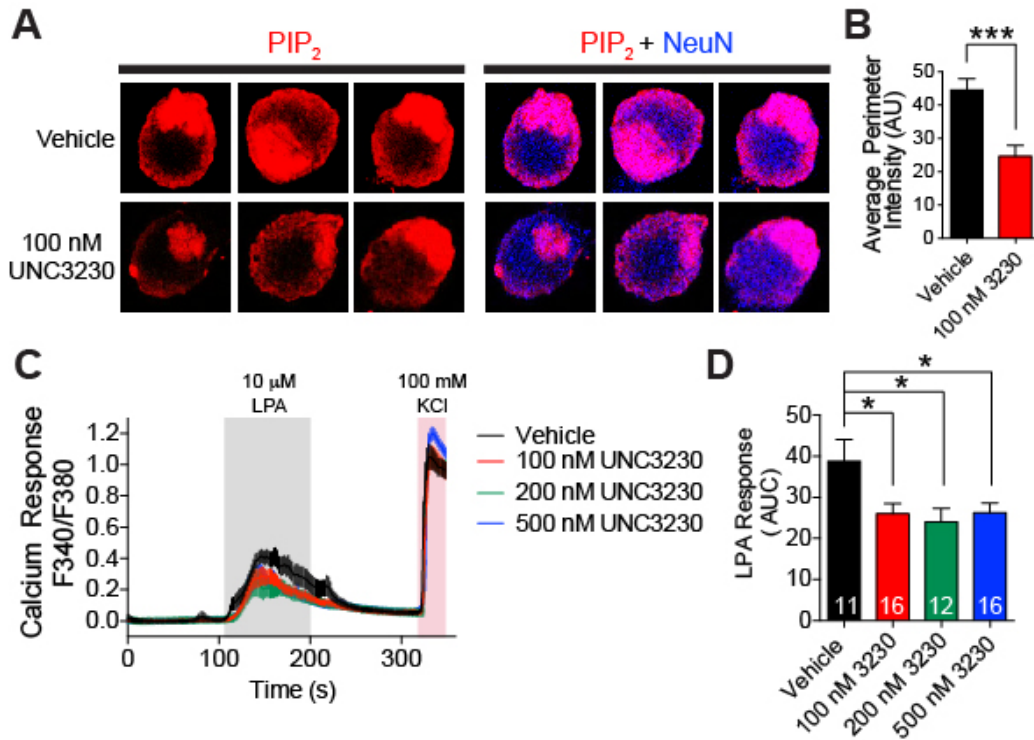
**Figure 4.5. The two most potent inhibitors of PIP5K1C have the same core structure and nanomolar potency.**

**(A)** Compound **1** (also referred to as UNC1 in abstract and UNC3230) and **(B)** Compound **2** two are the two most potent compounds identified and have the same thiazole carboxamide core structure with IC<sub>50</sub> values of 130 and 120 nM, respectively. Data are presented as mean ± SD.



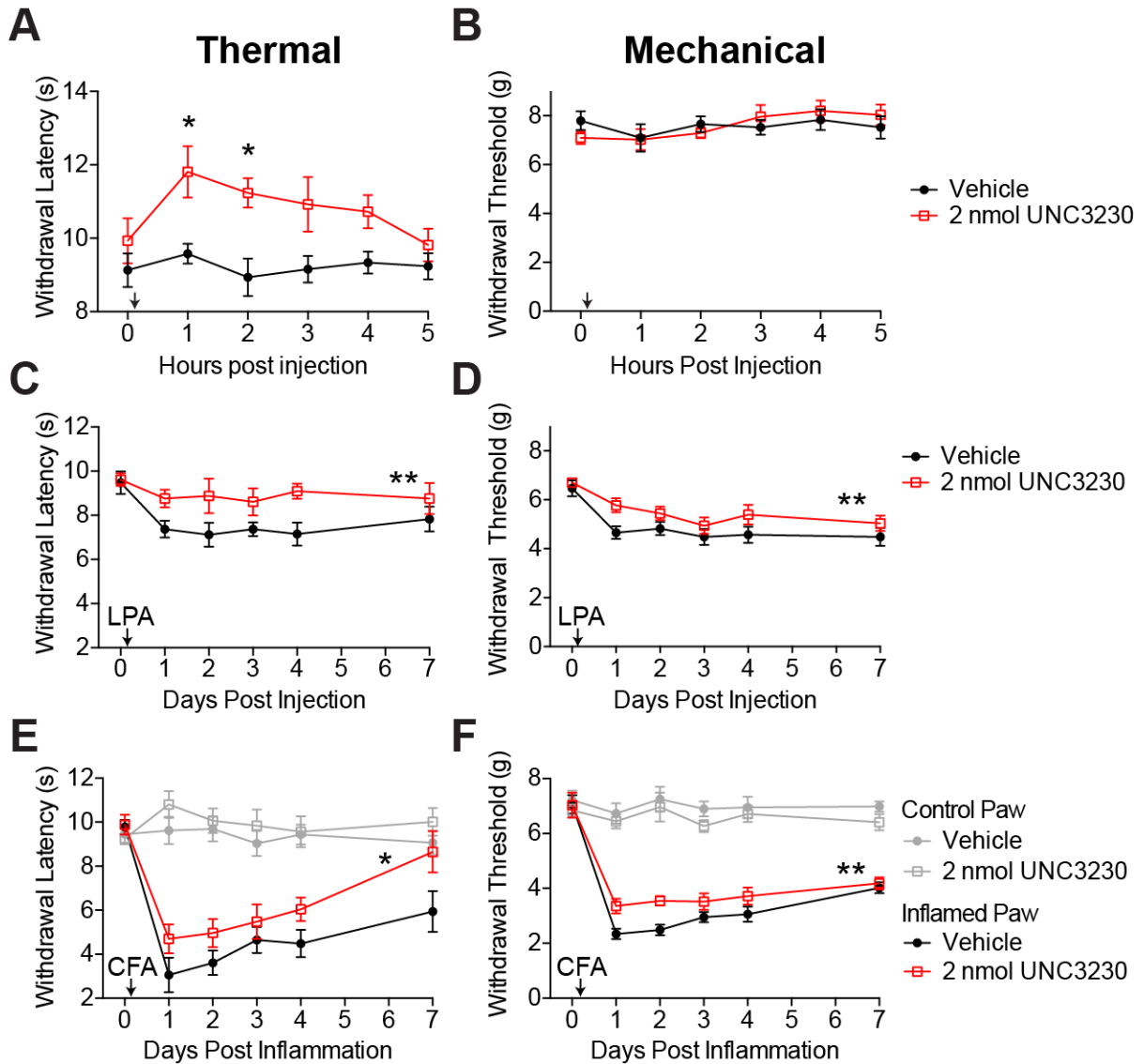
**Figure 4.6. UNC3230 is a selective small molecule PIP5K1C inhibitor.**

**(A)** Representative traces showing substrate and product peak separation in assay performed  $\pm$  UNC3230 (10  $\mu$ M). **(B)** UNC3230 structure and inhibitory concentration-50 ( $IC_{50}$ ) dose-response curve, using LabChip assay. **(C)** Selectivity of UNC3230 relative to a diverse panel of kinases, using ProfilerPro (48 kinases) and KINOMEScan (100 kinases) assays. Table 1 lists all kinases that were tested. Circle size and color reflects percent activity/binding remaining in the presence of UNC3230 (10  $\mu$ M) relative to controls. Branches without circles denote kinases that were not tested. AGC: Containing PKA, PKG, PKC families; CAMK: Calcium/calmodulin-dependent protein kinase; CK1: Casein kinase 1; CMGC: Containing CDK, MAPK, GSK3, CLK families; STE: Homologs of yeast Sterile 7, Sterile 11, Sterile 20 kinases; TK: Tyrosine kinase; TKL: Tyrosine kinase-like. Image generated using TREEspot™ Software Tool and reprinted with permission from KINOMEScan®, a division of DiscoverRx Corporation, © DISCOVERX CORPORATION 2010. **(D-F)** KINOMEScan competitive binding assays with multiple doses of UNC3230, presented from **(D)** strongest  $K_d$  to **(F)** weakest  $K_d$ . All data are mean  $\pm$  SEM.



**Figure 4.7. UNC3230 reduces membrane PIP<sub>2</sub> levels in DRG neurons and GPCR signaling.**

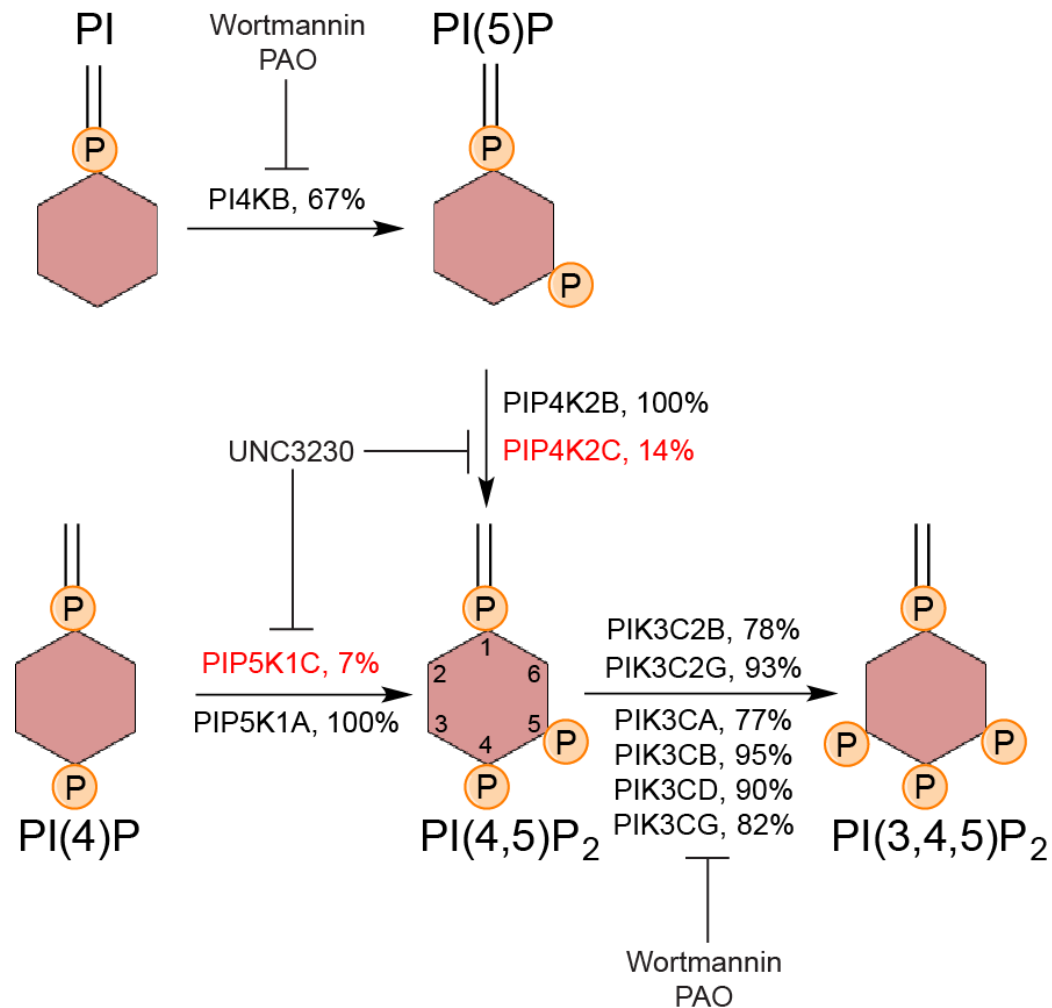
**(A)** PIP<sub>2</sub> antibody staining of WT DRG neurons after incubating with vehicle (0.002% DMSO) or 100 nM UNC3230 for 20 h. Co-stained with the neuronal marker NeuN (blue). **(B)** Quantification of the average perimeter (membrane) intensity. n=30-40 neurons per condition. **(C)** LPA-evoked calcium response in WT DRG neurons after incubating with vehicle or the indicated concentrations of UNC3230 for 20 h. After stimulation, cultures were washed with HBSS for 120 s to remove LPA, then stimulated for 30 s with 100 mM KCl to confirm neuron identity. **(D)** Quantification of the LPA-evoked calcium response by measuring the AUC of each responding neuron. Number of neurons quantified is indicated in bar graph. Data are mean ± SEM. \*p<0.005, \*\*\*p<0.005.



**Figure 4.8. UNC3230 reduces thermal and mechanical sensitization in models of chronic pain.**

(A) Thermal and (B) mechanical sensitivity of WT mice after administering vehicle or 2 nmol UNC3230 (i.t.). Arrow indicates injection. n=10 male mice per group. (C) Thermal and (D) mechanical sensitivity of WT mice in the LPA-induced neuropathic pain model. Vehicle or 2 nmol UNC3230 were administered i.t. One hour later, vehicle or 2 nmol UNC3230 was administered i.t. with 1 nmol LPA. n=10 male mice

per group. **(E)** Thermal and **(F)** mechanical sensitivity of WT mice in the CFA model of inflammatory pain. Vehicle or 2 nmol UNC3230 were administered i.t. Two hours later, CFA was injected into one hindpaw of each animal. The other hindpaw was not inflamed and served as a control. Vehicle or 2 nmol UNC3230 was administered (i.t.) 2 hours after CFA injection. n=10 male mice per group. **(A)** Unpaired t-tests were used to assess differences at each hour. **(C-F)** One-way ANOVAs were used to assess treatment effect over the 7-day time course. All data are mean  $\pm$  SEM. \*p<0.05, \*\*p<0.005.



**Figure 4.9. Selectivity of UNC3230 relative to lipid kinases that generate phosphoinositides.**

Shown are the gene symbols and percent activity/binding remaining in the presence of 10  $\mu$ M UNC3230 (dose-response curves were generated for the kinases shown in red; see Figure 4). Additional lipid kinases generate phosphoinositides (not shown; because recombinant versions were not available for testing). UNC3230 inhibits PIP4K2C and PIP5K1C. These lipid kinases generate PIP<sub>2</sub> directly from PI(5)P and PI(4)P, respectively. Wortmannin and phenylarsine oxide (PAO) inhibit lipid kinases that generate PI(4)P and PI(3,4,5)P<sub>2</sub>. PI = phosphatidylinositol.



## **Chapter V**

### **DISCUSSION AND PERSPECTIVE**

#### **Summary and Scope**

Nociceptive pain is essential for survival, protecting against harmful stimuli and promoting avoidance of harmful situations<sup>10, 12</sup>. However, peripheral sensitization of neurons within the nociceptive system during nerve injury or inflammation leads to the development of maladaptive chronic pain<sup>4, 6, 10, 12</sup>. Chronic pain affects more than 35% of adults in the United States and costs over \$600 billion to treat annually<sup>1</sup>, largely due to loss of productivity costs from patients' inability to complete daily tasks. Furthermore, the staggering treatment cost is worsened by ineffective therapeutic options that require lengthy treatment duration<sup>1</sup>. In addition to being ineffective, current first-line therapeutics have harmful side effects such as opioid dependence, NSAID-induced gastrointestinal bleeding and hepatotoxicity (acetaminophen), highlighting the need for novel analgesic drug development<sup>2</sup>.

In order to develop more effective analgesic options, the underlying signaling mechanisms of pain pathology need to be thoroughly investigated to identify novel therapeutic targets. However, the complexity of the nociceptive system makes this a difficult task; there are many causes of pain, each of which activates a variety of nociceptive pathways via multiple pronociceptive receptors and ion channels. In

addition to the complexity of nociceptive pathway activation, the sensitization process that mediates chronic pain adds an additional level of complexity, occurring peripherally and/or centrally. Recent analgesic drug discovery efforts targeting individual pronociceptive receptors have been plagued by lack of efficacy, most likely due to the diversity of receptors and pain modalities<sup>3</sup>. One of the pronociceptive receptors recently targeted for analgesic drug development is the TRPV1 ion channel. TRPV1 functions both as a noxious heat detector and as a pH sensor following nerve injury and inflammation, in which the pH decreases<sup>3</sup>. Notably, antagonists of TRPV1 exhibit reductions in hyperalgesia in preclinical models of chronic pain; however, when evaluated in human clinical trials, TRPV1 antagonism results in severe hyperthermia. This interference with TRPV1-mediated thermoregulation has prevented regulatory approval for the use of TRPV1 antagonists as therapeutics in the clinic<sup>132, 133</sup>. Other compounds that have showed modest efficacy in preclinical models include antagonists of prostanoid receptors which are activated by prostaglandin E<sub>2</sub> during inflammation<sup>134</sup>, neurokinin-1 receptor which is activated by substance P following injury and inflammation<sup>135</sup>, bradykinin 1 receptor which is activated during inflammation<sup>136</sup> and tyrosine receptor kinase receptor A (TrkA) which is activated by nerve growth factor (NGF) following injury and inflammation<sup>137</sup>. Unfortunately, antagonism of any of these receptors has yet to yield effective analgesics for use in humans. Once again, lack of efficacy is likely due to the receptor diversity within the nociceptive system, the diversity of signaling mechanisms involved in each pain modality, and detrimental on-target effects on other physiological processes including cardiovascular function<sup>3, 134</sup>.

A more recent approach to overcome issues with receptor diversity has been to focus on signaling proteins that are downstream of these receptors such as protein kinase C epsilon (PKC $\epsilon$ ) and mitogen-activated protein kinases (MAPKs). Although inhibitors of these kinases have exhibited reduced thermal hyperalgesia and mechanical allodynia in rodent models of chronic pain, their efficacy did not translate to use in humans<sup>55, 58, 59</sup>. Furthermore, ubiquitous expression of these downstream effectors may limit their future use due to unwanted, on-target effects in other tissues.

This work aimed to characterize a novel molecular target in nociceptive neurons that could provide an exciting new direction for analgesic drug development, bypassing the inefficiency and adverse side effects of previous efforts. We used genetic approaches to characterize the role of PIP5K1C in nociceptive signaling and sensitization and developed a small molecule inhibitor to pharmacologically validate PIP5K1C as a novel target for analgesic drug development. The major findings of this work are 1) PIP5K1C is a critical regulator of nociceptive signaling and sensitization, acting via synthesis of PIP<sub>2</sub> which is at a critical convergence point for many pain promoting pathways, 2) development of a high-throughput assay identified the first reported inhibitor of PIP5K1C (UNC3230), an approach that could be extended to other novel kinases that modulate pain, 3) UNC3230 is a potent and selective inhibitor of PIP5K1C that reduces pronociceptive signaling similar in magnitude to reductions observed in a *Pip5k1c* haploinsufficiency model and 4) reductions in PIP5K1C catalytic activity, either via genetic or

pharmacological approaches, profoundly reduces thermal and mechanical nociceptive sensitization in multiple rodent models of chronic pain.

The major implications of this work include the identification of a novel regulatory kinase in the complex nociceptive system, which will promote future studies of lipid kinases in nociceptive signaling, and the validation of PIP5K1C as an analgesic drug target, which provides the critical foundational work to guide future analgesic drug development. Importantly, the restricted expression of PIP5K1C in neurons may eliminate many of the unwanted side effects observed with antagonism of other pronociceptive receptors and previously studied downstream effectors that are ubiquitously expressed. In addition, PIP<sub>2</sub> and PIP5K1C represent a central regulatory point for multiple pain promoting pathways, which could allow inhibitors of PIP5K1C to overcome issues of receptor and pathway diversity that have plagued previous analgesic drug development strategies.

### **Key Findings**

This work provides the first evidence that PIP5K1C generates at least half of all PIP<sub>2</sub> in DRG neurons. Furthermore, PIP5K1C is an important regulator of nociceptive signaling and sensitization, including thermal and mechanical hypersensitivity in models of neuropathic and inflammatory pain<sup>1</sup>. These conclusions are supported by experiments with *Pip5k1c*<sup>+/-</sup> mice and with a small molecule inhibitor of PIP5K1C. *Pip5k1c* haploinsufficiency reduced PIP<sub>2</sub> levels in adult DRG by ~50% without affecting PIP<sub>2</sub> levels in adult brain or spinal cord making it unlikely that the observed antinociceptive phenotypes were due to *Pip5k1c*

haploinsufficiency in other regions of the nervous system. Moreover, intrathecal delivery of a small molecule inhibitor, UNC3230, recapitulated these antinociceptive phenotypes, suggesting that localized inhibition of PIP5K1C in adults (and not during development) is sufficient to reduce nociceptive sensitization.

We speculate that PIP<sub>2</sub> levels were reduced in DRG of *Pip5k1c*<sup>+/-</sup> mice but not in spinal cord or brain because of a greater dependence on *Pip5k1c* in DRG relative to these other tissues. In support of this hypothesis, PIP<sub>2</sub> levels were not reduced in the brain of *Pip5k1c*<sup>+/-</sup> mice<sup>51</sup>, but were reduced by 50% in the brain of embryonic *Pip5k1c*<sup>-/-</sup> mice<sup>51, 138</sup>. Thus, PIP<sub>2</sub> levels in the central nervous system appear to be insensitive to *Pip5k1c* haploinsufficiency. Additionally, PIP<sub>2</sub> levels were not reduced in the brain of embryonic *Pip5k1a*, *Pip5k1b* double knockout mice, suggesting other enzymes besides *Pip5k1a*, *Pip5k1b*, and *Pip5k1c* generate PIP<sub>2</sub> in the nervous system<sup>51</sup>. This greater dependence on *Pip5k1c* in DRG makes PIP5K1C a particularly attractive target for analgesic drug development, as inhibition of PIP5K1C has the potential to lower PIP<sub>2</sub> levels in sensory neurons without perturbing PIP<sub>2</sub> levels in other cell types, including those in the brain.

**PIP5K1C modulates pronociceptive signaling and sensitization via PIP<sub>2</sub>-dependent mechanism(s).**

GPCR- and TRVP1-evoked calcium signaling was significantly blunted in *Pip5k1c*<sup>+/-</sup> neurons. Similarly, neuronal excitability that is mediated by PIP<sub>2</sub>-dependent ion channels was significantly attenuated in *Pip5k1c*<sup>+/-</sup> neurons. These data suggest that PIP<sub>2</sub> required for PLC-catalyzed GPCR signaling and the direct

regulatory interactions of PIP<sub>2</sub> with the C terminus of ion channels regulate at least three pronociceptive signaling pathways. Likewise, these data suggest that PIP5K1C regulates these pathways via synthesis of PIP<sub>2</sub>. PIP<sub>2</sub>-dependence was supported by complete restoration of signaling deficits (GPCR, TRPV1, and ion channel mediated) in *Pip5k1c*<sup>+/-</sup> neurons following exogenous delivery of PIP<sub>2</sub>. Consistent with these findings, others have demonstrated that exogenous PIP<sub>2</sub> delivery rescued histamine-evoked calcium responses in HeLa cells following *Pip5k1c* knockdown with small interfering RNA (siRNA)<sup>41</sup>. Additionally, ATP-evoked calcium release from purinergic receptors was significantly blunted in *Pip5k1c*<sup>+/-</sup> lateral nonsensory cells<sup>52</sup>, further indicating that *Pip5k1c* regulates receptor signaling.

*Pip5k1c* regulates many additional processes downstream of PIP<sub>2</sub>, including actin dynamics, synaptic vesicle release and NMDA-induced AMPA receptor endocytosis<sup>67, 131, 139, 140</sup>. However, neurotransmission was not impaired between sensory neurons and spinal neurons in *Pip5k1c*<sup>+/-</sup> mice, making it unlikely that vesicle recycling deficits accounted for reduced behavioral sensitization. In contrast, we did observe deficits in cytoskeletal (actin and tubulin) dynamics in *Pip5k1c*<sup>+/-</sup> neurons, indicating there are likely multiple PIP<sub>2</sub>-dependent processes contributing to the deficits in nociceptive signaling and sensitization. Importantly, increases in tubulin expression in *Pip5k1c*<sup>+/-</sup> neurons could contribute to the reductions observed in TRPV1- and GPCR-mediated calcium signaling via tubulin-PIP<sub>2</sub>-PLC interactions. In fact, increases in tubulin levels inhibit PLC1β-mediated signaling, an important step in both GPCR and TRPV1 signaling<sup>29, 32</sup>. Thus, it is likely that increases in

tubulin expression in *Pip5k1c*<sup>+/-</sup> neurons are partially responsible for the signaling deficits. Furthermore, it is known that changes in actin and tubulin dynamics influence lipid bilayer properties and subsequently receptor stability and functionality<sup>33, 97, 139</sup>, and could be contributing to the observed signaling deficits in *Pip5k1c*<sup>+/-</sup> neurons. Collectively, our data highlight the importance of PIP<sub>2</sub> for efficient pronociceptive signaling and reveal that reductions in PIP5K1C lead to PIP<sub>2</sub>-dependent reductions in pronociceptive signaling; however, the exact mechanism by which this occurs requires further investigation.

Importantly, thermal and mechanical nociceptive sensitization in models of chronic inflammatory and neuropathic pain was enduringly blunted in *Pip5k1c*<sup>+/-</sup> mice in a PIP<sub>2</sub>-dependent manner. This critical finding has significant implications for the field of pain signaling. Discovery of novel regulatory proteins that mediate nociceptive sensitization allow for a more complete understanding of the complex sensitization process. In addition, our findings will promote investigation of other lipid kinases that could be targeted to reduce nociceptive sensitization. Furthermore, our findings provided rationale to investigate PIP5K1C as a drug target, considering the fact that kinases are highly druggable targets<sup>141</sup>.

### **PIP5K1C is a novel analgesic drug target**

The antinociceptive phenotypes in *Pip5k1c*<sup>+/-</sup> mice prompted the development of a high-throughput screen for PIP5K1C inhibitors. From this screen, we identified UNC3230, a compound that inhibited PIP5K1C in the low nanomolar range and reduced receptor signaling and nociceptive sensitization in a fashion analogous to

*Pip5k1c* haploinsufficiency. We evaluated the specificity of UNC3230 relative to a large panel of kinases and discovered that UNC3230 has remarkable selectivity for PIP5K1C and PIP4K2C, two lipid kinases that directly generate PIP<sub>2</sub>. However, we cannot exclude the possibility that UNC3230 also inhibits kinases that we did not test, including additional kinases that generate PIP<sub>2</sub>. Nevertheless, given that UNC3230 reduces PIP<sub>2</sub> levels in cultured DRG neurons, our data suggest that UNC3230 has on-target biochemical effects.

Our genetic and pharmacological data validate PIP5K1C as a therapeutic target for chronic pain; however, further optimization of hits from our high-throughput screen is needed. For example, UNC3230 has a narrow efficacy window and solubility issues that limited our ability to perform dose-responses *in vitro* and *in vivo*. However, these shortcomings may be overcome through subsequent medicinal chemistry optimization. PIP5K1C inhibitors could provide a valuable alternative to opioid and non-steroidal anti-inflammatory analgesics.

PIP5K1C is highly and somewhat selectively expressed in neuronal tissue (in addition to very minimal expression in the kidney) indicating that PIP5K1C inhibitors may bypass unwanted side effects that have plagued previous analgesic drug development focused on individual receptors and ubiquitously expressed downstream effectors<sup>55, 59, 88, 134, 135, 142</sup>. Localized administration (intrathecal) of PIP5K1C inhibitors provides the greatest potential for mitigating on-target adverse effects given that renal function may be altered following systemic administration due to expression of PIP5K1C in the kidneys. The main challenge for PIP5K1C inhibition as an orally available analgesic is prevention of blood-brain barrier (BBB)



penetration. Compounds can be designed (based on UNC3230 or future scaffolds) that do not penetrate the BBB, which will restrict their activity to the peripheral nervous system and make the potential for an orally available PIP5K1C inhibitor with minimal on-target adverse effects very possible. As mentioned previously, UNC3230 already exhibits excellent selectivity. Most notably, UNC3230 does not inhibit human PIP5K1A (homologous to mouse PIP5K1B), which is ubiquitously expressed, further enhancing the potential for continued development of inhibitors with minimal adverse off-target effects.

### **Implications for phosphoinositide signaling**

Our findings also could extend beyond PIP5K1C and promote research into additional enzymes lipid kinases, phosphatases, and lipid transporters that affect PIP<sub>2</sub> levels in DRG neurons. Indeed, a recent functional genomics study identified phospholipid signaling and lipid kinases as key regulators of heat nociception in flies<sup>143</sup>. This study also found that *Pip5k1a*<sup>-/-</sup> mice displayed hypersensitivity to noxious heat and capsaicin. However, *Pip5k1a* is expressed at much lower levels in DRG and does not contribute to PIP<sub>2</sub> levels in the nervous system<sup>51</sup>, so precisely how and where *Pip5k1a* regulates heat nociception in mice is unknown. Given the sometimes differing or opposing roles of *Pip5k1c* and *Pip5k1a* in the same processes<sup>47, 48, 97, 144, 145</sup>, it is reasonable to speculate that *Pip5k1c* and *Pip5k1a* may have opposing functions in DRG neurons. Furthermore, given the complexity of nociceptive signaling and the low level of expression of *Pip5k1a* in DRG neurons,

*Pip5k1a* could be modulating nociceptive processes at the level of the spinal cord or brain.

Moreover, PIP5K1C inhibitors will likely have uses as tool compounds that will aid in studies of PIP5K1C in other processes such as endocytosis, synaptic vesicle trafficking, and focal adhesion dynamics. Current methods to study these processes include obtaining primary neuron cultures from *Pip5k1c*<sup>-/-</sup> embryos or transiently transfecting PIP5K1C in common cell culture lines including human embryonic kidney (HEK) and HeLa cells<sup>41, 45, 131</sup>. Obtaining primary neuron cultures from knockout mice is time and resource-intensive and only allows examination of this processes following deletion of the entire protein for an extended period of time, thwarting efforts to investigate transient inhibition of PIP5K1C catalytic activity. Use of transient transfection in HEK or HeLa cells prevents studying the enzyme at physiologically relevant concentrations and tissue type (PIP5K1C is found primarily in neurons). Transient inhibition of PIP5K1C with the identified small molecules will allow studies to determine which PIP5K1C-dependent processes are independent of or dependent upon catalytic activity<sup>48</sup>. In addition, the identified inhibitors can be used as a complementary approach to genetic studies to differentiate between phenotypes that arise from chronic inhibition of the protein (genetic knockout mice) and acute inhibition of the catalytic activity (pharmacological transient inhibition). Lastly, characterization of the effects of PIP5K1C inhibition on phosphoinositide-dependent processes outside of the nociceptive system is necessary to inform studies aimed at future development of these inhibitors as analgesics.

## **Homozygous deletion of PIP5K1C in sensory neurons reduces DRG nerve innervation into target tissue**

Although this was an unexpected finding, decreased nerve innervation in *Pip5k1c<sup>fl/fl</sup>* mice provides helpful insight into the role of PIP5K1C in DRG processes that are not part of the nociceptive system. Interestingly, the phenotype observed in *Pip5k1c<sup>fl/fl</sup>* mice is different from previous reports of proprioceptive phenotypes. Although *Pip5k1c<sup>fl/fl</sup>* mice have the characteristic reductions in nerve innervation that accompany proprioceptive phenotypes that have been reported in the literature, elimination of parvalbumin positive neurons that are critical for proprioceptive function was not observed in *Pip5k1c<sup>fl/fl</sup>* mice<sup>101, 102</sup>. These data indicate the mechanism of reduced nerve innervation in *Pip5k1c<sup>fl/fl</sup>* mice differs from other reported phenotypes. Furthermore, it indicates that homozygous deletion of *Pip5k1c* does not result in the observed phenotypes due to a loss of neurons within the DRG; rather, the phenotype most likely arises from a global inability of DRG neurons to extend their axons into the peripheral tissue.

Given the observed cytoskeletal alterations and receptor-mediated signaling deficits in *Pip5k1c<sup>+/-</sup>* mice, it is reasonable to expect that *Pip5k1c<sup>fl/fl</sup>* mice would also exhibit these defects. We speculate that if signaling deficits of *Pip5k1c<sup>fl/fl</sup>* mice are similar to or more pronounced than those observed with *Pip5k1c<sup>+/-</sup>* mice, it is likely that PIP<sub>2</sub>-dependent Trk receptors that mediate neurotrophin axonal guidance for innervation are contributing to the observed phenotype. Furthermore, we speculate that if actin and tubulin defects of *Pip5k1c<sup>fl/fl</sup>* mice are similar to or more pronounced than those observed with *Pip5k1c<sup>+/-</sup>* mice, these deficits are likely contributing to the

observed phenotype given that concerted cytoskeletal rearrangement is required for axon innervation. Additional characterization of *Pip5k1c<sup>fl/fl</sup>* mice is needed to fully elucidate the mechanism(s) responsible for the proprioceptive phenotype. It is important to note that nerve innervation deficits are likely due to chronic reductions in PIP5K1C and PIP<sub>2</sub> during embryonic development. However, experiments with inducible conditional knockout mice (homozygous deletion of PIP5K1C in adult mice) are needed to confirm that deletion of PIP5K1C during development is the cause of the proprioceptive phenotype. We speculate that deleting PIP5K1C in adults (using an inducible Cre) will not result in a proprioceptive phenotype. Given that PIP5K1C inhibitors are administered to adult mice and that nerve innervation deficits are most likely a result of reduced PIP5K1C during embryonic development, alterations in nerve innervation following administration of small molecule PIP5K1C is unlikely. However, experiments to evaluate nerve innervation following inhibitor treatment are needed.

Characterization of conditional heterozygous mice, *Pip5k1c<sup>fl/wt</sup>*, is currently ongoing to test our original hypothesis that reductions in PIP5K1C synthesis of PIP<sub>2</sub> in the DRG are responsible for the antinociceptive phenotypes observed in *Pip5k1c<sup>+/-</sup>* mice. We hypothesize that conditional deletion of one allele of PIP5K1C will reduce PIP<sub>2</sub> in the DRG by at least 50%, the level of reduction observed in *Pip5k1c<sup>+/-</sup>* mice, and attenuate nociceptive signaling and sensitization in a similar manner to the reductions observed in *Pip5k1c<sup>+/-</sup>* mice.

## Human implications

Humans heterozygous for a mutation in *PIP5K1C* that results in a non-functional protein develop normally and appear healthy<sup>94</sup>. Since humans can clearly tolerate a life-long reduction in *PIP5K1C* gene dosage, drugs that transiently inhibit *PIP5K1C* have the potential to be well tolerated with chronic use. While loss of high frequency hearing was observed in *Pip5k1c*<sup>+/-</sup> mice, this is not likely to be an issue in humans since humans cannot hear above 20 kHz<sup>146</sup>. In contrast to the benign heterozygous mutation, humans carrying two non-functional *PIP5K1C* alleles (homozygous mutation), develop lethal congenital contracture syndrome type 3 (LCCS3), which is characterized by muscle atrophy, joint contractures and death within 24 hours of birth<sup>94</sup>. The lethality of the human phenotype closely mimics the perinatal lethality observed in the *Pip5k1c*<sup>-/-</sup> mice<sup>45</sup>; although, the link between reduced  $PIP_2$  and the characteristic joint contractures and muscle atrophy in the human disease has not been determined. The exact cause of lethality in the knockout mice generated by Di Paolo et al.<sup>45</sup> was never investigated; however, the gene trap knockout mice that resulted in embryonic lethality generated by Wang et al<sup>138</sup> revealed cardiovascular and neuronal abnormalities that were mediated by deficits in actin-dependent processes in cardiomyocytes and neuroepithelium. Wang et al and Di Paolo et al published their findings prior to the report of *PIP5K1C* mutations in LCCS3 by Narkis, et. Al. and thus no insights were provided on the murine findings and the link to the characteristics of the human phenotype. Interestingly, the data from our studies and from Wang, et. al. supports the hypothesis that the interaction between  $PIP_2$  and cytoskeletal proteins such as actin

and tubulin is the critical link between PIP5K1C mutations and the human phenotype.

Our data with *Pip5k1c*<sup>+/-</sup> mice reveal a critical role of PIP<sub>2</sub> in regulating physiological actin and tubulin dynamics,<sup>27</sup> two key components of muscle contraction that promote muscle contraction, strength, and force<sup>147, 148</sup>. In addition to the altered expression pattern of actin and the increase in tubulin expression, RNA sequencing of DRG from *Pip5k1c*<sup>+/-</sup> mice revealed more than 2-fold increases in several troponin T mRNAs compared to WT controls. It is reasonable to speculate that these changes in cytoskeletal mRNAs may serve as a compensatory mechanism for the loss of PIP<sub>2</sub> interactions with actin and tubulin once PIP5K1C expression is reduced. However, analysis of protein expression of these cytoskeletal filaments is still needed. Although our analysis was completed with DRG neurons, it is possible that these changes may occur in the muscle as well. Although PIP5K1C expression is thought to be restricted to neuronal tissues in mice, the expression profile of PIP5K1C in humans has not been determined. Furthermore, PIP5K1C is minimally expressed in murine skeletal muscle (expression in smooth muscle has never been investigated)<sup>45</sup>. Furthermore, alterations in actin and tubulin would likely decrease nerve innervation of alpha motor neurons into the muscle (as observed when conditionally deleting PIP5K1C). Even if there were no changes in expression levels of cytoskeletal proteins involved in muscle contraction, the mislocalization of actin observed would likely be enough to alter contractibility given that actin serves as the scaffold for myosin, tropomyosin, and troponin interactions that result in contraction<sup>148-150</sup>. Indeed, disruption of the actin

cytoskeleton with cytochalasin B reduced contractile speed<sup>149</sup>. Collectively, our data suggests a link between reduced PIP<sub>2</sub> synthesis and alterations in cytoskeletal proteins that may explain the LCCS3 phenotype in humans. In fact, mutations in genes that encode thin-filament proteins including actin and troponin T result in skeletal myopathies similar to LCCS3<sup>96</sup>. Although our data provides a suggestive link between PIP5K1C reductions of PIP<sub>2</sub> and the muscle/joint phenotypes of LCCS3, additional studies are required to determine the expression profile of PIP5K1C in humans and the extent to which cytoskeletal genes and proteins are expressed in humans carrying homozygous mutations in *PIP5K1C*.

Importantly, there are no reported muscle contraction/atrophy phenotypes reported in humans carrying a heterozygous mutation of *PIP5K1C*. Furthermore, as mentioned above, heterozygous mutations in *PIP5K1C* are well tolerated in humans making it likely that PIP5K1C analgesics would be well tolerated. Thus, we conclude that although our preliminary studies with actin and tubulin provide a suggestive link between homozygous mutation in *PIP5K1C* and the muscle contracture phenotype, it is unlikely that LCCS3-like symptoms would arise from acute administration of PIP5K1C analgesics in the adult. In support of this conclusion, there were no phenotypes similar to those in LCCS3 observed in *Pip5k1c*<sup>+/-</sup> mice or following administration of UNC3230. Moreover, the LCCS3 phenotype is likely due to reduced PIP<sub>2</sub> synthesis during embryonic development, further supporting our hypothesis that LCCS3-like phenotypes would not result from small molecule inhibition in adults. Development of more effective inhibitors (>50% reduction in PIP<sub>2</sub> synthesis) and/or investigation of *Pip5k1c* conditionally deleted during

adulthood only (inducible conditional knockout mice) are needed to provide more conclusive evidence that the nerve innervation phenotype (Chapter III) and LCCS3 human phenotype are a result of PIP5K1C loss during development. In addition, delivery of PIP5K1C-targeted analgesics could be (and have been) limited to the spinal region, eliminating all concerns that could arise from PIP5K1C inhibition within the muscle or other tissues. Our studies with *Pip5k1c*<sup>+/-</sup> mice and UNC3230 indicate that a 50% reduction in PIP<sub>2</sub>-synthesis is sufficient to attenuate nociceptive signaling and sensitization, thus complete loss of PIP5K1C function would not be required for effective analgesic activity. Development of a more effective PIP5K1C inhibitor that would abrogate PIP<sub>2</sub> levels and mimic the complete loss of PIP5K1C activity that results from homozygous mutation is needed to evaluate the full analgesic potential of PIP5K1C inhibitors and the risk of developing muscle contracture phenotypes.

It is currently unknown if humans with homozygous mutations of *PIP5K1C* have reduced inflammatory pain responses, such as those found in *Pip5k1c*<sup>+/-</sup> mice. Importantly, future studies with these human carriers have the potential to directly assess the importance of PIP5K1C in human pain perception. Lastly, individuals that carry one non-functional allele of *PIP5K1C* are Bedouins and live in the Negev desert of Israel—an environment that is arid and subject to extreme temperatures. Like sickle-cell anemia, where heterozygotes have a survival advantage in regions where malaria is endemic, mutations in *PIP5K1C* could provide a survival advantage in the desert, where somatosensory stimuli can be extreme. Although this is suggestive of a link between the observed phenotypes in *Pip5k1c*<sup>+/-</sup> mice and



humans carrying *PIP5K1C* heterozygous mutations, further characterization is needed to implicate the pathway in humans.

## Conclusions

The aim of this dissertation was to rigorously characterize the role of PIP5K1C, a potentially druggable kinase, in nociceptive signaling and sensitization. To accomplish this aim we utilized two approaches in parallel, genetic deletion of the *Pip5k1c* (*Pip5k1c*<sup>+/-</sup> knockout mice) and pharmacological (small molecule) inhibition of PIP5K1C. Completion of this work revealed a central regulatory role of PIP5K1C in GPCR- and ion channel-mediated pronociceptive signaling. Similarly, PIP5K1C regulates nociceptive sensitization in models of neuropathic and inflammatory chronic pain. Our work with *Pip5k1c*<sup>+/-</sup> mice identified a novel regulatory mechanism that will influence future studies of the nociceptive system and has the potential to prompt studies of pain perception in humans that carry a heterozygous mutation in *PIP5K1C*. In addition, a novel PIP5K1C high-throughput screen identified the first reported PIP5K1C inhibitor, which has broad implications for the field of phosphoinositide signaling and analgesic drug development.

## APPENDIX 1: PERSONAL CONTRIBUTIONS TO DISSERTATION CHAPTERS

With guidance from Dr. Mark Zylka, I completed all experiments and analyzed all data in Chapters II and III with the following exceptions. For Chapter II, Megumi Aita at the UNC *in situ* hybridization core performed the double fluorescence *in situ* hybridization using probes prepared by members of Dr. Mark Zylka's laboratory (Figure 2.1D-E). Bonnie Taylor-Blake completed all immunohistochemical staining (Figures 2.1F-G and 2.11A-J). Dr. Sarah Street completed all electrophysiological studies (experimentation and analysis; Figures 2.6A-B and 2.11K-N). Walter Dutton performed behavioral experiments using the LPA-induced neuropathic pain model (Figure 2.9A-B). Dr. Eric McCoy performed the light touch mechanical sensitivity assay (Figure 2.10D) and the UNC Behavioral Phenotyping Core completed the rotarod studies (Figure 2.10A). For Chapter III, Bonnie Taylor-Blake completed all immunohistochemical analysis of hindpaw glabrous skin, volar pad, and hairy skin (Figure 3.5).

For Chapter IV, I completed all assay development, primary screening, and data analysis with guidance from Cathy Simpson and William Janzen. The UNC CICBDD provided the LOPAC and kinase-focused libraries for screening. Chatura Jayakody prepared all screening plates. Michael Stashko completed selectivity screening of 48 kinases using the ProfilerPro platform. Selectivity screening of 100 kinases was completed at DiscoverX and Dan Lockhart generated the KinomeTree diagram using DiscoverX software. Dr. Anqi Ma synthesized large quantities of UNC3230 for testing *in vitro* and *in vivo*.

## REFERENCES

1. Medicine, I. o. *Relieving Pain in America: A Blueprint for Transforming Prevention, Care, Education, and Research*; 9780309214841 030921484X; Washington (DC), 2011.
2. Melnikova, I. Pain market. *Nat Rev Drug Discov* **2010**, 9, 589-90.
3. Gold, M. S.; Gebhart, G. F. Nociceptor sensitization in pain pathogenesis. *Nat Med* **2010**, 16, 1248-57.
4. Woolf, C. J.; Ma, Q. Nociceptors--noxious stimulus detectors. *Neuron* **2007**, 55, 353-64.
5. Stone, L. S.; Molliver, D. C. In search of analgesia: emerging roles of GPCRs in pain. *Mol Interv* **2009**, 9, 234-51.
6. Basbaum, A. I.; Bautista, D. M.; Scherrer, G.; Julius, D. Cellular and molecular mechanisms of pain. *Cell* **2009**, 139, 267-84.
7. Cavanaugh, D. J.; Chesler, A. T.; Braz, J. M.; Shah, N. M.; Julius, D.; Basbaum, A. I. Restriction of transient receptor potential vanilloid-1 to the peptidergic subset of primary afferent neurons follows its developmental downregulation in nonpeptidergic neurons. *J Neurosci* **2011**, 31, 10119-27.
8. Zylka, M. J.; Rice, F. L.; Anderson, D. J. Topographically distinct epidermal nociceptive circuits revealed by axonal tracers targeted to Mrgprd. *Neuron* **2005**, 45, 17-25.
9. Zylka, M. J. Nonpeptidergic circuits feel your pain. *Neuron* **2005**, 47, 771-2.
10. Schaible, H. G. Peripheral and central mechanisms of pain generation. *Handb Exp Pharmacol* **2007**, 3-28.
11. Julius, D.; Basbaum, A. I. Molecular mechanisms of nociception. *Nature* **2001**, 413, 203-10.

12. Woolf, C. J. Pain: moving from symptom control toward mechanism-specific pharmacologic management. *Ann Intern Med* **2004**, 140, 441-51.
13. Scholz, J.; Woolf, C. J. Can we conquer pain? *Nat Neurosci* **2002**, 5 Suppl, 1062-7.
14. Lukacs, V.; Thyagarajan, B.; Varnai, P.; Balla, A.; Balla, T.; Rohacs, T. Dual regulation of TRPV1 by phosphoinositides. *J Neurosci* **2007**, 27, 7070-80.
15. Lukacs, V.; Yudin, Y.; Hammond, G. R.; Sharma, E.; Fukami, K.; Rohacs, T. Distinctive changes in plasma membrane phosphoinositides underlie differential regulation of TRPV1 in nociceptive neurons. *J Neurosci* **2013**, 33, 11451-63.
16. Rohacs, T.; Thyagarajan, B.; Lukacs, V. Phospholipase C mediated modulation of TRPV1 channels. *Mol Neurobiol* **2008**, 37, 153-63.
17. Rosenbaum, T.; Simon, S. A. TRPV1 Receptors and Signal Transduction. In *TRP Ion Channel Function in Sensory Transduction and Cellular Signaling Cascades*, Liedtke, W. B.; Heller, S., Eds. Boca Raton (FL), 2007.
18. Gold, M. S.; Gebhart, G. F. Nociceptor sensitization in pain pathogenesis. *Nat Med* **2010**, 16, 1248-57.
19. Medicine, I. o. *Relieving pain in america: a blueprint for transforming prevention, care, education and research*. The National Academies Press: 2011; Vol. 1, p 1-382.
20. Hucho, T. B.; Dina, O. A.; Levine, J. D. Epac mediates a cAMP-to-PKC signaling in inflammatory pain: an isolectin B4(+) neuron-specific mechanism. *J Neurosci* **2005**, 25, 6119-26.
21. Weng, X.; Smith, T.; Sathish, J.; Djouhri, L. Chronic inflammatory pain is associated with increased excitability and hyperpolarization-activated current (I<sub>h</sub>) in C- but not Delta-nociceptors. *Pain* **2012**, 153, 900-14.
22. Fishcer, M. J. M., Mak, S.W.K, and McNaughton, P.A. Sensitisation of Nociceptors--What are Ion Channels Doing? *The Open Pain Journal* **2010**, 3, 82-96.

23. Gamper, N.; Shapiro, M. S. Target-specific PIP(2) signalling: how might it work? *J Physiol* **2007**, 582, 967-75.
24. Gamper, N.; Reznikov, V.; Yamada, Y.; Yang, J.; Shapiro, M. S. Phosphatidylinositol [correction] 4,5-bisphosphate signals underlie receptor-specific Gq/11-mediated modulation of N-type Ca<sup>2+</sup> channels. *J Neurosci* **2004**, 24, 10980-92.
25. Suh, B. C.; Hille, B. PIP2 is a necessary cofactor for ion channel function: how and why? *Annu Rev Biophys* **2008**, 37, 175-95.
26. Suh, B. C.; Leal, K.; Hille, B. Modulation of high-voltage activated Ca(2+) channels by membrane phosphatidylinositol 4,5-bisphosphate. *Neuron* **2010**, 67, 224-38.
27. Zhang, L.; Mao, Y. S.; Janmey, P. A.; Yin, H. L. Phosphatidylinositol 4, 5 bisphosphate and the actin cytoskeleton. *Subcell Biochem* **2012**, 59, 177-215.
28. McLaughlin, S.; Wang, J.; Gambhir, A.; Murray, D. PIP(2) and proteins: interactions, organization, and information flow. *Annu Rev Biophys Biomol Struct* **2002**, 31, 151-75.
29. Popova, J. S.; Garrison, J. C.; Rhee, S. G.; Rasenick, M. M. Tubulin, Gq, and phosphatidylinositol 4,5-bisphosphate interact to regulate phospholipase Cbeta1 signaling. *J Biol Chem* **1997**, 272, 6760-5.
30. Rasenick, M. M.; Wang, N. Exchange of guanine nucleotides between tubulin and GTP-binding proteins that regulate adenylate cyclase: cytoskeletal modification of neuronal signal transduction. *J Neurochem* **1988**, 51, 300-11.
31. Siderovski, D. P.; Willard, F. S. The GAPs, GEFs, and GDIs of heterotrimeric G-protein alpha subunits. *Int J Biol Sci* **2005**, 1, 51-66.
32. Popova, J. S.; Greene, A. K.; Wang, J.; Rasenick, M. M. Phosphatidylinositol 4,5-bisphosphate modifies tubulin participation in phospholipase Cbeta1 signaling. *J Neurosci* **2002**, 22, 1668-78.

33. Storti, B.; Bizzarri, R.; Cardarelli, F.; Beltram, F. Intact microtubules preserve transient receptor potential vanilloid 1 (TRPV1) functionality through receptor binding. *J Biol Chem* **2012**, 287, 7803-11.
34. Yan, J.; Jin, T. Signaling network from GPCR to the actin cytoskeleton during chemotaxis. *Bioarchitecture* **2012**, 2, 15-18.
35. Ganguly, S.; Saxena, R.; Chattopadhyay, A. Reorganization of the actin cytoskeleton upon G-protein coupled receptor signaling. *Biochim Biophys Acta* **2011**, 1808, 1921-9.
36. Kranenburg, O.; Poland, M.; Gebbink, M.; Oomen, L.; Moolenaar, W. H. Dissociation of LPA-induced cytoskeletal contraction from stress fiber formation by differential localization of RhoA. *J Cell Sci* **1997**, 110 ( Pt 19), 2417-27.
37. Fukushima, N.; Kimura, Y.; Chun, J. A single receptor encoded by vzg-1/lpA1/edg-2 couples to G proteins and mediates multiple cellular responses to lysophosphatidic acid. *Proc Natl Acad Sci U S A* **1998**, 95, 6151-6.
38. Elmes, S. J.; Millns, P. J.; Smart, D.; Kendall, D. A.; Chapman, V. Evidence for biological effects of exogenous LPA on rat primary afferent and spinal cord neurons. *Brain Res* **2004**, 1022, 205-13.
39. Inoue, M.; Rashid, M. H.; Fujita, R.; Contos, J. J.; Chun, J.; Ueda, H. Initiation of neuropathic pain requires lysophosphatidic acid receptor signaling. *Nat Med* **2004**, 10, 712-8.
40. Dina, O. A.; McCarter, G. C.; de Coupade, C.; Levine, J. D. Role of the sensory neuron cytoskeleton in second messenger signaling for inflammatory pain. *Neuron* **2003**, 39, 613-24.
41. Wang, Y. J.; Li, W. H.; Wang, J.; Xu, K.; Dong, P.; Luo, X.; Yin, H. L. Critical role of PIP5K $\gamma$ 87 in InsP3-mediated Ca<sup>2+</sup> signaling. *J Cell Biol* **2004**, 167, 1005-10.
42. Xie, Z.; Chang, S. M.; Pennypacker, S. D.; Liao, E. Y.; Bikle, D. D. Phosphatidylinositol-4-phosphate 5-kinase 1 $\alpha$  mediates extracellular calcium-induced keratinocyte differentiation. *Mol Biol Cell* **2009**, 20, 1695-704.

43. Ishihara, H.; Shibasaki, Y.; Kizuki, N.; Katagiri, H.; Yazaki, Y.; Asano, T.; Oka, Y. Cloning of cDNAs encoding two isoforms of 68-kDa type I phosphatidylinositol-4-phosphate 5-kinase. *J Biol Chem* **1996**, 271, 23611-4.
44. Doughman, R. L.; Firestone, A. J.; Wojtasiak, M. L.; Bunce, M. W.; Anderson, R. A. Membrane ruffling requires coordination between type I alpha phosphatidylinositol phosphate kinase and Rac signaling. *J Biol Chem* **2003**, 278, 23036-45.
45. Di Paolo, G.; Moskowitz, H. S.; Gipson, K.; Wenk, M. R.; Voronov, S.; Obayashi, M.; Flavell, R.; Fitzsimonds, R. M.; Ryan, T. A.; De Camilli, P. Impaired PtdIns(4,5)P<sub>2</sub> synthesis in nerve terminals produces defects in synaptic vesicle trafficking. *Nature* **2004**, 431, 415-22.
46. Wenk, M. R.; Pellegrini, L.; Klenchin, V. A.; Di Paolo, G.; Chang, S.; Daniell, L.; Arioka, M.; Martin, T. F.; De Camilli, P. PIP kinase Igamma is the major PI(4,5)P<sub>2</sub> synthesizing enzyme at the synapse. *Neuron* **2001**, 32, 79-88.
47. Mao, Y. S.; Yamaga, M.; Zhu, X.; Wei, Y.; Sun, H. Q.; Wang, J.; Yun, M.; Wang, Y.; Di Paolo, G.; Bennett, M.; Mellman, I.; Abrams, C. S.; De Camilli, P.; Lu, C. Y.; Yin, H. L. Essential and unique roles of PIP5K-gamma and -alpha in Fcgamma receptor-mediated phagocytosis. *J Cell Biol* **2009**, 184, 281-96.
48. Mao, Y. S.; Yin, H. L. Regulation of the actin cytoskeleton by phosphatidylinositol 4-phosphate 5 kinases. *Pflugers Arch* **2007**, 455, 5-18.
49. Bairstow, S. F.; Ling, K.; Su, X.; Firestone, A. J.; Carbonara, C.; Anderson, R. A. Type I gamma phosphatidylinositol phosphate kinase directly interacts with AP2 and regulates endocytosis. *J Biol Chem* **2006**, 281, 20632-42.
50. Ling, K.; Doughman, R. L.; Firestone, A. J.; Bunce, M. W.; Anderson, R. A. Type I gamma phosphatidylinositol phosphate kinase targets and regulates focal adhesions. *Nature* **2002**, 420, 89-93.
51. Volpicelli-Daley, L. A.; Lucast, L.; Gong, L. W.; Liu, L.; Sasaki, J.; Sasaki, T.; Abrams, C. S.; Kanaho, Y.; De Camilli, P. Phosphatidylinositol-4-phosphate 5-kinases and phosphatidylinositol 4,5-bisphosphate synthesis in the brain. *J Biol Chem* **2010**, 285, 28708-14.

52. Rodriguez, L.; Simeonato, E.; Scimemi, P.; Anselmi, F.; Cali, B.; Crispino, G.; Ciubotaru, C. D.; Bortolozzi, M.; Ramirez, F. G.; Majumder, P.; Arslan, E.; De Camilli, P.; Pozzan, T.; Mammano, F. Reduced phosphatidylinositol 4,5-bisphosphate synthesis impairs inner ear Ca<sup>2+</sup> signaling and high-frequency hearing acquisition. *Proc Natl Acad Sci U S A* **2012**, 109, 14013-8.
53. Russ, A. P.; Lampel, S. The druggable genome: an update. *Drug Discov Today* **2005**, 10, 1607-10.
54. Pagano, M. A.; Cesaro, L.; Meggio, F.; Pinna, L. A. Protein kinase CK2: a newcomer in the 'druggable kinome'. *Biochem Soc Trans* **2006**, 34, 1303-6.
55. Anand, P.; Shenoy, R.; Palmer, J. E.; Baines, A. J.; Lai, R. Y.; Robertson, J.; Bird, N.; Ostefeld, T.; Chizh, B. A. Clinical trial of the p38 MAP kinase inhibitor dilmapirod in neuropathic pain following nerve injury. *Eur J Pain* **2011**, 15, 1040-8.
56. Aley, K. O.; Martin, A.; McMahon, T.; Mok, J.; Levine, J. D.; Messing, R. O. Nociceptor sensitization by extracellular signal-regulated kinases. *J Neurosci* **2001**, 21, 6933-9.
57. Aley, K. O.; Messing, R. O.; Mochly-Rosen, D.; Levine, J. D. Chronic hypersensitivity for inflammatory nociceptor sensitization mediated by the epsilon isozyme of protein kinase C. *J Neurosci* **2000**, 20, 4680-5.
58. Cesare, P.; Dekker, L. V.; Sardini, A.; Parker, P. J.; McNaughton, P. A. Specific involvement of PKC-epsilon in sensitization of the neuronal response to painful heat. *Neuron* **1999**, 23, 617-24.
59. Cousins, M. J.; Pickthorn, K.; Huang, S.; Critchley, L.; Bell, G. The safety and efficacy of KAI-1678- an inhibitor of epsilon protein kinase C (epsilonPKC)- versus lidocaine and placebo for the treatment of postherpetic neuralgia: a crossover study design. *Pain Med* **2013**, 14, 533-40.
60. Moodie, J. E.; Bisley, E. J.; Huang, S.; Pickthorn, K.; Bell, G. A single-center, randomized, double-blind, active, and placebo-controlled study of KAI-1678, a novel PKC-epsilon inhibitor, in the treatment of acute postoperative orthopedic pain. *Pain Med* **2013**, 14, 916-24.



61. Ostenfeld, T.; Krishen, A.; Lai, R. Y.; Bullman, J.; Baines, A. J.; Green, J.; Anand, P.; Kelly, M. Analgesic efficacy and safety of the novel p38 MAP kinase inhibitor, losmapimod, in patients with neuropathic pain following peripheral nerve injury: a double-blind, placebo-controlled study. *Eur J Pain* **2013**, *17*, 844-57.
62. Rohacs, T. Phosphoinositide regulation of non-canonical transient receptor potential channels. *Cell Calcium* **2009**, *45*, 554-65.
63. Ufret-Vincenty, C. A.; Klein, R. M.; Hua, L.; Angueyra, J.; Gordon, S. E. Localization of the PIP2 sensor of TRPV1 ion channels. *J Biol Chem* **2011**, *286*, 9688-98.
64. Ishihara, H.; Shibasaki, Y.; Kizuki, N.; Wada, T.; Yazaki, Y.; Asano, T.; Oka, Y. Type I phosphatidylinositol-4-phosphate 5-kinases. Cloning of the third isoform and deletion/substitution analysis of members of this novel lipid kinase family. *J Biol Chem* **1998**, *273*, 8741-8.
65. Bittner, M. A.; Holz, R. W. Phosphatidylinositol-4,5-bisphosphate: actin dynamics and the regulation of ATP-dependent and -independent secretion. *Mol Pharmacol* **2005**, *67*, 1089-98.
66. Roach, A. N.; Wang, Z.; Wu, P.; Zhang, F.; Chan, R. B.; Yonekubo, Y.; Di Paolo, G.; Gorfe, A. A.; Du, G. Phosphatidic acid regulation of PIPKI is critical for actin cytoskeletal reorganization. *J Lipid Res* **2012**, *53*, 2598-609.
67. van den Bout, I.; Divecha, N. PIP5K-driven PtdIns(4,5)P2 synthesis: regulation and cellular functions. *J Cell Sci* **2009**, *122*, 3837-50.
68. White, J. K.; Gerdin, A. K.; Karp, N. A.; Ryder, E.; Buljan, M.; Bussell, J. N.; Salisbury, J.; Clare, S.; Ingham, N. J.; Podrini, C.; Houghton, R.; Estabel, J.; Bottomley, J. R.; Melvin, D. G.; Sunter, D.; Adams, N. C.; Tannahill, D.; Logan, D. W.; Macarthur, D. G.; Flint, J.; Mahajan, V. B.; Tsang, S. H.; Smyth, I.; Watt, F. M.; Skarnes, W. C.; Dougan, G.; Adams, D. J.; Ramirez-Solis, R.; Bradley, A.; Steel, K. P. Genome-wide generation and systematic phenotyping of knockout mice reveals new roles for many genes. *Cell* **2013**, *154*, 452-64.

69. Zylka, M. J.; Dong, X.; Southwell, A. L.; Anderson, D. J. Atypical expansion in mice of the sensory neuron-specific Mrg G protein-coupled receptor family. *Proc Natl Acad Sci U S A* **2003**, 100, 10043-8.
70. Pinaud, R.; Mello, C. V.; Velho, T. A.; Wynne, R. D.; Tremere, L. A. Detection of two mRNA species at single-cell resolution by double-fluorescence in situ hybridization. *Nat Protoc* **2008**, 3, 1370-9.
71. Zylka, M. J.; Sowa, N. A.; Taylor-Blake, B.; Twomey, M. A.; Herrala, A.; Voikar, V.; Vihko, P. Prostatic acid phosphatase is an ectonucleotidase and suppresses pain by generating adenosine. *Neuron* **2008**, 60, 111-22.
72. McCoy, E. S.; Taylor-Blake, B.; Street, S. E.; Pribisko, A. L.; Zheng, J.; Zylka, M. J. Peptidergic CGRPalpha Primary Sensory Neurons Encode Heat and Itch and Tonicly Suppress Sensitivity to Cold. *Neuron* **2013**, 78, 138-51.
73. McCoy, E. S.; Taylor-Blake, B.; Zylka, M. J. CGRPalpha-expressing sensory neurons respond to stimuli that evoke sensations of pain and itch. *PLoS One* **2012**, 7, e36355.
74. Wang, H.; Zylka, M. J. Mrgprd-expressing polymodal nociceptive neurons innervate most known classes of substantia gelatinosa neurons. *J Neurosci* **2009**, 29, 13202-9.
75. Street, S. E.; Walsh, P. L.; Sowa, N. A.; Taylor-Blake, B.; Guillot, T. S.; Vihko, P.; Wightman, R. M.; Zylka, M. J. PAP and NT5E inhibit nociceptive neurotransmission by rapidly hydrolyzing nucleotides to adenosine. *Mol Pain* **2011**, 7, 80.
76. Caterina, M. J.; Schumacher, M. A.; Tominaga, M.; Rosen, T. A.; Levine, J. D.; Julius, D. The capsaicin receptor: a heat-activated ion channel in the pain pathway. *Nature* **1997**, 389, 816-24.
77. Shields, S. D.; Eckert, W. A., 3rd; Basbaum, A. I. Spared nerve injury model of neuropathic pain in the mouse: a behavioral and anatomic analysis. *J Pain* **2003**, 4, 465-70.

78. Ma, L.; Matsumoto, M.; Xie, W.; Inoue, M.; Ueda, H. Evidence for lysophosphatidic acid 1 receptor signaling in the early phase of neuropathic pain mechanisms in experiments using Ki-16425, a lysophosphatidic acid 1 receptor antagonist. *J Neurochem* **2009**, 109, 603-10.
79. Cunha, T. M.; Verri, W. A., Jr.; Vivancos, G. G.; Moreira, I. F.; Reis, S.; Parada, C. A.; Cunha, F. Q.; Ferreira, S. H. An electronic pressure-meter nociception paw test for mice. *Braz J Med Biol Res* **2004**, 37, 401-7.
80. Hargreaves, K.; Dubner, R.; Brown, F.; Flores, C.; Joris, J. A new and sensitive method for measuring thermal nociception in cutaneous hyperalgesia. *Pain* **1988**, 32, 77-88.
81. Fairbanks, C. A. Spinal delivery of analgesics in experimental models of pain and analgesia. *Adv Drug Deliv Rev* **2003**, 55, 1007-41.
82. Garrison, S. R.; Dietrich, A.; Stucky, C. L. TRPC1 contributes to light-touch sensation and mechanical responses in low-threshold cutaneous sensory neurons. *J Neurophysiol* **2012**, 107, 913-22.
83. Hara, Y.; Fukaya, M.; Tamaki, H.; Sakagami, H. Type I phosphatidylinositol 4-phosphate 5-kinase gamma is required for neuronal migration in the mouse developing cerebral cortex. *Eur J Neurosci* **2013**, 38, 2659-71.
84. Sowa, N. A.; Street, S. E.; Vihko, P.; Zylka, M. J. Prostatic acid phosphatase reduces thermal sensitivity and chronic pain sensitization by depleting phosphatidylinositol 4,5-bisphosphate. *J Neurosci* **2010**, 30, 10282-93.
85. Prescott, E. D.; Julius, D. A modular PIP2 binding site as a determinant of capsaicin receptor sensitivity. *Science* **2003**, 300, 1284-8.
86. Cui, Y.; Yang, F.; Cao, X.; Yarov-Yarovoy, V.; Wang, K.; Zheng, J. Selective disruption of high sensitivity heat activation but not capsaicin activation of TRPV1 channels by pore turret mutations. *J Gen Physiol* **2012**, 139, 273-83.
87. Kassuya, C. A.; Ferreira, J.; Claudino, R. F.; Calixto, J. B. Intraplantar PGE2 causes nociceptive behaviour and mechanical allodynia: the role of prostanoid E receptors and protein kinases. *Br J Pharmacol* **2007**, 150, 727-37.

88. Stock, J. L.; Shinjo, K.; Burkhardt, J.; Roach, M.; Taniguchi, K.; Ishikawa, T.; Kim, H. S.; Flannery, P. J.; Coffman, T. M.; McNeish, J. D.; Audoly, L. P. The prostaglandin E2 EP1 receptor mediates pain perception and regulates blood pressure. *J Clin Invest* **2001**, 107, 325-31.
89. Omote, K.; Yamamoto, H.; Kawamata, T.; Nakayama, Y.; Namiki, A. The effects of intrathecal administration of an antagonist for prostaglandin E receptor subtype EP(1) on mechanical and thermal hyperalgesia in a rat model of postoperative pain. *Anesth Analg* **2002**, 95, 1708-12, table of contents.
90. Minami, T.; Nishihara, I.; Uda, R.; Ito, S.; Hyodo, M.; Hayaishi, O. Characterization of EP-receptor subtypes involved in allodynia and hyperalgesia induced by intrathecal administration of prostaglandin E2 to mice. *Br J Pharmacol* **1994**, 112, 735-40.
91. Renback, K.; Inoue, M.; Ueda, H. Lysophosphatidic acid-induced, pertussis toxin-sensitive nociception through a substance P release from peripheral nerve endings in mice. *Neurosci Lett* **1999**, 270, 59-61.
92. Papakonstanti, E. A.; Stournaras, C. Cell responses regulated by early reorganization of actin cytoskeleton. *FEBS Lett* **2008**, 582, 2120-7.
93. Morgan, J. R.; Di Paolo, G.; Werner, H.; Shchedrina, V. A.; Pypaert, M.; Pieribone, V. A.; De Camilli, P. A role for talin in presynaptic function. *J Cell Biol* **2004**, 167, 43-50.
94. Narkis, G.; Ofir, R.; Landau, D.; Manor, E.; Volokita, M.; Hershkowitz, R.; Elbedour, K.; Birk, O. S. Lethal contractural syndrome type 3 (LCCS3) is caused by a mutation in PIP5K1C, which encodes PIPKI gamma of the phosphatidylinositol pathway. *Am J Hum Genet* **2007**, 81, 530-9.
95. Nowak, K. J.; Ravenscroft, G.; Laing, N. G. Skeletal muscle alpha-actin diseases (actinopathies): pathology and mechanisms. *Acta Neuropathol* **2013**, 125, 19-32.
96. Ochala, J. Thin filament proteins mutations associated with skeletal myopathies: defective regulation of muscle contraction. *J Mol Med (Berl)* **2008**, 86, 1197-204.

97. Noda, Y.; Niwa, S.; Homma, N.; Fukuda, H.; Imajo-Ohmi, S.; Hirokawa, N. Phosphatidylinositol 4-phosphate 5-kinase alpha (PIP2Kalpha) regulates neuronal microtubule depolymerase kinesin, KIF2A and suppresses elongation of axon branches. *Proc Natl Acad Sci U S A* **2012**, 109, 1725-30.
98. Hasegawa, H.; Abbott, S.; Han, B. X.; Qi, Y.; Wang, F. Analyzing somatosensory axon projections with the sensory neuron-specific Advillin gene. *J Neurosci* **2007**, 27, 14404-14.
99. Zhou, X.; Wang, L.; Hasegawa, H.; Amin, P.; Han, B. X.; Kaneko, S.; He, Y.; Wang, F. Deletion of PIK3C3/Vps34 in sensory neurons causes rapid neurodegeneration by disrupting the endosomal but not the autophagic pathway. *Proc Natl Acad Sci U S A* **2010**, 107, 9424-9.
100. Zurborg, S.; Piszczek, A.; Martinez, C.; Hublitz, P.; Al Banchaabouchi, M.; Moreira, P.; Perlas, E.; Heppenstall, P. A. Generation and characterization of an Advillin-Cre driver mouse line. *Mol Pain* **2011**, 7, 66.
101. Ringstedt, T.; Kucera, J.; Lendahl, U.; Ernfors, P.; Ibanez, C. F. Limb proprioceptive deficits without neuronal loss in transgenic mice overexpressing neurotrophin-3 in the developing nervous system. *Development* **1997**, 124, 2603-13.
102. Chen, X. J.; Levedakou, E. N.; Millen, K. J.; Wollmann, R. L.; Soliven, B.; Popko, B. Proprioceptive sensory neuropathy in mice with a mutation in the cytoplasmic Dynein heavy chain 1 gene. *J Neurosci* **2007**, 27, 14515-24.
103. Kumar, N.; Zhao, P.; Tomar, A.; Galea, C. A.; Khurana, S. Association of villin with phosphatidylinositol 4,5-bisphosphate regulates the actin cytoskeleton. *J Biol Chem* **2004**, 279, 3096-110.
104. Dent, E. W.; Gertler, F. B. Cytoskeletal dynamics and transport in growth cone motility and axon guidance. *Neuron* **2003**, 40, 209-27.
105. Huang, E. J.; Reichardt, L. F. Trk receptors: roles in neuronal signal transduction. *Annu Rev Biochem* **2003**, 72, 609-42.

106. Patel, T. D.; Jackman, A.; Rice, F. L.; Kucera, J.; Snider, W. D. Development of sensory neurons in the absence of NGF/TrkA signaling in vivo. *Neuron* **2000**, 25, 345-57.
107. Stirling, L. C.; Forlani, G.; Baker, M. D.; Wood, J. N.; Matthews, E. A.; Dickenson, A. H.; Nassar, M. A. Nociceptor-specific gene deletion using heterozygous NaV1.8-Cre recombinase mice. *Pain* **2005**, 113, 27-36.
108. Cavanaugh, D. J.; Chesler, A. T.; Jackson, A. C.; Sigal, Y. M.; Yamanaka, H.; Grant, R.; O'Donnell, D.; Nicoll, R. A.; Shah, N. M.; Julius, D.; Basbaum, A. I. Trpv1 reporter mice reveal highly restricted brain distribution and functional expression in arteriolar smooth muscle cells. *J Neurosci* **2011**, 31, 5067-77.
109. Lau, J.; Minett, M. S.; Zhao, J.; Dennehy, U.; Wang, F.; Wood, J. N.; Bogdanov, Y. D. Temporal control of gene deletion in sensory ganglia using a tamoxifen-inducible Advillin-Cre-ERT2 recombinase mouse. *Mol Pain* **2011**, 7, 100.
110. Cleary, J. M.; Shapiro, G. I. Development of phosphoinositide-3 kinase pathway inhibitors for advanced cancer. *Curr Oncol Rep* **2010**, 12, 87-94.
111. Delage, E.; Puyaubert, J.; Zachowski, A.; Ruelland, E. Signal transduction pathways involving phosphatidylinositol 4-phosphate and phosphatidylinositol 4,5-bisphosphate: convergences and divergences among eukaryotic kingdoms. *Prog Lipid Res* **2013**, 52, 1-14.
112. Wymann, M. P.; Schneider, R. Lipid signalling in disease. *Nat Rev Mol Cell Biol* **2008**, 9, 162-76.
113. Balla, T.; Szentpetery, Z.; Kim, Y. J. Phosphoinositide signaling: new tools and insights. *Physiology (Bethesda)* **2009**, 24, 231-44.
114. French, K. J.; Schrecengost, R. S.; Lee, B. D.; Zhuang, Y.; Smith, S. N.; Eberly, J. L.; Yun, J. K.; Smith, C. D. Discovery and evaluation of inhibitors of human sphingosine kinase. *Cancer Res* **2003**, 63, 5962-9.
115. Alshaker, H.; Sauer, L.; Monteil, D.; Ottaviani, S.; Srivats, S.; Bohler, T.; Pchejetski, D. Therapeutic potential of targeting SK1 in human cancers. *Adv Cancer Res* **2013**, 117, 143-200.

116. Lamia, K. A.; Peroni, O. D.; Kim, Y. B.; Rameh, L. E.; Kahn, B. B.; Cantley, L. C. Increased insulin sensitivity and reduced adiposity in phosphatidylinositol 5-phosphate 4-kinase beta-/- mice. *Mol Cell Biol* **2004**, *24*, 5080-7.
117. Davis, M. I.; Sasaki, A. T.; Shen, M.; Emerling, B. M.; Thorne, N.; Michael, S.; Pragani, R.; Boxer, M.; Sumita, K.; Takeuchi, K.; Auld, D. S.; Li, Z.; Cantley, L. C.; Simeonov, A. A homogeneous, high-throughput assay for phosphatidylinositol 5-phosphate 4-kinase with a novel, rapid substrate preparation. *PLoS One* **2013**, *8*, e54127.
118. Hutti, J. E.; Porter, M. A.; Cheely, A. W.; Cantley, L. C.; Wang, X.; Kireev, D.; Baldwin, A. S.; Janzen, W. P. Development of a high-throughput assay for identifying inhibitors of TBK1 and IKKepsilon. *PLoS One* **2012**, *7*, e41494.
119. Sciences, C. L. LabChip Mobility-Shift Assay: Phosphatidylinositol-3 Kinase PI3Ka. *LC3000-AP-212* **2008**, LC3000-AP-212, 1-4.
120. Lin, S.; Fischl, A. S.; Bi, X.; Parce, W. Separation of phospholipids in microfluidic chip device: application to high-throughput screening assays for lipid-modifying enzymes. *Anal Biochem* **2003**, *314*, 97-107.
121. Lee, K. Y. Loss of lipid to plastic tubing. *J Lipid Res* **1971**, *12*, 635-6.
122. Copeland, R. A. Mechanistic considerations in high-throughput screening. *Anal Biochem* **2003**, *320*, 1-12.
123. Lipinski, C. A. Drug-like properties and the causes of poor solubility and poor permeability. *J Pharmacol Toxicol Methods* **2000**, *44*, 235-49.
124. Walters, W. P.; Murcko, M. A. Prediction of 'drug-likeness'. *Adv Drug Deliv Rev* **2002**, *54*, 255-71.
125. Weiss, W. A.; Taylor, S. S.; Shokat, K. M. Recognizing and exploiting differences between RNAi and small-molecule inhibitors. *Nat Chem Biol* **2007**, *3*, 739-44.
126. Karaman, M. W.; Herrgard, S.; Treiber, D. K.; Gallant, P.; Atteridge, C. E.; Campbell, B. T.; Chan, K. W.; Ciceri, P.; Davis, M. I.; Edeen, P. T.; Faraoni, R.;

- Floyd, M.; Hunt, J. P.; Lockhart, D. J.; Milanov, Z. V.; Morrison, M. J.; Pallares, G.; Patel, H. K.; Pritchard, S.; Wodicka, L. M.; Zarrinkar, P. P. A quantitative analysis of kinase inhibitor selectivity. *Nat Biotechnol* **2008**, 26, 127-32.
127. Sorensen, S. D.; Linseman, D. A.; McEwen, E. L.; Heacock, A. M.; Fisher, S. K. A role for a wortmannin-sensitive phosphatidylinositol-4-kinase in the endocytosis of muscarinic cholinergic receptors. *Mol Pharmacol* **1998**, 53, 827-36.
128. Cavasotto, C. N.; Phatak, S. S. Homology modeling in drug discovery: current trends and applications. *Drug Discov Today* **2009**, 14, 676-83.
129. Hillisch, A.; Pineda, L. F.; Hilgenfeld, R. Utility of homology models in the drug discovery process. *Drug Discov Today* **2004**, 9, 659-69.
130. Hammond, G. R.; Fischer, M. J.; Anderson, K. E.; Holdich, J.; Koteci, A.; Balla, T.; Irvine, R. F. PI4P and PI(4,5)P2 are essential but independent lipid determinants of membrane identity. *Science* **2012**, 337, 727-30.
131. Toth, D. J.; Toth, J. T.; Gulyas, G.; Balla, A.; Balla, T.; Hunyady, L.; Varnai, P. Acute depletion of plasma membrane phosphatidylinositol 4,5-bisphosphate impairs specific steps in endocytosis of the G-protein-coupled receptor. *J Cell Sci* **2012**, 125, 2185-97.
132. Szallasi, A.; Sheta, M. Targeting TRPV1 for pain relief: limits, losers and laurels. *Expert Opin Investig Drugs* **2012**, 21, 1351-69.
133. Szolcsanyi, J.; Pinter, E. Transient receptor potential vanilloid 1 as a therapeutic target in analgesia. *Expert Opin Ther Targets* **2013**, 17, 641-57.
134. Jones, R. L.; Giembycz, M. A.; Woodward, D. F. Prostanoid receptor antagonists: development strategies and therapeutic applications. *Br J Pharmacol* **2009**, 158, 104-45.
135. Hill, R. NK1 (substance P) receptor antagonists--why are they not analgesic in humans? *Trends Pharmacol Sci* **2000**, 21, 244-6.



136. Gomis, A.; Meini, S.; Miralles, A.; Valenti, C.; Giuliani, S.; Belmonte, C.; Maggi, C. A. Blockade of nociceptive sensory afferent activity of the rat knee joint by the bradykinin B2 receptor antagonist fasinibant. *Osteoarthritis Cartilage* **2013**, *21*, 1346-54.
137. Mantyh, P. W.; Koltzenburg, M.; Mendell, L. M.; Tive, L.; Shelton, D. L. Antagonism of nerve growth factor-TrkA signaling and the relief of pain. *Anesthesiology* **2011**, *115*, 189-204.
138. Wang, Y.; Lian, L.; Golden, J. A.; Morrissey, E. E.; Abrams, C. S. PIP5KI gamma is required for cardiovascular and neuronal development. *Proc Natl Acad Sci U S A* **2007**, *104*, 11748-53.
139. Rusinova, R.; Hobart, E. A.; Koeppe, R. E., 2nd; Andersen, O. S. Phosphoinositides alter lipid bilayer properties. *J Gen Physiol* **2013**, *141*, 673-90.
140. Unoki, T.; Matsuda, S.; Kakegawa, W.; Van, N. T.; Kohda, K.; Suzuki, A.; Funakoshi, Y.; Hasegawa, H.; Yuzaki, M.; Kanaho, Y. NMDA receptor-mediated PIP5K activation to produce PI(4,5)P(2) is essential for AMPA receptor endocytosis during LTD. *Neuron* **2012**, *73*, 135-48.
141. Hopkins, A. L.; Groom, C. R. The druggable genome. *Nat Rev Drug Discov* **2002**, *1*, 727-30.
142. Anand, P.; Bley, K. Topical capsaicin for pain management: therapeutic potential and mechanisms of action of the new high-concentration capsaicin 8% patch. *Br J Anaesth* **2011**, *107*, 490-502.
143. Neely, G. G.; Rao, S.; Costigan, M.; Mair, N.; Racz, I.; Milinkeviciute, G.; Meixner, A.; Nayanala, S.; Griffin, R. S.; Belfer, I.; Dai, F.; Smith, S.; Diatchenko, L.; Marengo, S.; Haubner, B. J.; Novatchkova, M.; Gibson, D.; Maixner, W.; Pospisilik, J. A.; Hirsch, E.; Wishaw, I. Q.; Zimmer, A.; Gupta, V.; Sasaki, J.; Kanaho, Y.; Sasaki, T.; Kress, M.; Woolf, C. J.; Penninger, J. M. Construction of a global pain systems network highlights phospholipid signaling as a regulator of heat nociception. *PLoS Genet* **2012**, *8*, e1003071.
144. Nguyen, T. T.; Kim, Y. M.; Kim, T. D.; Le, O. T.; Kim, J. J.; Kang, H. C.; Hasegawa, H.; Kanaho, Y.; Jou, I.; Lee, S. Y. Phosphatidylinositol 4-phosphate

5-kinase alpha facilitates Toll-like receptor 4-mediated microglial inflammation through regulation of TIRAP location. *J Biol Chem* **2013**.

145. Vasudevan, L.; Jeromin, A.; Volpicelli-Daley, L.; De Camilli, P.; Holowka, D.; Baird, B. The beta- and gamma-isoforms of type I PIP5K regulate distinct stages of Ca<sup>2+</sup> signaling in mast cells. *J Cell Sci* **2009**, 122, 2567-74.
146. Brant, L. J.; Fozard, J. L. Age changes in pure-tone hearing thresholds in a longitudinal study of normal human aging. *J Acoust Soc Am* **1990**, 88, 813-20.
147. Herzog, W.; Leonard, T.; Joumaa, V.; DuVall, M.; Panchangam, A. The three filament model of skeletal muscle stability and force production. *Mol Cell Biomech* **2012**, 9, 175-91.
148. Carpenter, C. L. Actin cytoskeleton and cell signaling. *Crit Care Med* **2000**, 28, N94-9.
149. Battistella-Patterson, A. S.; Wang, S.; Wright, G. L. Effect of disruption of the cytoskeleton on smooth muscle contraction. *Can J Physiol Pharmacol* **1997**, 75, 1287-99.
150. Ben-Aissa, K.; Patino-Lopez, G.; Belkina, N. V.; Maniti, O.; Rosales, T.; Hao, J. J.; Kruhlak, M. J.; Knutson, J. R.; Picart, C.; Shaw, S. Activation of moesin, a protein that links actin cytoskeleton to the plasma membrane, occurs by phosphatidylinositol 4,5-bisphosphate (PIP<sub>2</sub>) binding sequentially to two sites and releasing an autoinhibitory linker. *J Biol Chem* **2012**, 287, 16311-23.